

ISSN 2622-9374 (Online)

Asian Institute of Research
**Engineering and Technology Quarterly
Reviews**

Vol. 3, No.2 December 2020



ASIAN INSTITUTE OF RESEARCH
Connecting Scholars Worldwide



Asian Institute of Research
Engineering and Technology Quarterly Reviews
Vol.3, No.2 December 2020

Table of Contents	i
Engineering and Technology Quarterly Reviews Editorial Board	ii
One-pot Synthesis of Spirooxindole Derivatives Catalyzed by Bi₂Fe₄O₉ Nanoparticles Abdul Rauof Rashid, Azizullah Yosufi, Mohammad Ali Khlili	46
Applying Capability Indices with Moving Average and Range Control Charts to Evaluate a Product in a Local Aluminum Plant Tareq M. Ali	52
Eigenvalue of Adjacent Matrix of Zero Divisor Graphs on Rings Hemati Sherin	63
Comparative Study of Water Quality From Boreholes and Hand-Dug Wells: Case of Namatapa in Bangwe Township Jabulani Matsimbe	67
Becoming Incomplete House: the Environmental Implication of the Traditional Balinese House Transformation in Tourism Area I Dewa Gede Agung Diasana Putra	74
Assessment of the Scale of Artisanal Mining in Bangwe Township, Blantyre Jabulani Matsimbe	84
OpenFOAM Based Approach for the Prediction of the Dam Break with an Obstacle Syamsuri	91
Forced Outage Analysis of Brazilian Thermal Power Plants using the Kruskal-Wallis Test Leonardo dos Santos e Santos	98
Application of the BowTie Method in Accident Analysis: Case of Kaziwiziwi Coal Mine Jabulani Matsimbe, Steven Ghambi, Abdul Samson	127
Assessment of Safety Culture and Maturity in Mining Environments: Case of Njuli Quarry Jabulani Matsimbe, Steven Ghambi, Abdul Samson	137

Engineering and Technology Quarterly Reviews Editorial Board

Editor-In-Chief

Prof. Fausto P. Garcia Marquez (Spain)

Editorial Board

Prof. Magdi S. Mahmoud (Saudi Arabia)
Prof. Dr. Erivelto Luís de Souza (Brazil)
Prof. Yves Rybarczyk (Portugal)
Prof. Evangelos J. Sapountzakis (Greece)
Prof. Dr. Abdel Ghani Aissaoui (Algeria)
Assoc. Prof. Kenan Hazirbaba (United Arab Emirates)
Assoc. Prof. Adinel Gavrus (France)
Moeiz Miraoui, Ph.D. Eng (Tunisia)
Dr. Man Fung LO (Hong Kong)
Assistant. Prof. Ramzi R. Barwari (Iraq)
Dr. Cezarina Adina Tofan (Romania)
Assistant Prof. Krzysztof Wolk (Poland)
Assistant Prof. Triantafyllos K Makarios (Greece)
Assoc. Prof. Faisal Talib (India)
Claudiu Pirnau, Ph.D. (Romania)
Assistant Prof. Dr. Nadeem Qaiser Mehmood (Pakistan)
Assistant. Prof. Dr. Dhananjaya Reddy (India)
Assoc. Prof. Pedro A. Castillo Valdivieso (Spain)
Assoc. Prof. Balkrishna Eknath Narkhede (India)
Assistant. Prof. Nouh Alhindawi (Jordan)
Assistant Professor Dr. Kaveh Ostad-Ali-Askari (Iran)
Assoc. Prof. Antoanela Naaji (Romania)
Dr. Miguel Nuno Miranda (Portugal)
Assoc. Prof. Jianwei Cheng (China)
Assoc. Prof. Dr. Ahmad Mashhour (Bahrain)
Assoc. Prof. Jaroslaw Krzywanski (Poland)
Amar Oukil, Ph.D. (Oman)
Dr. Asif Irshad Khan (Saudi Arabia)
Assistant. Prof. Sutapa Das (India)
Assistant. Prof. César M. A. Vasques (Portugal)

One-pot Synthesis of Spirooxindole Derivatives Catalyzed by Bi₂Fe₄O₉ Nanoparticles

Abdul Rauof Rashid¹, Azizullah Yosufi², Mohammad Ali Khlili³

¹ Department of Chemistry, Faculty of Natural Science, University of Bamyan, Bamyan, Afghanistan. Email: abd.rauofrashid@gmail.com

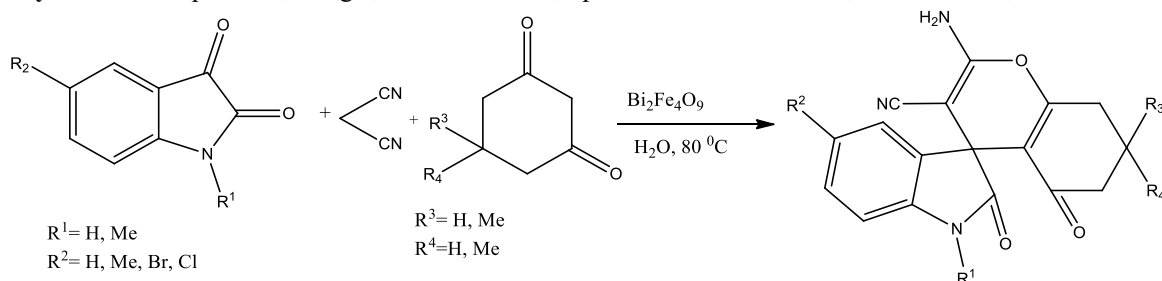
² Department of Chemistry, Faculty of Natural Science, University of Bamyan, Bamyan, Afghanistan. Email: yosofi88@gmail.com

³ Department of Science, Teacher Training Center (TTC), of Bamyan, Bamyan, Afghanistan. Email: m.alikhalili@yahoo.com

Abstract

In this study regarding the catalytic application of Bismuth Ferrite nanoparticles in the synthesis of heterocyclic compounds, we synthesized Bi₂Fe₄O₉ nanoparticles by sol-gel combustion method from bismuth nitrate pentahydrate [Bi(NO₃)₃·5H₂O] and iron nitrate nonahydrate [Fe(NO₃)₃·9H₂O] as starting materials. Structural and microstructural were characterized using X-ray diffraction (XRD), Field Emission Scanning Electron Microscopy (FESM), Vibrating-Visible Spectroscopy (VSM) and infrared spectroscopy (IR). The average size of nanoparticles was determined 36, 3 nm, by XRD and Scherer's equation. The results show that the pure phase of Bi₂Fe₄O₉ can be formed by this method. Then it is used in the one-pot synthesis of spirooxindole derivatives via three-component reaction of isatins, malononitrile and 1,3-dicarbonyl compounds in water as a green solvent in the temperature of 80°C. The reaction yields 88-98 percentages of the products. The catalyst was reused several times in the same reaction yielding unchanged products.

Keywords: Nanoparticles, Sol-gel, Bismuth Ferrite, Spirooxindole Derivatives, Malononitrile, Green Solvent



1. Introduction

Multicomponent reactions are those in which three or more reactants take part as one-pot reactants in a chemical reaction and yield a product [Ugi, 2001- Climent, 2012]. This kind of reactions is one of the important reactions in Chemistry which has been known for 150 years; it also has been widely used and studied in Organic Chemistry recently. The first multicomponent reaction is the synthesis of strecker α -amino cyanide [Stercker, 1882]. The overall properties of multicomponent reactions are; they are completed in one pot yielding high percentages of products, using accessible reactants, simple synthesis, needless to separate the intermediate substances and

environmental friendly. Multicomponent reaction is an important method for producing complex products like heterocyclic compounds[Bhaskar,2012- Dömling,2010]. Heterocyclic compounds generally, and spirooxinadole -five membered nitrogen containing cyclic compounds especially have vital role in the chemistry of drugs. The synthesis of oxinadole is still a challenge in Organic and Industrial Chemistry[Allahresani,2016-Bhaskar,2012]. The core of most drug factors and natural alkaloids is spirooxinadole[Shanthi,2007]. Recently the spirooxinadole derivatives are synthesized by different methods utilizing various catalysts[Hassani,2018]. The usual synthesizing way of these compounds is condensation of tripartite isatine, 1,3-dicarbonyl and one part of active methylene[Hemmat,2019]. The spirooxinadole derivatives are having biological and pharmaceutical activities[Allahresani,2011] such as; anti-tumor[Yu,2013], anti-micro organs[Nandakumar,2010], anti-fungal, anti-malaria[Thangamani,2010-Yeung,2010], antibiotic[Ghahremanzadeh,2016] and anti HIV[KL,2006]. Therefore the synthesis of these compounds is important in Organic Chemistry and industry of drugs. This article explores the synthesis of spirooxinadole derivatives from one-pot malononitrile, isatine, 1,3-dicarbonyl compounds and water as solvent with the existence of bismuth ferrate ($\text{Bi}_2\text{Fe}_4\text{O}_9$)

2. Experimental

2.1. Used chemicals

All the utilized chemicals and solvents including bismuth nitrate pentahydrated, iron nitrate nonahydrated, citric acid, nitric acid and ammonia are provided from Merck Company.

2.2. Procedure

Pour 1 mmole (0.148g) Isatine, 1 mmole (0.112g) cyclohexane-1,3-dione, 1 mmole (0.066g) malononitrile, catalyst $\text{Bi}_2\text{Fe}_4\text{O}_9$ and 6 mL of water in a round- based balloon with a magnetic stirrer at 80°C stir it and watch the progress of the reaction by TLC for controlling.

Once the reaction is completed and the solvent is removed, solve the yielded mixture in acetone and draw out the catalyst by centrifuge from the mixture. Then crystalize it in Ethanol which yields 88 – 95% of the product.

3. Optimizing conditions of reaction in synthesis of spirooxinadole derivatives

3.1. Optimization of solvent

pour 1 mmole (0.148g) Isatine, 1 mmole (0.112g) cyclohexane-1,3-dione, 1 mmole (0.066g) Malononitrile, catalyst $\text{Bi}_2\text{Fe}_4\text{O}_9$ and various solvents (water, solution of water and ethanol 1:1, solution of ethyl acetate and ethanol) in a round-based balloon and stir it at 80°C. Observe the progress of the reaction with TLC. After the completion of the reaction solve the mixture in acetone and draw out the catalyst with a centrifuge from the mixture. Then solve the mixture of the reaction in water and ethyl acetate, after that isolate the water and organic phases from each other with a decanter funnel. Once the solvent is removed from the mixture, the product is crystalized in Ethanol. The outcome of the test is illustrated in the table of 3-1.

Table 3-1: Optimization of solvent

No	Solvent	Temperature (°C)	Time (min)	Percentage of product
1	Water	80	10	95-98
2	Water and ethanol (1:1)	80	25	85-90
3	Ethyl acetate	Reflux	25	15-20
4	Ethanol	Reflux	20	80-85

3.2. Optimizing the amount of catalyst

pour 1 mmole (0.148g) Isatine, 1 mmole (0.112g) cyclohexane-1,3-dione, 1 mmole (0.066g) Malononitrile, different amounts (0.05, 0.012, 0.08, and 0.04g) of catalyst $\text{Bi}_2\text{Fe}_4\text{O}_9$ in a round-based balloon and complete the reaction as before mentioned. Its outcome is entered in table 3-2, as you see the best result is obtained with 0.012g $\text{Bi}_2\text{Fe}_4\text{O}_9$.

Table 3-2: Optimization of the amount of catalyst

Number	Amount of catalyst (g)	Time (min)	Percentage of the product (%)
1	0.004	20	50-55
2	0.008	30	80-85

3	0.012	10	95-98
4	0.05	10	95-98

3.3. Optimizing the Temperature

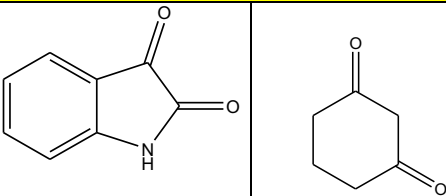
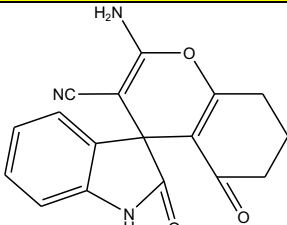
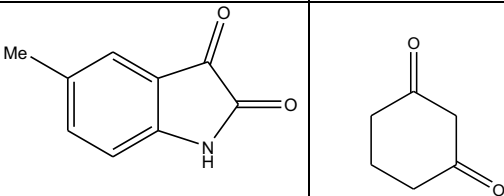
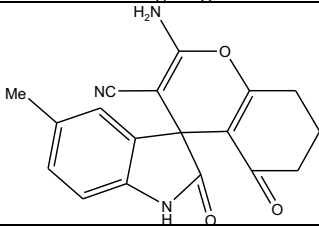
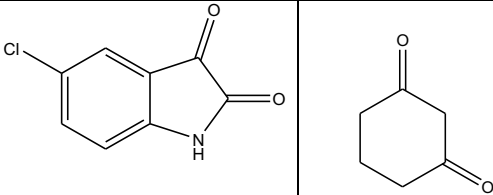
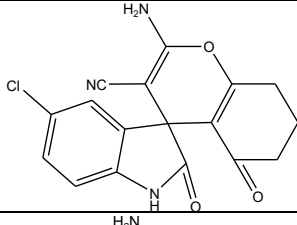
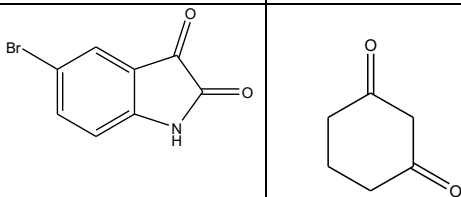
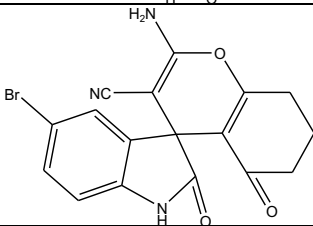
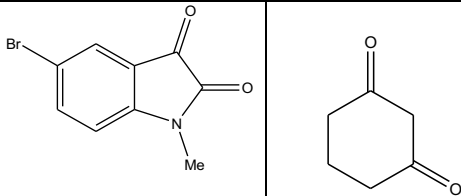
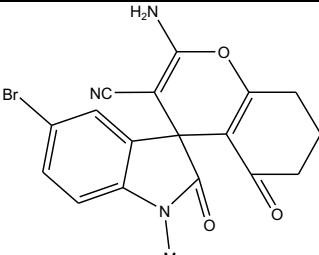
Pour 1 mmole (0.148g) Isatine, 1 mmole (0.112g) cyclohexane-1,3-dione, 1 mmole (0.066g) Malononitrile, 5mL of water as solvent and 0.012g $\text{Bi}_2\text{Fe}_4\text{O}_9$ as catalyst in a round-based balloon and stir it with a magnetic stirrer in various temperature degrees (25, 80, and 100°C). Watch and control the progress of the reaction with the previously mentioned way. The data from the experiment is entered in the table 3-3 which shows the highest amount of yield is produced at 80°C.

Table 3-3: Optimization of temperature

Number	Amount of catalyst (g)	Temperature (°C)	Time (min)	Percentage of the Product
1	0.012	25	30	30-40
2	0.012	80	10	95-98
3	0.012	100	10	95-98

The synthesis result of spirooxinadole derivatives from 1 mmole Isatine, 1 mmole diketone derivatives, 1 mmole Malononitrile in 6 mL of water and 0.012 g catalyst in 10 minutes are entered in table 3-4.

Table 3-4: synthesis of spirooxinadole derivatives with the existence of $\text{Bi}_2\text{Fe}_4\text{O}_9$ as catalyst and water as solvent.

Number	Reactants	Product	Percentage
1			98
2			93
3			95
4			95
5			90

6				97
7				93
8				95
9				95
10				88

3.4. Synthetic mechanism of spirooxinadole derivatives with the existence of $\text{Bi}_2\text{Fe}_4\text{O}_9$ nano-particles as catalyst

Figure 3-1 illustrates suggested mechanism for synthesis of spirooxinadole derivatives. Firstly the catalyst $\text{Bi}_2\text{Fe}_4\text{O}_9$ activates the carbonyl group of Isatine, then Malononitrile functions as nucleophile on the activated group of Isatine and forms the second intermediate state. The mentioned intermediate state makes the third intermediate state. Finally adding cyclohexane-1,3-dione on the yielded compound causes the target product to be produced.

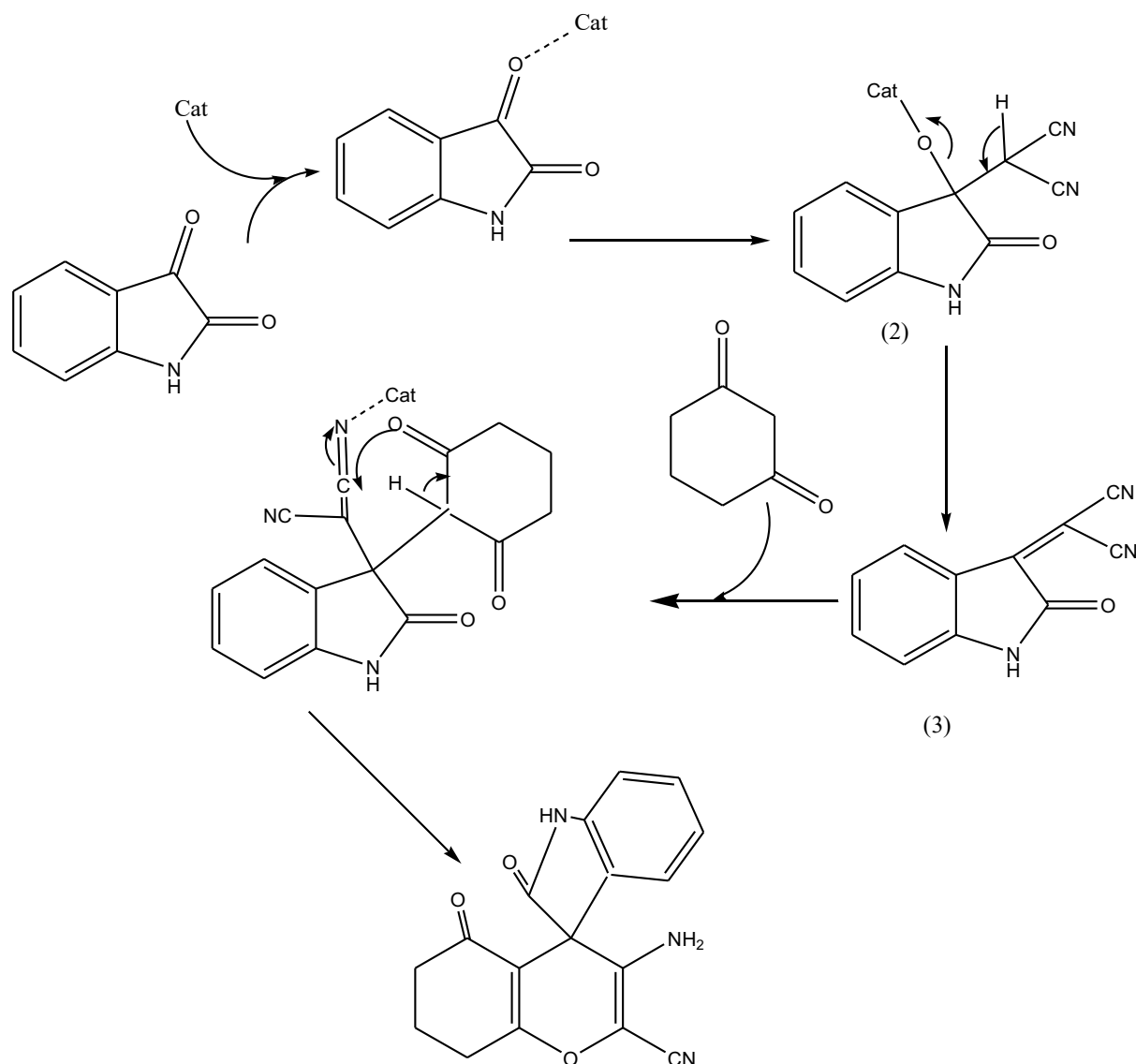


Figure 3.1: Synthetic mechanism of spirooxinadole derivatives with the existence of $\text{Bi}_2\text{Fe}_4\text{O}_9$.

Conclusion

As it is clear that catalysts play vital roles on chemical reactions rate, firstly $\text{Bi}_2\text{Fe}_4\text{O}_9$ as nano-catalyst has been synthesized for the first time by the sol-gel combustion method and has been signified by FESE, EDX, VSM and IR analysis. Then Malononitrile, Isatine, 1,3-dicarbonyl compounds have been utilized in water as solvent in 80°C of temperature. The products of the reaction were produced with 88-98 %. finally, the catalyst has been recovered and used for similar reactions several time.

The applied method in this research for synthesis of spirooxinadole derivatives with the existence of $\text{Bi}_2\text{Fe}_4\text{O}_9$ as nano-catalyst in water as solvent has several advantages such as application of homogenous catalyst, its nontoxicity and stability against temperature, simple retrieval of the catalyst, high percentage and purity of the products, simple method and not producing additional products.

References

- Ugi, I., 2001. Recent progress in the chemistry of multicomponent reactions. *Pure and Applied Chemistry*, 73(1), pp.187-191.
- Climent, M.J., Corma, A. and Iborra, S., 2012. Homogeneous and heterogeneous catalysts for multicomponent reactions. *RSC advances*, 2(1), pp.16-58.
- Stercker, A. Libeigs Ann. Chem. 1882, 215, 1.

- Bhaskar, G., Arun, Y., Balachandran, C., Saikumar, C. and Perumal, P.T., 2012. Synthesis of novel spirooxindole derivatives by one pot multicomponent reaction and their antimicrobial activity. *European journal of medicinal chemistry*, 51, pp.79-91.
- Dömling, A. and Ugi, I., 2000. Multicomponent reactions with isocyanides. *Angewandte Chemie International Edition*, 39(18), pp.3168-3210.
- Allahresani, A., Taheri, B. and Nasser, M.A., 2018. Synthesis of spirooxindole derivatives catalyzed by GN/SO₃ H nanocomposite as a heterogeneous solid acid. *Research on Chemical Intermediates*, 44(11), pp.6979-6993.
- Bhaskar, G., Arun, Y., Balachandran, C., Saikumar, C. and Perumal, P.T., 2012. Synthesis of novel spirooxindole derivatives by one pot multicomponent reaction and their antimicrobial activity. *European journal of medicinal chemistry*, 51, pp.79-91.
- Shanthi, G., Subbulakshmi, G. and Perumal, P.T., 2007. A new InCl₃-catalyzed, facile and efficient method for the synthesis of spirooxindoles under conventional and solvent-free microwave conditions. *Tetrahedron*, 63(9), pp.2057-2063.
- Hassani, H., Zakerinasab, B. and Nozarie, A., 2018. Sulfonic acid supported on Fe₂O₃/VO₂ nanocatalyst: a highly efficient and reusable nanocatalyst for synthesis of spirooxindole derivatives. *Asian Journal of Green Chemistry*, 2(1), pp.59-69.
- Hemmat, K., Nasser, M.A. and Allahresani, A., 2019. CoFe₂O₄@ SiO₂@ Co (III) Salen Complex: A Magnetically Recyclable Heterogeneous Catalyst for the Synthesis of Quinoline Derivatives in Water. *ChemistrySelect*, 4(14), pp.4339-4346.
- Allahresani, A., Taheri, B. and Nasser, M.A., 2018. A green synthesis of spirooxindole derivatives catalyzed by SiO₂@ gC₃N₄ nanocomposite. *Research on Chemical Intermediates*, 44(2), pp.1173-1188.
- Yu, F., Huang, R., Ni, H., Fan, J., Yan, S. and Lin, J., 2013. Three-component stereoselective synthesis of spirooxindole derivatives. *Green chemistry*, 15(2), pp.453-462.
- Nandakumar, A., Thirumurugan, P., Perumal, P.T., Vembu, P., Ponnuswamy, M.N. and Ramesh, P., 2010. One-pot multicomponent synthesis and anti-microbial evaluation of 2'-(indol-3-yl)-2-oxospiro (indoline-3, 4'-pyran) derivatives. *Bioorganic & medicinal chemistry letters*, 20(14), pp.4252-4258.
- Thangamani, A., 2010. Regiospecific synthesis and biological evaluation of spirooxindolopyrrolizidines via [3+2] cycloaddition of azomethine ylide. *European journal of medicinal chemistry*, 45(12), pp.6120-6126.
- Yeung, B.K., Zou, B., Rottmann, M., Lakshminarayana, S.B., Ang, S.H., Leong, S.Y., Tan, J., Wong, J., Keller-Maerki, S., Fischli, C. and Goh, A., 2010. Spirotetrahydro β -carboline (spiroindolones): a new class of potent and orally efficacious compounds for the treatment of malaria. *Journal of medicinal chemistry*, 53(14), pp.5155-5164.
- Ghahremanzadeh, R., Rashid, Z., Zarnani, A.H. and Naeimi, H., 2013. Synthesis of novel spirooxindoles in water by using MnFe₂O₄ nanoparticles as an efficient magnetically recoverable and reusable catalyst. *Applied Catalysis A: General*, 467, pp.270-278.
- KL, J.T.K., 2006. Wolff K. Yin H. Bieza K. Caldwell J. Bursulaya B. Wu TY.-H. He Y. *Bioorg. Med. Chem. Lett*, 16, p.2105.

Applying Capability Indices with Moving Average and Range Control Charts to Evaluate a Product in a Local Aluminum Plant

Tareq M. Ali¹

¹ Department of Applied Sciences, University of Technology, Baghdad, Iraq

Correspondence: Tareq M. Ali, Applied Sciences Department, University of Technology, Al-Sinaa Street, Baghdad, Iraq. E-mail: tarekza2001@yahoo.com

Abstract

The study of production processes capability is one of the most important statistical process control techniques (SPC). This study allows answering an important question; is the manufacturing system capable of producing a product with fewer defects and according to the wishes and requirements of consumer and customer? The main objective of this study is the assessment of a process capability and indices for the production process of aluminum sections regarding to weight, hardness, coating, tensile strength and heat treatment in a local aluminum plant, these aluminum sections and parts are widely used in industry, building, rails, and many other applications. The study was carried out in one of the local aluminum factory for the production of specific engineering sections, some capability indices were applied to the most affective characteristics on the quality of these produced sections; as weight, hardness, coating, tensile strength, heat treatment, these indices were applied after confirming the statistical control of the production process using the quality control charts, specifically moving average and range control charts.

Keywords: Capability Indices, Defects, Heat Treatment, Control Charts

1. Introduction

A process has been well-defined as a series of interdependent methods, operations, or steps consuming resources and changing the inputs to outputs. Every step or operation is added to the following for achieving an aim or a favorite result. In each process, there is a specific quantity of variation that cannot be removed, but it can be monitored, measured, decreased and controlled. When one looks at a simple instant of preparing a cup of coffee, one can specify the steps, inputs, apparatus and the process output.

The necessary steps (as inputs) require switching on the coffee producer, measure and add the water as well as coffee, and then the output being a cup of coffee. The variation can take place in the quantity of water or coffee presented in this process and the coffee producer performance. Each cup of coffee is not precisely the similar but in the majority states, when measurements are precise and sensibly consistent, it flavors similar. Via using the controls of process, taking the precise measurements and utilizing reliable, highly maintained apparatuses, the process variation can possess less influence upon the output quality.

In order to make the process able to produce an acceptable product on a reliable basis, Process Capability (Cp) can be used. Cp is a statistical measurement of the ability of a process for producing parts within identified specification on a consistent basis. For determining how the process is working, one can compute the followings: Cp, Process Capability Index (Cpk), Preliminary Process Capability (Pp), and Preliminary Process Capability Index (Ppk), based upon the process condition and the procedure of obtaining the value of standard deviation (or sigma). The computations of (Cp) and (Cpk) utilize the sample deviation or the deviation of mean within the rational sub-groups. The computations of (Pp) and (Ppk) employ the standard deviation depending upon the investigated studied data (the whole population). The indices of (Cp) and (Cpk) are utilized for evaluating the current, set processes in the statistical control. The indices (Pp) and (Ppk) are employed for evaluating a fresh process or one, which isn't in the statistical control.

The (Cp) and (Cpk) assess the process output compared to the limits of specification obtained via the value of target and the range of tolerance. (Cp) says when the process is able to make parts within the specifications, and (Cpk) expresses at the point when the process is focused between the specification limits. If engineers design components, they ought to regard the capability of machine or the process chosen to manufacture the component. For illustration, if one uses an actual world instant, imagine one drives a vehicle over a bridge. The width vehicle width is equal to the data spread or range. The guardrails on every side of bridge are the limits of specification. One ought to keep the vehicle on bridge for reaching the other side. The value of (Cp) is equal to the distance that the vehicle keeps away from the guardrails, and the (Cpk) denotes how well one is driving down the mid of bridge. Clearly, when the data spread is narrower (the width of car is smaller), the more distance exists between guardrails and vehicle and the more probable one stays on bridge.

The (Cp) index is an important sign of the capability of process. The value of (Cp) is computed utilizing the limits of specification and the process standard deviation. Major of companies need that the process ($Cp \geq 1.33$). The process center's (Cpk) index moves a step more via testing how near a process is achieving to the limits of specification regarding the usual variation of process. The bigger value of (Cpk), the nearer the data mean being to the value of target. The (Cpk) is computed utilizing the limits of specification, standard deviation (or sigma), and the magnitude of mean. The value of (Cpk) has to be within (1) and (3). When this value is < 1 , the process should be improved.

The (Cp) and (Cpk) indices are merely as good as the data utilized. The accurate capability of process investigations is relied on (3) rudimentary assumptions concerning the data:

There're no distinctive variation causes in process and it's in a statistical control state. Some distinctive causes ought to be revealed and determined.

The data fits a normal distribution, displaying a bell-shaped curve and can be computed to (\pm three sigma). There're states if the data doesn't fit a normal distribution.

Data of sample is a population's representative. Data has to be arbitrarily gathered from a big run of manufacture. Numerous companies need at minimum (25) to rather (50) measurements of sample be gathered.

2. Process Capability

Process capability is described as the process inherent variability in the nonappearance of every undesirable causes; the least variability, of which the process being fit with the variability owing only to the regular causes.

Distinctively, the processes pursues the distribution of normal probability, it that's correct, the process measurements high percentage drops between ($\pm 3\sigma$) of the mean or center of process.

That's, a nearly (0.27%) of the measurements would normally drop outside the limits of ($\pm 3\sigma$), and the stability of them (nearly 99.73%) would be inside the limits of ($\pm 3\sigma$).

Because the limits of process range from (-3σ) to ($+3\sigma$), the whole spread quantities to around (6σ) entire variation. When one compares the spread of process with the spread of specification, one distinctively has one of the three following states [3]:

State I:

A truly competent process, the spread of process is fine inside the spread of specification $6\sigma < (USL - LSL)$, Fig.1.stateI

Where:

USL: Upper specification limit

LSL: Lower specification limit

σ : Process standard deviation

State II:

A hardly capable process, the spread of process is just around matching (6σ), Fig.1.stateII

Where:

$$6\sigma = (USL - LSL)$$

If a spread of process being just around equal to the spread of specification, this process is capable of satisfying the specifications, but hardly so. This proposes that when the mean of processes shifts just slightly to the left or to the right, an important output quantity will surpass one of the limits of specification. This process should be observed carefully for detecting the movements from mean. The control charts are brilliant way for doing this.

State III:

The spread of process is more than the specification range, Fig.1.stateIII

Where:

$$6\sigma > (USL - LSL)$$

I

f the process of process is larger than the range of specification, this process isn't capable of satisfying the specifications irrespective of where the mean or center of process is situated. That's really a sorry state, often this takes place, and the responsible people aren't even conscious of it.

The over process modification is one result, leading to even more variability; the substitutes comprise [1]:

- Varying the process to a high dependable technique or investigating the process cautiously in a try to decrease the variability of process.
- Living with the present process and sorting (100%) of products.
- Re-centering the process for minimizing the whole losses outside the limits of specification.
- Ending the process and getting out of such business.

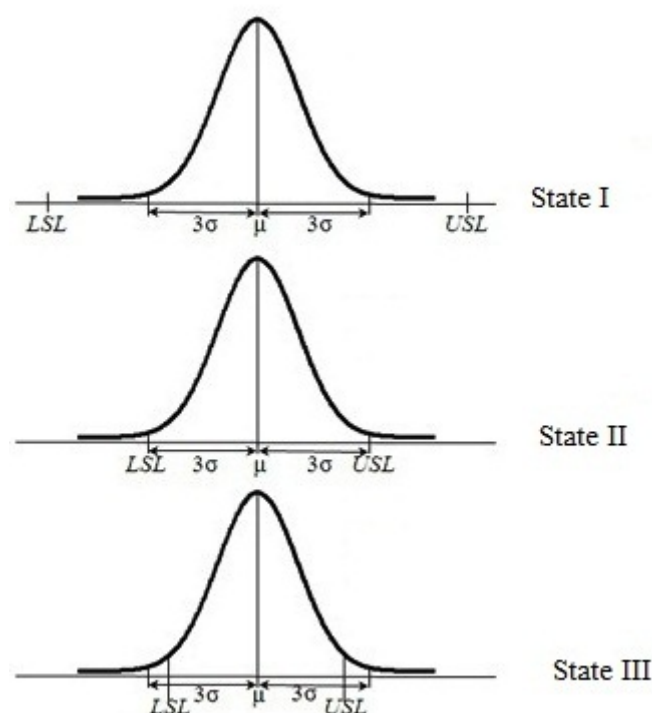


Figure1. States of process capability

3. Capability Indices

These are simple measures for rapidly describing the relation between process variability and the specification limits spread.

Similar to numerous simple measures, like the stages (A), (B), (C), (D), and (F) in university, the capability indices don't totally define what is taking place with the process.

They're beneficial if the assumptions for utilizing them are satisfied for comparing the capabilities of processes.

Capability indices (C_p , C_{pu} , C_{pl} , C_{pk} , and C_{pm})

The term of the simple capability index (C_p) is the ratio of the spread of specification to the spread of process; the last is characterized via (6) standard deviations or (6σ).

$$C_p = \frac{USL - LSL}{6\sigma}$$

Where:

$100(1/C_p)$ is construed as the specifications' width percentage utilized via process.

The earlier (C_p) equation assumes that the process possesses both the upper and the lower limits of specification. Nevertheless, numerous applied cases can offer merely a single limit of specification. In such situation, the one-sided (C_p) is described via [6]:

$$C_{pu} = \frac{USL - \mu}{3\sigma} \quad (\text{Upper specification only})$$

$$C_{pl} = \frac{\mu - LSL}{3\sigma} \quad (\text{Lower specification only})$$

One can notice that the (C_p) measures the centered process capability. But, the whole processes aren't essentially be usually centered at the nominal dimension, that means, the processes may also go off-center, then the real capability of processes that are non-centered will be lower than that directed via (C_p). In a situation if the process is going off-center, the process capability being measured via the pursuing ratio (Process Capability Index C_{pk}):

$$C_{pk} = \min [C_{pu}, C_{pl}]$$

$$C_{pk} = \min \left[\frac{USL - \mu}{3\sigma}, \frac{\mu - LSL}{3\sigma} \right]$$

- 1) If ($C_{pk} = C_p$), at that point this process is centered at the specifications midpoint.
- 2) If ($C_{pk} < C_p$), at that point this process is going off-center.
- 3) If ($C_{pk} = 0$), the mean of process is precisely equivalent to one of specification limits.
- 4) If ($C_{pk} < 0$), then the process mean locates outside the specification limits.
- 5) If ($C_{pk} < -1$), then the whole process locates outside the specification limits.

Sometimes, one has two production processes with different means and standard deviations, but they have the same value of specification limits and C_{pk} , as shown in Table1.

Table 1: Two production processes different means and standard deviations

Process	A	B
Mean	50.0 cN	57.5 cN
Standard deviation	5.0 cN	2.5 cN
Specification limits	35cN, 65cN	35cN, 65cN
C_p	1	2
C_{pk}	1	1

The way for addressing such difficulty is to employ the ratio of process capability, which is a better centering indicator. One such modified being [6]:

$$C_{pm} = \frac{USL - LSL}{6\tau}$$

Where:

T is the square root of the anticipated squared deviation from the target (T).

$$T = \frac{1}{2} (USL + LSL)$$

Then:

$$\tau^2 = \sigma^2 + (\mu - T)^2$$

$$C_{pm} = \frac{USL - LSL}{6\sqrt{\sigma^2 + (\mu - T)^2}}$$

$$C_{pm} = (USL - LSL) / 6\sigma \sqrt{1 + \left[\frac{\mu - T}{\sigma}\right]^2}$$

$$C_{pm} = C_p / \sqrt{1 + \left[(\mu - T) / \sigma\right]^2}$$

4. Moving Averages Control Charts

The (X) and (R) charts track the processes' performance that possesses lengthy runs of production or reiterated services, but occasionally there may be inadequate no. of sample measurements for creating the conventional (X) and (R) charts, for instant, just a single sample may be taken from a process. Instead of plotting every individual reading, it may be very suitable to implement the moving average and the moving range charts for combining (n) no. of the individual values for creating an average. If taking a fresh individual reading, the oldest value that forms the preceding average is rejected; the fresh reading being combined with the residual values from the preceding average for forming a fresh average.

That's too familiar in an uninterrupted process of chemical industry, where merely a single reading is likely at a time. Via the combination of the individual values made over time, the moving averages smoothen out the variations of short term and offer the trends in data, for such cause, moving average charts being often utilized for the seasonal outputs. The control limits of the moving average charts are the same of the traditional (X) and (R) charts, as follow:

$$\bar{\bar{X}} = \frac{\sum \bar{X}}{g}$$

$$\bar{R} = \frac{\sum R}{g}$$

$$UCL_X = \bar{\bar{X}} + A_2 \bar{R}$$

$$LCL_X = \bar{\bar{X}} - A_2 \bar{R}$$

$$UCL_R = D_4 \bar{R}$$

$$LCL_R = D_3 \bar{R}$$

Where:

g: Number of \bar{X}_i readings

5. Total Percentage outside the Specifications

For the purpose of determining the percentage of defects outside the upper and lower limit of standard, the value of (Z) must be determined for them as follows:

$$Z_{USL} = (USL - \bar{\bar{X}}) / \sigma$$

$$Z_{LSL} = (\bar{\bar{X}} - LSL) / \sigma$$

After determining the value of Z_{USL} and Z_{LSL} , the (Z-score) table is used to determine the percentage of defects outside the upper and lower limits of the standard.

6. Sections Produced in the Company

Arab Aluminum Industry Co. Ltd. (ARAL) was established in 1976, it was founded to achieve a fully integrated aluminum extrusion industry.

The ARAL features of the extensive fabricating facilities include:

- 1- A die-making plant and die-correction shop
- 2- A billet casting plant
- 3- Four hydraulic presses ranging from (640) to (2000) tons, with billet diameters ranging from (4) to (8) inches.
- 4- Two complete anodizing lines equipped with 72000 and 42000 amps rectifiers.
- 5- Two horizontal electrostatic paint lines.
- 6- A poly urethane thermal "Fill Lines".

The production facilities and manufacturing processes are shown in Table 2, and the different types of profiles that produced in this company are depicted in Fig. 2.

Table 2: Production facilities and manufacturing processes

Stages	Process	Process Description	Quality Inspection
1	Logs Manufacturing	Melting pure aluminum and placing it in a Cryolite bath.	
2	Logs Heating	Heating Logs in a three-heat zone furnace.	
3	Cutting Logs into Billets	Fully automated shear for the required length.	
4	Extrusion of Billets	Pressing billets through a heated die to obtain the required profile.	
5	Measuring Dimensions and Surface Finish.	Making graphite mark over the surface and using micrometer to ensure if it is accepted. If it is not, the die will be sent back to the die correction workshop to correct the error.	Check the dimensions and surface finishing
6	Weighing the Profile	The profile is weighed to ensure if it is accepted. If it is not, the die will be sent back to the die correction workshop to correct the error.	Check the weight
7	Aging for Accepted Profiles	Accepted profiles will be heat treated in the aging furnace for 8-10 hours at 190°C.	
8	Chemical Treatment	After aging, the profile will subject to a chemical treatment in another department	Check the oxide thickness
9	Rejected Profiles Recycling	Rejected profiles will be recycled by means of melting and casting again to take the logs shape.	

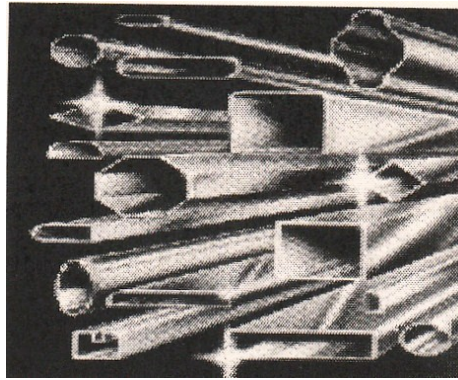


Figure 2: Sections produced in a company

In this study, one of these sections was selected to determine the process capability and quality indices on one of the properties specified in the specification (Weight property), see Fig. 3 and Table 3.

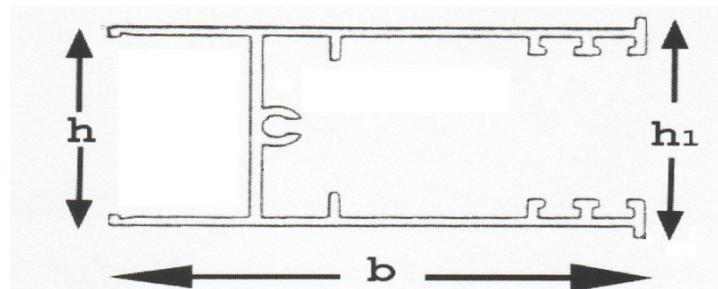


Figure 3: The selected section

Table 3: Specifications of the selected section dimensions

Property Specification	Weight (g/m)	b (mm)	h (mm)	h ₁ (mm)
USL	878	83	37.7	42
LSL	764	70	30	28

Moving average and moving range charts are selected for this purpose, thirty consecutive samples were drawn from the section in Fig.3 at specified intervals, and their dimensions and weights for one meter were recorded, for sample size=1, and $g = 3$, as shown in the Table 4.

Table 4: Subgroups weight and dimensions

Subgroups	Weight (g/m)	Dimensions (mm)			Subgroups	Weight (g/m)	Dimensions (mm)		
		b	h	h ₁			b	h	h ₁
1	790	73.2	34.7	37.5	16	849	79.8	34.2	36.8
2	787	70.1	33.9	38.9	17	790	70.5	35.5	41.6
3	820	78.3	35.4	39.1	18	813	84.2	36.4	39.1
4	843	79.5	32.7	37.8	19	834	78.0	37.1	40.3
5	85.1	80.2	36.4	39.7	20	773	81.7	32.3	35.5
6	796	72.3	33.5	38.6	21	851	86.2	37.3	41.8
7	868	84.1	35.1	40.2	22	880	82.5	37.1	41.3
8	805	71.6	35.8	37.4	23	805	74.1	36.0	38.7
9	813	77.0	35.7	41.0	24	817	69.3	32.9	38.8
10	781	69.3	33.2	36.7	25	795	72.5	35.2	41.2
11	850	78.7	34.1	43.2	26	821	77.4	34.5	35.3
12	810	76.5	33.7	39.8	27	498	75.1	38.0	39.2
13	832	70.4	34.9	37.4	28	817	73.2	33.9	38.8
14	843	77.2	34.7	37.8	29	848	81.3	35.0	40.7
15	821	80.1	35.8	41.0	30	833	76.7	36.7	39.8

The condition of determining the process capability of the production and its quality parameters is that the production process must be under statistical control, to achieve this requirement, quality control charts should be used to ensure or to reach a statistical control of the production process. Calculations for moving average and range control charts are illustrated in Table 5, and then the control limits are calculated as below:

Table 5: Calculated values for the moving average and range control charts

Subgroups	Weight (g/m)	3P Sum (W)	3P AVG (W)	3P Range (W)
1	790			
2	787			
3	820	2397	799	33
4	843	2450	816.67	56
5	851	2514	838	31
6	796	2490	830	55
7	868	2515	838.33	72
8	805	2469	823	72
9	813	2486	828.67	63
10	781	2399	799.67	32
11	850	2444	814.67	69
12	810	2441	813.67	69
13	832	2492	830.67	40
14	843	2485	828.33	33
15	821	2496	832	22
16	849	2513	837.67	28
17	790	2460	820	59
18	813	2452	817.33	59
19	834	2437	812.33	44
20	773	2420	806.67	61
21	851	2458	819.33	78
22	850	2474	824.67	78
23	805	2506	835.33	56

24	817	2472	824	45
25	795	2417	805.67	22
26	821	2433	811	26
27	798	2414	804.67	26
28	817	2436	812	23
29	848	2463	821	50
30	833	2498	832.67	31
		Sum	22977	1333

$$\bar{\bar{X}} = 22977/28$$

$$\bar{\bar{X}} = 820.6 \text{ g/m}$$

$$UCL_x = \bar{\bar{X}} + A_2 \bar{R}$$

$$UCL_x = 820.6 + (1.023 \times 47.6)$$

$$UCL_x = 869.3 \text{ g/m}$$

$$LCL_x = \bar{\bar{X}} - A_2 \bar{R}$$

$$LCL_x = 820.6 - (1.023 \times 47.6)$$

$$LCL_x = 771.9 \text{ g/m}$$

$$\bar{R} = 1333 / 28$$

$$\bar{R} = 47.6 \text{ g/m}$$

$$UCL_R = D_4 \bar{R}$$

$$UCL_R = 2.575 \times 47.6$$

$$UCL_R = 122.57 \text{ g/m}$$

$$LCL_R = D_3 \bar{R}$$

$$LCL_R = 0 \times 47.6$$

$$LCL_R = 0$$

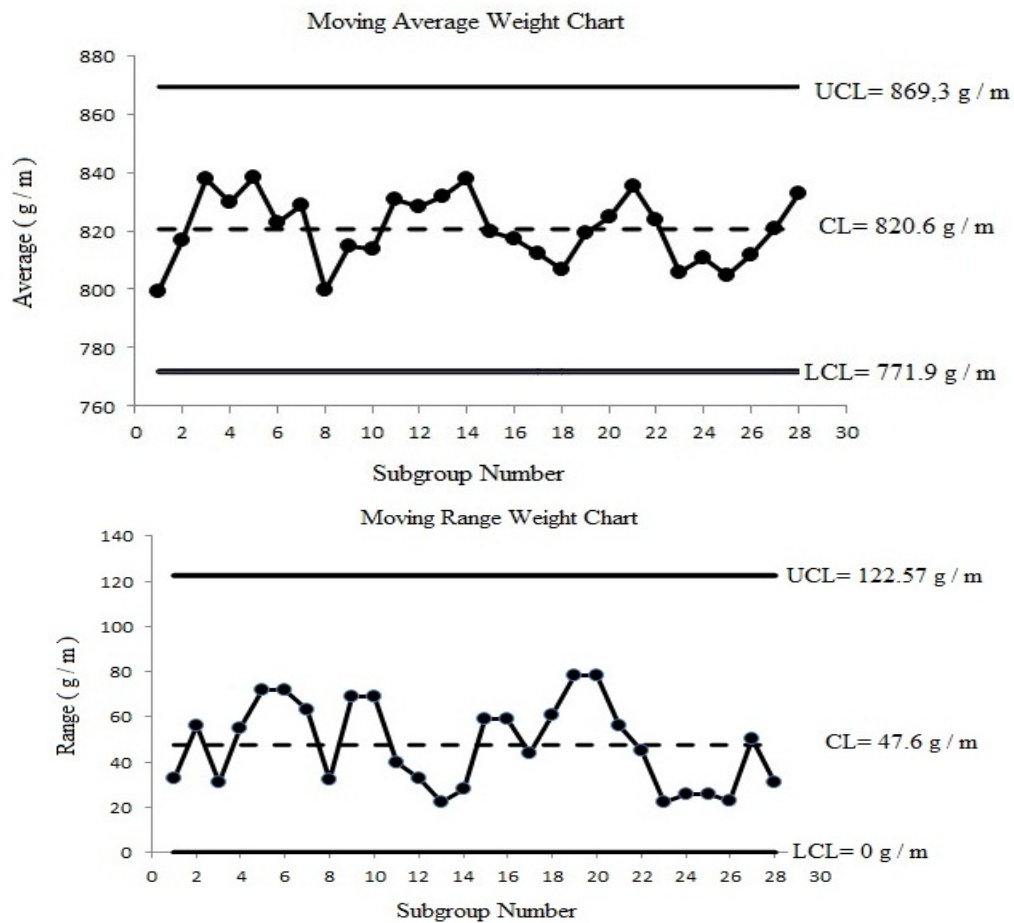


Figure4. Moving average and moving range control charts for profile ABS115 weight

From moving average and moving range control charts for profile ABS115 weight in Fig.4, it is clear that the production process is statistically controlled and there is no indication of the existence of assignable causes, thus one can determine the process capability and indices.

7. Process capability and indices for the weight of profile ABS115

The specification limits are $USL = 878 \text{ g/m}$ and $LSL = 764 \text{ g/m}$.

From this specification, one can say that the nominal mean value of process (T) is:

$$T = \frac{USL + LSL}{2}$$

$$T = (878 + 764) / 2$$

$$T = 821 \text{ g/m}$$

Now, the estimation of process standard deviation (σ) can be calculated:

$$\sigma = \frac{\bar{R}}{d_2}$$

d_2 = Constant for the variable control charts depending on a sample size.

$$\sigma = \frac{47.6}{1.693}$$

$$\sigma = 28.11 \text{ g/m}$$

$$6\sigma = 6 \times 28.11$$

$$6\sigma = 168.66 \text{ g/m}$$

$$C_p = \frac{USL - LSL}{6\sigma}$$

$$C_p = \frac{878 - 764}{168.66}$$

$$C_p = 0.67$$

The specifications' width percentage utilized via the process = $100(1/C_p)$

The specifications' width percentage utilized via the process = $100(1/0.670)$

The specifications' width percentage utilized via the process = 149.25 %

$$C_{pk} = \min \left[\frac{USL - \mu}{3\sigma}, \frac{\mu - LSL}{3\sigma} \right]$$

$$C_{pk} = \min [0.68, 0.66]$$

$$C_{pk} = 0.66$$

$$C_{pm} = C_p / \sqrt{1 + [(\mu - T)/\sigma]^2}$$

$$C_{pm} = 0.67 / \sqrt{1 + [(820.6 - 821)/28.11]^2}$$

$$C_{pm} = 0.67$$

8. Defective Percentage

$$Z_{USL} = \frac{878 - 820.6}{28.11}$$

$$Z_{USL} = 2.04$$

From (Z score) table, the number corresponding to 2.04 is 0.9773, for this:

The percentage of defective outside upper control limit = $1 - 0.9773$

The percentage of defective outside upper control limit = $0.0227 = 2.27\%$

$$Z_{LSL} = \frac{820.6 - 764}{28.11}$$

$$Z_{LSL} = 2.01$$

From (Z score) table, the number corresponding to 2.01 is 0.9778, for this:

The percentage of defective outside lower control limit = $1 - 0.9778$

The percentage of defective outside lower control limit = $0.0222 = 2.22\%$

Total defective percentage = $2.27 + 2.22$

Total defective percentage = 4.49%

9. Conclusion

It was observed that the production process was statistically controlled for the weight of the chosen section, but when measuring the process capability, the result was 0.67; this means that the production process occupies

149% of the standard specified for the weight of the section, for this, not all statistically controlled processes can produce products without defects, but the statistical control means that the production process is free of non-assignable causes and it works under assignable causes only.

It has been shown that the capacity of the capability of process (C_p) is larger than the process capability index (C_{pk}) value by about 0.01; this means the process is running off center, as mentioned before.

The production process goal is $T = 821 \text{ gm/m}$, and the average production process deviates from it by 0.4 gm/m , as its value $\bar{X} = 820.6 \text{ gm/m}$, and this is confirmed by $C_{pk} < C_p$.

It is possible to reduce or eliminate this slight deviation in the process average \bar{X} by shifting its value by 0.4 g/m towards the upper specification limit, but it will cause an increase in the defects percentage outside the upper limit of specification and reduce the defects percentage outside the lower limit of specification.

References

- Bissell (1990). *How reliable is your capability index*. Royal Statistical Society.
- ISO 22514- 4(2016). *Statistical Methods in Process Management-Capability and Performance*: part 4: process capability estimates and performance measures.
- Kaya, I., Kahraman , C., (2011). *Process Capability Analyses with Fuzzy Parameters; Expert Systems with Applications*. An International Journal archive, 38 (9) , 11918-11927.
- Kotz , S., Johnson, N.L., (2002). *Process Capability Indices: A Review*. Journal of Quality Technology, 34, 1-19.
- Montgomery, D.C. (2009). *Statistical Quality Control: A Modern Introduction*. Wiley, New york.
- Mahshid, R. Mansourvar , Z., Hansen, HN.(2018). *Tolerance Analysis in Manufacturing Using Process Capability Ratio with Measurement Uncertainty*, Precision Engineering. 201-210.
- Nelson, L.S. (1999). *The Calculation of Process Capability Indices*. Journal of Quality Technology, 31, 249 - 50.
- Perakis, M., Xekalaki, E. (2004). *A New Method for Constructing Confidence Intervals for the Index Cpm*. Quality and Reliability Engineering International , 20 (7), 651-65.



Eigenvalue of Adjacent Matrix of Zero Divisor Graphs on Rings

Hemati Sherin¹

¹ Department of mathematics, faculty of natural science, Bamyan University, Bamyan, Afghanistan

Abstract

Let R be a commutative ring with identity $1 \neq 0$ and T be the ring of all $n \times n$ upper triangular matrices over R . The zero-divisor graph of T denoted by $\Gamma(T_n(R))$. In this paper, I define the adjacent Matrix of $\Gamma(R)$ and $\Gamma(T_n(R))$. Then I describe the relation between the non-zero Eigenvalues of adjacent Matrix of these graph and edges. After I use these result to determination of Eigenvalue adjacent matrix of $\Gamma(T_2(R))$.

Keywords: Eigenvalue, Adjacency Matrix, Zero Divisors Graph of Commutative Ring

1. INTRODUCTION

A graph is described by its adjacency matrix and we can analyses different problem with count its eigenvalue and other properties. Adjacent Matrix of a graph were first defined by Harary (Harary 1962). Jorgensen characterized the parameter sets for all directed strongly regular graphs with adjacent matrix of rank 3 or 4 (Jørgensen 2005).

Let R be a commutative ring with identity $1 \neq 0$ and $ZD(R)$ denote the set of zero-divisors of R . The zero-divisor graph of R , denoted $\Gamma(R)$, is the undirected graph. There is an edge in $\Gamma(R)$ between the vertices r and s if and only if $rs = 0$. Using the language of graph theory, the set of vertices of $\Gamma(R)$ is $V(\Gamma(R)) = ZD(R)$ and the set of edges of $\Gamma(R)$ is $E(\Gamma(R)) = \{(r, s) \mid rs = 0\}$.

Zero-divisor graphs were first defined for commutative rings by Beck (Beck 1988) when the coloring of graphs was studied, and later redefined by Anderson and Livingston (Anderson and Naseer 1993). Redmond (Redmond 2002) introduced the concept of the zero-divisor graph for a non-commutative ring R . Bapat describe the relation between the distinct Eigenvalues of adjacent Matrix a graph and its diameter (Bapat 2010). In this paper I introduced the relation between Eigenvalue and numbers of edges graph $\Gamma(R)$. Further extend result to graph $\Gamma(T_2(R))$.

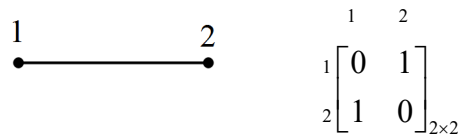
2. Eigenvalue of the adjacent matrix of zero divisor graph on commutative ring

I start with some examples from reference (Anderson and Livingston 1999) motivate next result.

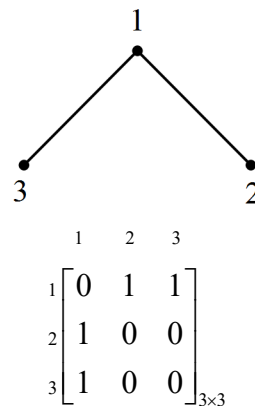
Example 2.1. (a) Assume ring R is $R = \frac{Z_2[x]}{\langle x^2 \rangle}$ or non-isomorphic rings R . Then $ZD(R) = \{\bar{0}, \bar{x}\}$ and

$\Gamma(R)$ has one vertex, adjacent matrix of $\Gamma(R)$ is $\begin{bmatrix} 0 \\ 1 \end{bmatrix}$.

(b) Assume ring R is $R = \frac{Z_3[x]}{\langle x^2 \rangle}$ or non-isomorphic rings R . then $ZD(R) = \{\bar{0}, \bar{x}, 2\bar{x}\}$ and $\Gamma(R)$, adjacent matrix of $\Gamma(R)$ is the follow.

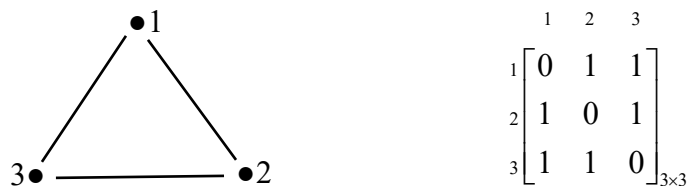


(c) Assume ring R is $R = \frac{Z_2[x]}{\langle x^3 \rangle}$ or non-isomorphic rings R . then $ZD(R) = \{\bar{0}, \bar{x}, \bar{x}^2, \overline{x+x^2}\}$ and $\Gamma(R)$, adjacent matrix of $\Gamma(R)$ is the follow.



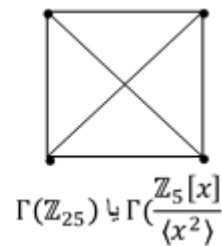
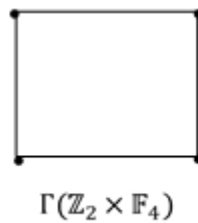
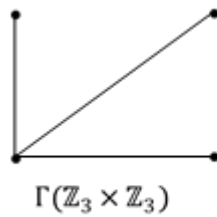
(c) Assume ring R is $R = \frac{Z_2[x, y]}{\langle x^2, xy, y^2 \rangle}$, $R = \frac{F_4[x]}{\langle x^2 \rangle}$ or non-isomorphic rings R . then

$ZD(R) = \{\bar{0}, \bar{x}, \bar{y}, \overline{x+y}\}$ or $ZD(R) = \{\bar{0}, \bar{x}, \overline{a_1x}, \overline{a_2x} / a_1, a_2 \in F_4\}$ and $\Gamma(R)$, adjacent matrix of $\Gamma(R)$ is the follow.



By part (a), (b), (c) all connected graphs with less than four vertices may be realized as $\Gamma(R)$. Of the eleven graphs with four vertices, only six are connected. Of these six, only the following three graphs may be realized

as $\Gamma(R)$.



We can easily proof that the $\Gamma(R)$ can be a triangle or a square. But, $\Gamma(R)$ cannot be an n -gon for any $n \geq 5$.

Lemma 2.2. Let R be a commutative ring with identity and $\Gamma(R)$ is zero divisor graph of ring R with number of vertices $n \leq 3$ and non-cyclic, then its non-zero Eigenvalue of adjacent matrix is equal square root numbers of edges.

Proof. If graph has one vertex, then result is clear. If graph has two vertices, then

$$|A - \lambda I| = 0 \Rightarrow \begin{vmatrix} 0 & 1 \\ 1 & 0 \end{vmatrix} - \lambda \begin{vmatrix} 1 & 0 \\ 0 & 1 \end{vmatrix} = \begin{vmatrix} -\lambda & 1 \\ 1 & -\lambda \end{vmatrix} = \lambda^2 - 1 = 0 \Rightarrow \lambda = \pm\sqrt{1}.$$

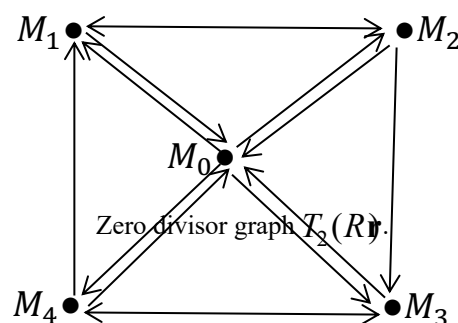
If graph has three vertices, then

$$|A - \lambda I| = 0 \Rightarrow \begin{vmatrix} 0 & 1 & 1 \\ 1 & 0 & 0 \\ 1 & 0 & 0 \end{vmatrix} - \lambda \begin{vmatrix} 1 & 0 & 0 \\ 0 & 1 & 0 \\ 0 & 0 & 1 \end{vmatrix} = 0 \Rightarrow \begin{vmatrix} -\lambda & 1 & 1 \\ 1 & -\lambda & 0 \\ 1 & 0 & -\lambda \end{vmatrix} = 0 \Rightarrow \lambda = \pm\sqrt{2}. \quad \square$$

3. Eigenvalue of the adjacent matrix of zero divisor graph on triangular matrix ring

At first by use reference (Li and Tucci 2013), we study zero divisor graph of $T_2(R)$. in general, every element

of $T_2(R)$ will be denoted $\begin{bmatrix} x_1 & x_2 \\ 0 & x_3 \end{bmatrix}$ where each $x_j \in R$.



And adjacent matrix of $T_2(R)$ is follow that:

$$A(T_2(R)) = \begin{matrix} & \begin{matrix} M_0 & M_1 & M_2 & M_3 & M_4 \end{matrix} \\ \begin{matrix} M_0 \\ M_1 \\ M_2 \\ M_3 \\ M_4 \end{matrix} & \begin{bmatrix} 0 & 1 & 1 & 1 & 1 \\ 1 & 0 & 1 & 0 & 1 \\ 1 & 1 & 0 & 1 & 0 \\ 1 & 0 & 1 & 0 & 1 \\ 1 & 1 & 0 & 1 & 0 \end{bmatrix} \end{matrix}_{5 \times 5}$$

Theorem 3.1. Let $\Gamma(T_2(R))$ be zero divisor graph of triangular matrices 2×2 . Then Eigenvalue of the adjacent matrix this graph are 1 with multiplicity 1 and -2, 0 with multiplicity 2.

Proof. By the properties of determinant, rank this matrix is not 5 or 4. Now we study determinant matrix 3×3 .

$$\begin{vmatrix} 0 & 1 & 1 \\ 1 & 0 & 1 \\ 1 & 0 & 0 \end{vmatrix} = (-1)^{1+2} (1) \begin{vmatrix} 1 & 1 \\ 1 & 0 \end{vmatrix} = -[(0-1)] = 1.$$

So rank $A(T_2(R)) = 3$. Therefore this matrix has 3 non- Eigenvalues. it follows that

$$\Rightarrow \lambda^4 + 3\lambda^3 - 4\lambda = 0 \Rightarrow \lambda_1 = \lambda_2 = 0, \lambda_3 = \lambda_4 = -2 \wedge \lambda_5 = 1.$$

□

4. Conclusion

In conclusion, I define adjacent matrix of $\Gamma(R)$ and study relation between Eigenvalue and numbers of edges this graph. I will show that $\Gamma(R)$ with numbers of vertices $n \leq 3$ and non-cyclic, its non-zero Eigenvalue of adjacent matrix is equal square root numbers of edges. Further extend result to determination of Eigenvalue adjacent matrix of $\Gamma(T_2(R))$.

References

- Anderson, David F, and Philip S Livingston. 1999. "The zero-divisor graph of a commutative ring." *Journal of algebra* 217 (2):434-447.
- Anderson, DD, and M Naseer. 1993. "Beck's coloring of a commutative ring." *Journal of algebra* 159 (2):500-514.
- Anderson, David F. 2008. "On the diameter and girth of a zero-divisor graph, II." *Houston journal of mathematics* 34 (2):361-372.
- Bapat, Ravindra B. 2010. *Graphs and matrices*. Vol. 27: Springer.
- Beck, Istvan. 1988. "Coloring of commutative rings." *Journal of algebra* 116 (1):208-226.
- Harary, Frank. 1962. "The determinant of the adjacency matrix of a graph." *Siam Review* 4 (3):202-210.
- Jørgensen, Leif K. 2005. "Rank of adjacency matrices of directed (strongly) regular graphs." *Linear algebra and its applications* 407:233-241.
- Li, Aihua, and Ralph P Tucci. 2013. "Zero divisor graphs of upper triangular matrix rings." *Communications in Algebra* 41 (12):4622-4636.
- Li, B. 2011. "Zero-divisor graph of triangular matrix rings over commutative rings." *Int. J. Algebra* 5:255-260.
- Redmond, Shane P. 2002. "The zero-divisor graph of a non-commutative ring." *Internat. J. Commutative Rings*. v1 i4:203-211.



Comparative Study of Water Quality From Boreholes and Hand-Dug Wells: Case of Namatapa in Bangwe Township

Jabulani Matsimbe¹

¹ Department of Mining Engineering, Faculty of Engineering, The Polytechnic, University of Malawi, Blantyre, Malawi. Email: jmatimbe@poly.ac.mw

Abstract

Access to safe drinking water is a major problem in Malawi. Residents in Bangwe Township use water from boreholes and hand-dug wells for consumption. The question that arises is how safe is this water. Present study seeks to comparatively assess water quality from boreholes and hand-dug wells located at Namatapa, Bangwe Township. Water samples from two boreholes at 1 km apart and two hand-dug wells at 1.1 km apart were analysed for physicochemical and biological parameters using recommended methods. Sampling was done in the wet season over a period of three months. Results showed that coliforms exceeded the recommended guideline values for drinking water according to World Health Organisation and Malawi Bureau of standards. Values in excess of 462 cfu/100 ml and 10 cfu/100ml were observed in hand-dug wells and boreholes respectively. Suspended solids, Turbidity, pH, Nitrate and Total dissolved solids were all within the acceptable limits. The study results demystify the community belief that borehole water is always safer than hand-dug well water. Therefore, there is a need for authorities to provide portable water in the area so that residents should stop consuming untreated water from boreholes and hand-dug wells.

Keywords: Coliforms, Groundwater, Malawi, Physicochemical

1. Introduction

Access to portable water sources in rural and urban areas remains a serious challenge in many developing countries like Malawi (Mtewa et al. 2018). Water quality research done on communally shared water points in Lilaka, Mvula, Chikunda, Namiyango and Ntopwa of Bangwe township has shown that water from boreholes and wells exceeds the recommended guideline values for drinking water according to World Health Organisation, Malawi Bureau of standards and Ministry of Water development (Kaonga et al. 2013; Mtewa et al. 2018; Mkandawire T & Banda E 2009). There is no literature on the water quality of borehole and hand-dug well in Namatapa area, Bangwe Township. In addition, residents in the area think boreholes are a source of portable water as compared to hand-dug wells. Consumption of poor quality water majorly threatens the health of millions of people worldwide (Adekunle et al., 2007). Kalua and Chipeta (2005) reported that in Malawi, nearly 50% of all illnesses are related to waterborne diseases. From 2004 to 2005 and November 2007 to December 2007 Bangwe clinic registered 263 and 85 cholera cases, respectively, which was the highest level recorded by both peri-urban and rural clinics in Blantyre (Kaonga et al. 2013). Groundwater accounts for about 88% safe drinking water in rural areas where there is widely dispersed population and water treatment infrastructure and transportation does not exist (Alexander, 2008). Present study seeks to comparatively assess the water quality of

boreholes and hand-dug wells in Namatapa area. It is hoped that the output of this study will help update the water quality database on some overlooked areas like Namatapa in Bangwe Township (Figure 1, 2 and 3).

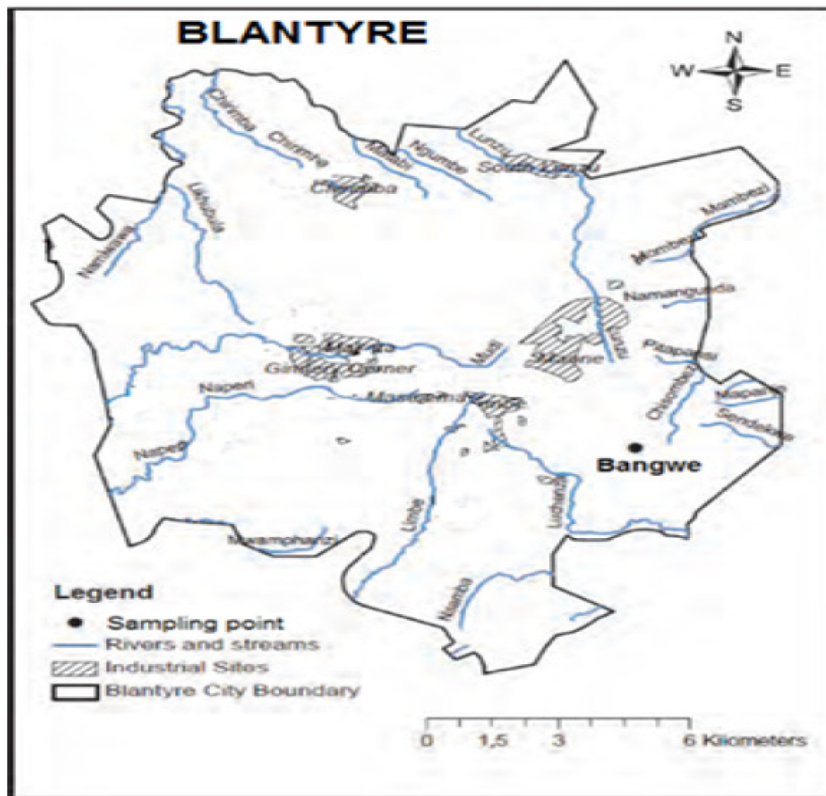


Figure 1. Map of Bangwe Township showing location of Namatapa area



Figure 2. Borehole #1 and #2



Figure 3. Hand-dug well #1 and #2

2. Materials and Methods

Study Area

Namatapa lies on Latitude -15.822806° and Longitude 35.074804° . Within its vicinity is Namatapa primary school, Namatapa youth centre, Namatapa market, Jannat Mosque and Pentecost church. Borehole #1 and Well #1 is located close to Namatapa primary school while Borehole #2 and Well #2 are located close to Jannat Masjid Mosque (Figure 4). The area is of particular importance due to availability of essential services whose users consume water from the boreholes and wells.

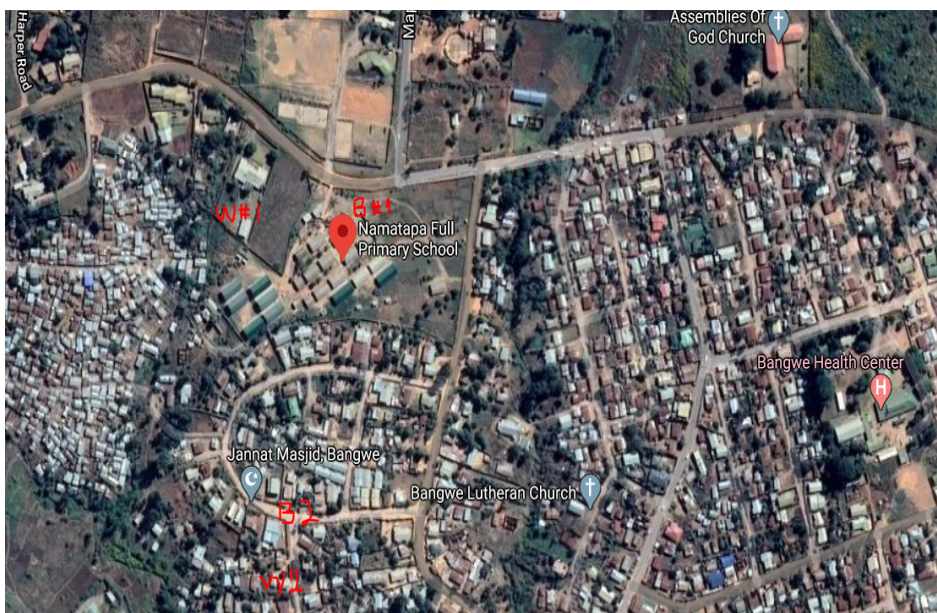


Figure 4. Satellite view of Namatapa area, Bangwe Township (Google Earth, 2020)

Sampling

Borehole and hand-dug well water samples were taken in sterile containers from two different locations around and within Namatapa. Water samples (in triplicates) were taken in the wet season (November 2019, December 2019, January 2020) so as to balance seasonal water quality patterns that might vary on localities.

Samples were transported to the Quality Control Laboratory at The Polytechnic for immediate analyses in accordance with standardized methods (APHA, 2017; WHO, 2011). All laboratory analyses were started on the

same day of sample collection. For each of the chemical parameters, 10 ml of the sample was dispensed into the cuvettes and the corresponding chemical reagents added (in accordance with the manufacturer's specification). Corresponding measurements were read-off the LCD display. The turbidity, pH and total dissolved solids were measured using the Hanna microprocessor turbidity meter, Beckman 350 pH meter and HM digital TDS meter, respectively. Filtering and weighing was done for suspended solids. The coliform and *Escherichia coli* counts were enumerated using the colilert-18 microbiological test kit (Membrane Filtration Technique). Calibration on all equipment was done according to the manufacturer's instructions.

3. Results and discussion

The results are expressed as mean \pm standard deviation, $n=3$. Table 2 shows the mean and standard deviation of borehole and hand-dug well water samples obtained from various locations around and within Namatapa area. The samples were tested for physicochemical and microbiological parameters compared with those recommended by Ministry of Water Development (MWD), Malawi Bureau of Standards (MBS), and World Health Organization (WHO).

The values of suspended solids for borehole and hand-dug well ranged from 0 -1 mg/l thus within those recommended by MWD, MBS and WHO [$<30\text{mg/l}$]. The low values in suspended solids could be due to the fact that all the water sources are covered. Turbidity values for borehole #1 [0.18 NTU], borehole #2 [0 NTU] and well #2 [2.44 NTU] except for well #1 [11.13 NTU] were within the recommended values of MWD, MBS, WHO [25 NTU, 5 NTU, 5 NTU respectively]. According to Inanc et al. 1998, surface runoff and storm water from rainfall can transport pollutants from the surfaces into underground aquifers thereby increasing the turbidity. Table 2 and Figure 5 shows that the pH values for borehole #1 [6.4], borehole #2 [6.16], well #2 [6.82] and well #1 [6.85] were within the recommended ranges of MWD, MBS, WHO [6.0 - 9.5, 6.5 - 9.5, 6.5 - 8.5 respectively]. The pH variations for well and borehole water could be due to solvation of organic matter in the soil matrix surrounding and in contact with the water wells (Mtewa, 2017). The Nitrate levels [0 – 0.5 mg/l] and Total dissolved levels as shown in Figure 6 [138 – 472 mg/l] for all borehole and well water samples were within the acceptable levels of MWD, MBS and WHO.

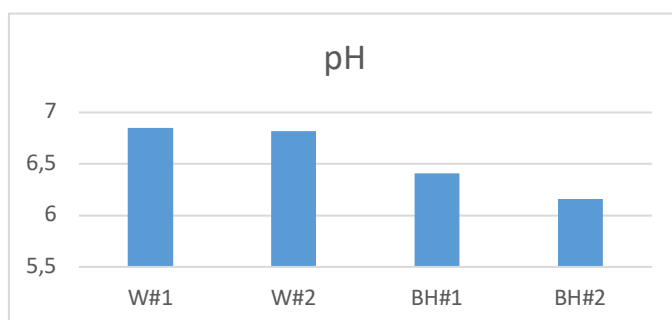


Figure 5. pH values for hand-dug well (W#1 & W#2) and borehole (BH#1 & BH#2)

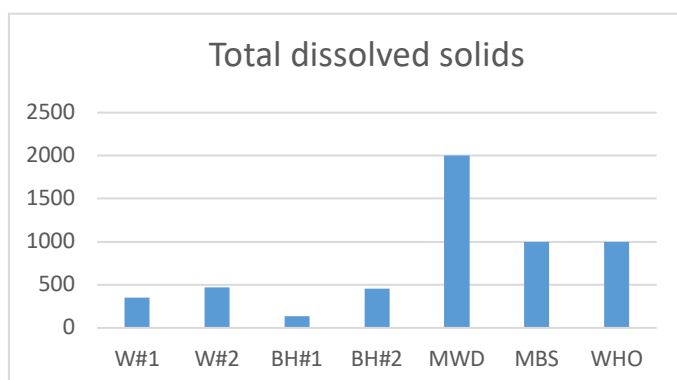


Figure 6. Total dissolved solid values for hand-dug well (W#1 & W#2) and borehole (BH#1 & BH#2) compared to MWD, MBS & WHO

Figure 7 shows that the faecal coliform values for borehole #1 [6 cfu/100ml], borehole #2 [5.7 cfu/100ml] except for well #1 [403 cfu/100ml] and well #2 [70 cfu/100ml] were within the recommended ranges for MWD [50 cfu/100ml]. Figure 8 shows that the total coliform values for borehole #2 [8.3 cfu/100ml], borehole #1 [10 cfu/100ml] except for well #1 [462 cfu/100ml] and well #2 [95 cfu/100ml] were within the recommended ranges for MWD [50 cfu/100ml].

All water samples exceeded the acceptable faecal and total coliform limit recommended by MBS and WHO [0 cfu/100ml]. Since water quality acceptable limits are based on MBS and WHO standards, the borehole and hand-dug well water is not safe for consumption without further treatment. Kaonga et al. 2013 found that faecal contamination is one of the causes of diarrhoea pathogens in less developed countries. According to Efe (2008), the longer water travels through soil formation the cleaner it becomes; this could account for the lower water quality values of borehole water which is at higher depth than well water.

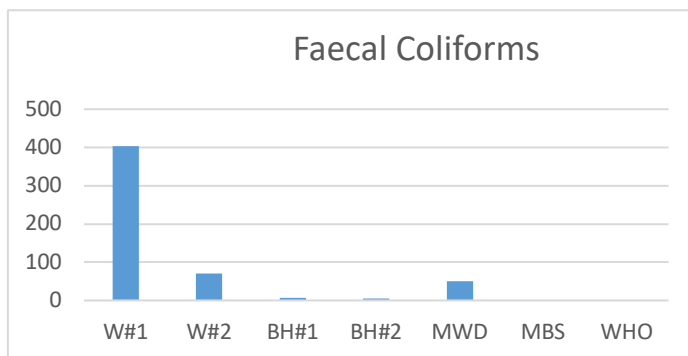


Figure 7. Faecal coliform values for hand-dug well (W#1 & W#2) and borehole (BH#1 & BH#2) compared to MWD, MBS & WHO

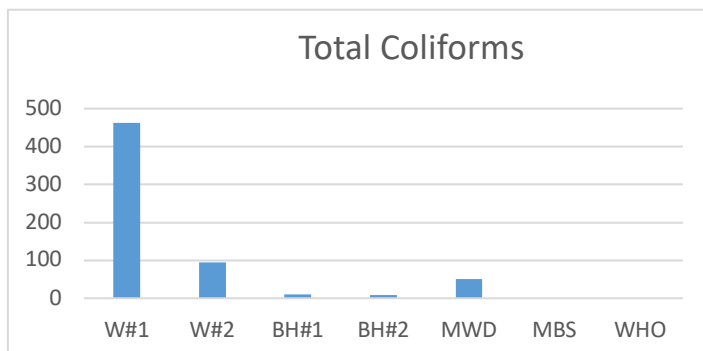


Figure 8. Total coliform values for hand-dug well (W#1 & W#2) and borehole (BH#1 & BH#2) compared to MWD, MBS & WHO

Table 2: Mean \pm standard deviation of water quality parameters

Parameter	Units	Sample Site For Well		Sample Site For Borehole		MWD	MBS	WHO
		W#1	W#2	BH#1	BH#2			
Suspended Solids	mg/l	1 \pm 1.00	0 \pm 0.00	0 \pm 0.00	0.3 \pm 0.58	30	30	30
Turbidity	NTU	11.13 \pm 5.18	2.44 \pm 1.98	0.18 \pm 0.31	0 \pm 0.00	25	5	5
pH	pH units	6.85 \pm 0.09	6.82 \pm 0.04	6.41 \pm 0.08	6.16 \pm 0.04	6.0-9.5	6.5-9.5	6.5-8.5
Nitrate	mg/l	0.12 \pm 0.01	0.079 \pm 0.03	0.076 \pm 0.04	0.48 \pm 0.40	100	100	45
Total dissolved solids	mg/l	349.2 \pm 4.10	471.5 \pm 8.91	138.2 \pm 7.26	454.9 \pm 5.50	2000	1000	1000
Faecal coliforms	cfu/100 ml	403 \pm 6.41	70 \pm 5.13	6 \pm 2.1	5.7 \pm 1.6	50	0	0
Total coliforms	cfu/100 ml	462 \pm 6.56	95 \pm 5.03	10 \pm 1.3	8.3 \pm 2.4	50	0	0

*cfu: colony forming units.

Random interviews on 20 Namatapa residents showed that 80% of the residents boil the water before consumption while 20% consume the water directly as it appears clean to the eye. It is considered that the process of heating water to a rolling boil, as recommended in the WHO Guidelines for Drinking-water Quality (WHO, 2011), is sufficient to inactivate pathogenic bacteria, viruses and protozoa.

4. Conclusion and recommendations

Many households in Malawi rely on groundwater supplies such as boreholes and hand-dug wells. This study reveals the need to sensitise borehole and well owners about the water quality from these sources as there is a general belief that boreholes are better and safer than hand-dug wells. Meanwhile, depth of water source is considered to be an important factor as most of the parameters that had lower mean values were from borehole samples which are usually deeper than hand-dug wells. Nevertheless, the borehole and hand-dug well water is not safe for consumption as it does not meet the standards recommended by MWD, MBS and WHO.

Conflict of Interest

The author has not declared any conflict of interests.

Acknowledgements

The author would like to thank University of Malawi, The Polytechnic for supporting the research.

References

- Adekunle IM, Adetunji MT, Gbadebo AM, Banjoko OB (2007). Assessment of Groundwater quality in a typical rural settlement in southeast Nigeria. *International Journal of Environmental Research and Public Health* 4(4):307-318.
- Alexander P. (2008). Evaluation of ground water quality of Mubi town in Adamawa State, Nigeria. *Afr. J. Biotechnol.* 7:1712-1715.
- American Public Health Association (APHA) (2017). *Standard methods for the examination of water and wastewater* (23rd Edition), APHA, ISBN 0875532233, Washington DC.
- Efe S. I. (2008). Quality of water from hand-dug wells in Onitsha metropolitan area. *J. Environ. Sci.* 6(23):5-12.
- Inanc B., Kinaci C., Sevimli M. F., Arikan O. & Ozturk M. (1998). Pollution prevention and restoration in the Golden Horn of Istanbul. *Water Sci. Technol.* 37(8):137-144.
- Kalua PWR, Chipeta WPC (2005). 'A Situation Analysis of Water Sector in Malawi.' A paper presented at the workshop on Situation Analysis of Water Sector in Malawi.
- Kaonga C, Kambala C, Mwendera C, Mkandawire T (2013). Water quality assessment in Bangwe Township, Blantyre City, Malawi. *African Journal of Environmental Science and Technology*, DOI: 10.5897/AJEST12.196
- Malawi Bureau of Standards (2005). *Malawi standard; drinking water – specification*. Malawi Standards Board, MS 214:2005.
- Malawi Government (2005). *Ministry of water development and irrigation, National Water Policy*. Lilongwe: Ministry of Irrigation and Water Development
- Mtewa AGK (2017). Antibacterial potency stability, pH and phytochemistry of some Malawian ready-to-serve aqueous herbal formulations used against enteric diseases. *International Journal of Herbal Medicine* 5(3):01-05.
- Mtewa T, Chauluka F, Mtewa A, Banda L, Kalindekaffe L (2018). Water quality assessment of various sources in Periurban areas of Malawi: A case of Bangwe township in Blantyre. *African Journal of Environmental Science and Technology*, DOI: 10.5897/AJEST2018.254
- WHO (2011). *Guidelines for drinking-water quality*, fourth edition. Geneva: World Health Organization (http://www.who.int/water_sanitation_health/publications/2011/dwq_guidelines/en/, accessed 13 August 2020).
- Mkandawire T, Banda E (2009). Assessment of drinking water quality of Mtopwa village in Bangwe Township, Blantyre. *Journal of Desalination*, DOI: 10.1016/j.desal.2008.05.101

Becoming Incomplete House: the Environmental Implication of the Traditional Balinese House Transformation in Tourism Area

I Dewa Gede Agung Diasana Putra¹

¹ Department of Architecture, Faculty of Engineering, Udayana University, Bali, Indonesia

Correspondence: I Dewa Gede Agung Diasana Putra, Department of Architecture, Faculty of Engineering, Udayana University Bali, Indonesia. E-mail: diasanaputra@unud.ac.id

Abstract

The traditional Balinese house in rural areas is designed to optimize the use of available resources, to minimize energy consumption, and to provide spaces for garbage processing and biodiversity. However, the change of rural to become urban areas in tourism areas is an interesting phenomenon. In this phenomenon, the use of house as tourist facilities and the increase of occupants in the house have caused the changes in its physical configurations in which the house becomes an incomplete house since some spaces are transformed into tourist facilities. The increase of its building density also affects many components of the environmental aspects in the house including energy consumption. The aim of this paper is to demonstrate this environmental implication especially energy consumption in the rural-urban interface areas. This aspect in a number of houses transformed for tourist facilities has been investigated through utility meter data collection. Architectural investigation and interviews were then used to consolidate memory and to reconstruct the spatial stories of the house. The transformed houses were selected randomly. This study states that the transformation has affected the use of natural resources in the house. The transformed houses are the owner's attempts to demonstrate the improvement of their social status.

Keywords: Rural-Urban Interface, Traditional Balinese House, Environmental Implication, Transformation

1. Introduction

The traditional Balinese house in rural areas is designed to optimize the use of available resources, to minimize energy consumption, and to provide spaces for garbage processing and biodiversity. However, the change of rural to become urban areas in tourism areas is an interesting phenomenon. In this phenomenon, the use of house as tourist facilities in the house has caused the changes in its physical configurations in which the increase of its building density affects energy consumptions.

The natural environmental conditions, which are closely linked to the culture, are the other factor to consider when creating the forms of the traditional Balinese house. The changes in its physical configurations followed by

the increase of its building density affect many components of the environmental aspects in the house. The aim of this paper is to demonstrate this environmental implication in the rural-urban interface areas. This paper will discuss energy consumption in the transformed houses. This aspect in a number of houses transformed for tourist facilities have been investigated through utility meter data collection. Architectural investigation and interviews were then used to consolidate memory and to reconstruct the spatial stories of the house. The transformed houses were selected randomly. This study states that the transformation has affected the use of natural resources in the house. The transformed houses are the owner's attempts to demonstrate the improvement of their social status.

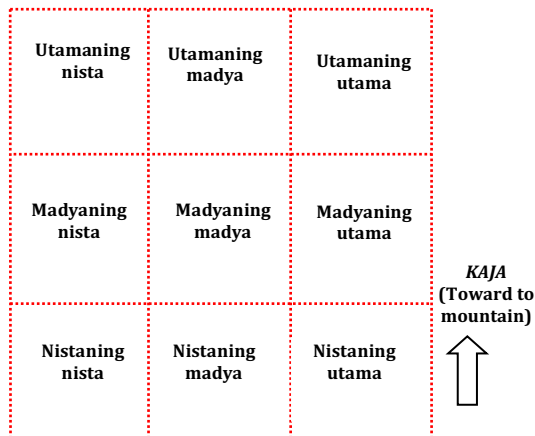
This paper investigates and explores environmental implication in the rural-urban interface areas that has been reconfigured as a response to address the specific challenges of the tourist economy. Initially, however, some theoretical considerations of how traditions in general are transmitted are presented. This is followed by a detailed description of the elements of the traditional Balinese house in relation to environmental implications. In subsequent sections, the paper explores how the implication of tourism activities on environmental conditions of the traditional Balinese house. Some conclusions are presented in the final section.

2. The Configuration of the Traditional Balinese House

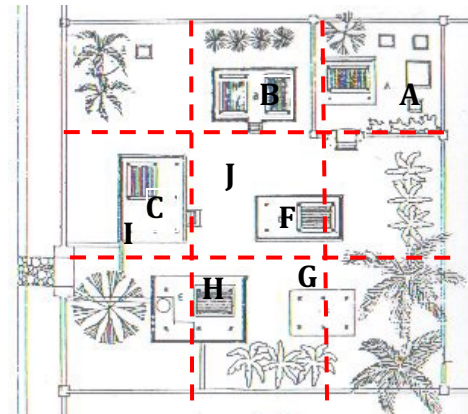
The traditional Balinese house is perceived and interpreted through the religious and spiritual concepts. The head is the most sacred area. In this part, the people build shrines and pavilions in such a way that the spaces are able to accommodate many ceremonial activities dedicated to God and ancestors. The body is the intermediate sphere where the people build many pavilions (*bales*) to accommodate domestic and ceremonial activities. The legs are the *nista* (below) area, also called *lebuh*. The legs consist of a backyard called *teba* and a front part of the house consisting of *telajakan*, wall, *angkul-angkul* and *aling-aling*.

Variety of social status and roles of the owners in their communities influences the variety of the form of the house. Geographical factors and historical events have also produced a diversity of cultural practices, including physical images of the house (Hobart, Ramseyer & Leeman 1996; Geertz 2004). The variety is inspired by the *desa-kala-patra* concept, where a house is built based on the condition of the land and the location, the time and the circumstance. This concept represents a flexibility of the Balinese culture that determines the approach to the construction of the house (Meganada 1990).

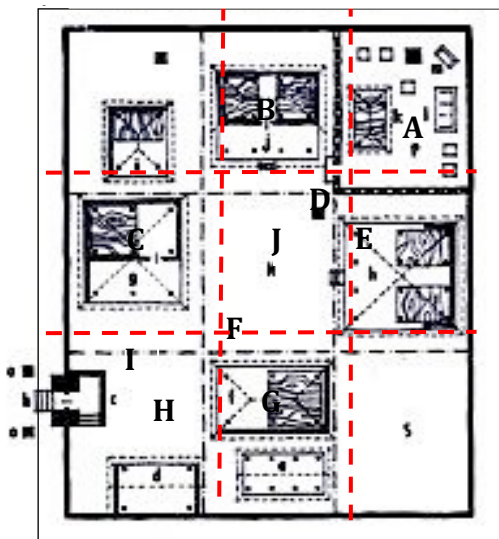
Such variations can be seen in many detailed drawings of the typical traditional house including the drawings by Tan (1967) and Budiardjo (1986), as well as the drawings by local writers such as Gelebet (1986) (Figure 1). However, the formations of the pavilions still represent the implementation of the *sanga mandala* concept, which has been considered as a template and standard record accompanying architectural discussion of Balinese architecture (Figure 3.8A). It can be seen in three example houses that are the result of previous studies. In every house, the family temple (A) is in *utamaning utama* zone, the bale *meten* (B) is in *madyaning utama* zone, and the *bale dauh* (C) is in *madyaning nista* zone. The differences of the pavilions are related to the size of the pavilions. The *bale meten* in House Plan 2 has a veranda, whereas House Plans 1 and 3 do not have a veranda (Figure 1). The variation of the family temples (A) is related to the number of the shrines. The more shrines there are, the wider the family temple. The other difference is the location of the family temple's gate, where the gate is optionally located in the west and south of the family temple wall directly entering to the *natah*. The *natah* located in the middle of the zone (*madyaning madya*) has different shapes because of the differences of the form and setting of the pavilions.



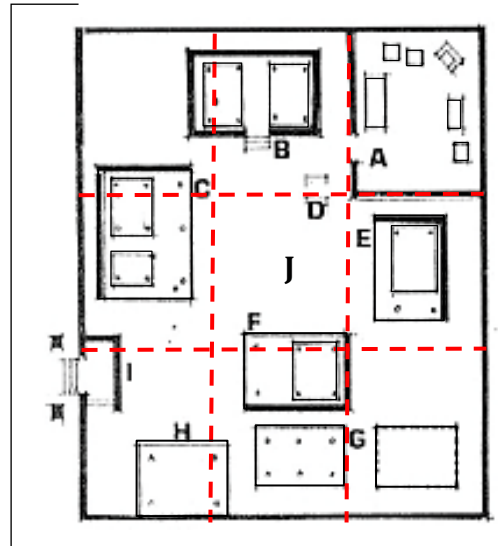
A. Schematic the sanga mandala concept



B. House Plan 1
Source: Gelebet 1986



C. House Plan 2
Source: Tan 1967



D. House Plan 3
Source: Budiharjo 1986

Legend

- | | | |
|---|--|---------------------------------------|
| A. Family temple (<i>merajan</i>) | D. Shrine in the <i>natah</i> | G. Granary (<i>jineng/klumpu</i>) |
| B. Northern pavilion (<i>bale daja</i>) | E. Eastern pavilion (<i>bale dangin</i>) | H. Kitchen (<i>paon/perantenan</i>) |
| C. Western pavilion (<i>bale dauh</i>) | F. <i>sumangen</i> | I. <i>Aling-aling</i> |
| | | J. Courtyard (<i>natah</i>) |

Figure 1: The variation of the traditional Balinese house configurations but still applying the *sanga mandala* concept

3. Human Beings and Natural Relationship in the House

The form of a traditional house differs from place to place and is a complex phenomenon that involves socio-cultural and environmental aspects. The environment, including resources of building materials and differing climates across different regions also play a role in creating forms of architecture (Kostof 1995; Fletcher 1975; Rapoport 1969). The environmental considerations in a built environment are not new in building design. People used this approach and realized that the environment is an important thing in their life. Therefore, they had a responsibility to preserve the natural world and other living things (Lusser 1995). This tradition is based on knowledge in a society and is shared as a local wisdom over generations. The local wisdom is a process of perceiving, thinking, acting and further knowing about the importance of the natural world (Cajete 2000; Nelson 2008).

In the traditional Balinese house, people plant vegetation, including coconut, jackfruit and bamboo, in the backyard called *teba* that provides many materials to support their activities. The coconut tree is used for a roof structure, the trunk of the jackfruit tree for columns called *saka* and the bamboo for rafters and partitions. Such trees are popular in Bali because they have many functions, not only for building materials but also for raw materials of offerings and for the needs of everyday life. The people also plant other trees including banana and many kinds of fruit and flowers in the *teba* so that they are easy to obtain when required. Besides that, the vegetation is seen to beautify the house, and importantly serves to reduce the internal temperature.

Plants have the potential to increase the thermal comfort in order to achieve energy efficiency in warm humid tropical climates including Bali (Trimariantio & Dudek 2011). The shade around the pavilions provided by vegetation reduces the heat from solar radiation that influences the internal temperature of the building (Trimariantio & Dudek 2011). The temperature outside and inside the building is reduced and a cool air motion entering the building creates thermal comfort for the occupants. The leaves of plants filter dusty wind into the building so that they create a healthier condition in the house. The roots of the plant and uncovered land in the *natah* or other spaces between pavilions are potential catchment areas in order to protect the ground water (Vikas 2001).

The abovementioned conditions show that the house has been a self-sustainable, which provides many materials needed by occupants including raw materials for building, daily demands and offerings. Over the last decades, some people change the courtyard when they need more rooms for their family members or obtaining economic benefit. This transformation has reduced biodiversity in the house and therefore, this condition has reduced the people's opportunity to obtain raw materials for building, offerings and daily basic needs in their house easily (Widja 2004). This study focusses on whether this condition occurs in the traditional Balinese house due to the transformation for tourist facilities.

4. Becoming an "Incomplete" House in the Transformation of the Traditional House

The investigation found that the transformation is not restricted to particular parts of the house, such as the potential economic areas including the front of the house. Rather, the transformation has spread to all parts of the house, including the profane areas where people perform domestic activities.

The front wall and the *telajakan* have changed enormously due to tourism development in the villages. Some of them have now vanished or transformed. The other front component of the house is the traditional gate (*angkul-angkul*), which is the visual identity of the house. Even though the house is hidden behind the tourist facilities, the *angkul-angkul* is a sign to recognize the house as a traditional Balinese dwelling. This phenomenon can be seen in Ubud where most traditional gates still exist. From the gates, people can easily identify the presence of a group of traditional houses among the tourist facilities. On the other hand, without the *angkul-angkul*, the presence of the houses is hard to recognize such as most houses in Kuta and Sanur. The entrance of the house is a space between the tourist facilities and from the street, it is hard to recognize the presence of the houses behind those facilities.

Every division has undergone different levels of transformation. This variation is due to each division having different cultural values and functions. The head constituting the most sacred spaces, where God and occupants' ancestors reside, underwent fewer and more limited transformations. Only a few family temples have been relocated to other parts of the house, or elevated to the higher level of a new structure. On the other hand, the expansion and multiplication of new structures has occurred in the body of the house, causing a reduction of open spaces. This increase of new structures for domestic and tourist activities has extended to the legs, the backyard. The backyard, which was a small forest without pavilions, has now become a site for accommodating domestic and tourist facilities. The limitation of space has forced people to live in the most profane areas of the house, which was a place for vegetation, animals and garbage processing, based on traditional guidelines.

From the perspective of the cosmological framework, the body is getting bigger while the legs are getting smaller and, in many cases, have disappeared. The house is likely to become disproportional and even incomplete. The house becomes like a human who still has a head with an enlarged body but without legs or

with very small legs. The traditional house pattern undergoes an ongoing process of the loss of some components, its cultural expression and traditional functions but economically, the house becomes more valuable than it was before the transformation.

However, the main function of the house is still residential with the addition of tourist facilities. In some cases, the economic benefits of tourism have caused the house now to be occupied by more than one family unit so that the number of occupants has increased. They share the spaces in the house to accommodate domestic and religious activities and to gain economic benefits from tourism by constructing new structures in the house. Since the transformations have caused the incompleteness of spaces in the house, the stages on which to perform traditions and maintain the continuity of religious activities, social practices and indeed how to perform them, have been adjusted.

4.1. Energy Consciousness in the Traditional House Design

A traditional house is usually designed and based on the environmental conditions, as a response of the people (Knapp 1989). The architecture of the traditional Balinese house responds to the warm humid climate by installing cross ventilation and shading components in the house to create thermal comfort for the inhabitants (Silaban 1991). Such a house has passive environmental properties that optimally utilises the potential of the local nature, to protect against and respond to high temperatures, high humidity and high solar radiation. According to this condition, proper ventilation and air movement are the requirements of the house setting in order to provide thermal comfort for the occupants (Antaryama 2000, cited in Trimariantio 2003). They are regarded as a popular passive cooling resource in hot and humid summer climates where the houses are designed to utilise the wind as a natural cooling source (Kusuma 1999). Using computer simulation, Kusuma further suggested that the setting produces the air circulation that easily moves around and enters a building. In the *natah*, the wind flows from the space between pavilions in the southern part and the gate to other parts of the house. This is a potential air motion to reduce high temperature, humidity and solar radiation. The motion also plays a role for air movement in the building through the ventilation between the wall and the roof in the pavilions (Figure 2).

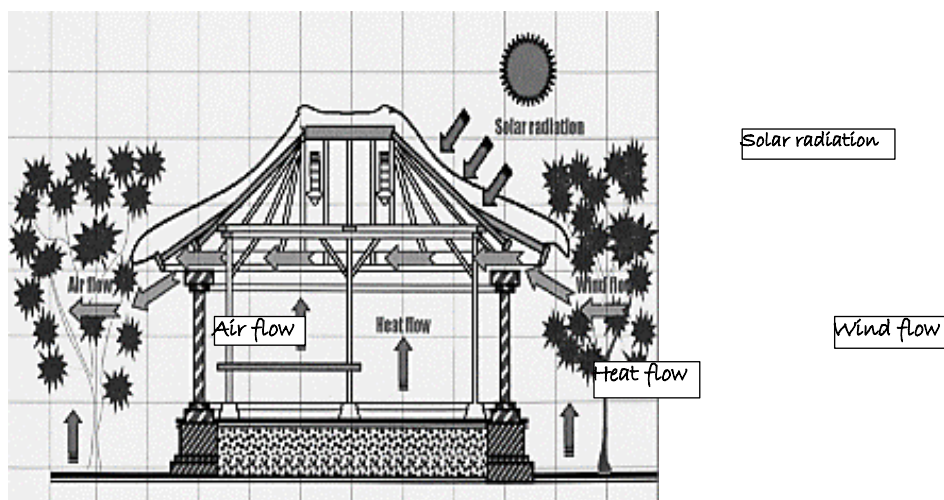


Figure 2: Air circulation in the traditional Balinese house

Source: Trimariantio 2003

The cooling air enters the room where traditionally the room is a single room and transfers the heat from the room to the outside. This circular flow will increase the thermal comfort in the room that is supported by the trees that function to reduce the outside temperature. Therefore, the thermal comfort that is created by this cooling air motion eliminates the need for artificial devices. The house is naturally comfortable for the occupants.

The house is regarded as an economical house, which is cheap in its development process and is a thrifty in energy use in its operation (Widja 2004). Over time, because of many factors such as an advance of technology, an increase of household size and family income, the house has been transformed. New structures have been built by demolishing walls and pavilions, and adjacent to pavilions and in the backyard by cutting down trees and no longer raising animals. These new constructions have changed the setting of the house and have caused an increase in house size. This enlargement reduces open spaces and the distance between pavilions in the house so that it decreases cross ventilation in the building and the opportunity for natural lighting (Sueca 2003). Therefore, people also want artificial lighting and air conditioning, which increases the use of energy (Trimariantio & Dudek 2011; Gill et al. 2011; Sullivan & Ward 2011; Dalem et al. 2010). If the transformed house in urban areas face problems related to energy consumption, do the same problems also occur in the transformed house in tourist destination?

4.2. Energy Consumption

The energy consumption for residential purposes in Indonesia in 2000 was 1,738 PJ. It was 39% of the total energy consumption in Indonesia (Sugiono et al. 2013). In 2010, this consumption increased to 1,820 PJ (Syahril et al. 2012), equal to 0.3 TWh. More than 61 million households consumed this energy where the estimation of the total floor area of dwelling units was 4 billion m² (BPS 2012). Based on these data, the average annual energy consumption per metre square of dwelling is approximately 70 kWh/m² or 5.8 kWh/m² per month. Since specific data for the standard of energy consumption in settlement areas is currently limited, this average intensity is used as a benchmark to calculate and compare the level of energy consumption.

Located in the tropical zone of the southern hemisphere, Bali has a warm humid climate all year round with seasons that can only be distinguished as wet and dry. The wet season falls between October and April, and the dry season occurs between May and September. With the warm humid climate, the temperature throughout the year averages between 25° to 30°C with high humidity that averages about 82%. The hottest months of the year in Bali are between November and March, with an average temperature around 30°C. On the other hand, the coolest months of the year are June, July, August and September with an average temperature around 25°C (BPS 2011). These conditions have influenced the use of energy in the building sector in Bali where there are no significant differences throughout the year (Permana & Kumar 2008).

The traditional Balinese house is a building adapted to the warm humid climate and optimally utilising the potential of nature (Silaban 1991) to use energy effectively (Trimariantio 2003; Yeang 1987; Yuan 1987). The house is environmentally friendly and is low cost and thrifty in its operation (Widja 2004). A veranda, a shallow overhang, and cross ventilation between the roof and walls are essential building elements to moderate the tropical climate (Gelebet 1986).

Traditionally, most energy use in the house occurred in the kitchen where women cooked every morning and prepared food for animals, especially pigs. In this place, the daily life of Balinese began when the mother lit the first fire for the day's cooking (Covarrubias 1974). This activity, which used firewood as fuel, was the main source of energy consumption. At night, people used limited light from a traditional lamp called a *damar* made from cotton and coconut oil on a coconut shell or small piece of pottery. In Kamasan, a *damar* was put in a little niche excavated in the wall of a *bale dauh* so that it produced charcoal used for drawing traditional paintings. For that reason, people in Kamasan kept a *damar* burning until the morning.

Along with the advance of technology and information, people started using kerosene for cooking and electricity for lighting and other household devices such as televisions, radios, fans, washing machines and refrigerators. When gas stoves were introduced, some people used these devices and abandoned kerosene stoves for cooking because the gas stoves were cheaper and cleaner than the kerosene ones. After the Indonesian Government launched the program of conversion from kerosene to liquid petroleum gas (LPG) in 2007 (KESDM 2011), most people used a gas stove for cooking.

In the transformed houses in the four villages, energy was supplied by electricity, LPG and a small amount of firewood in some houses. Since the energy consumption is similar throughout the year, the consumption of

electricity and LPG was collected from the monthly electricity bill and information from the owners. These data were then divided by the total floor area. In the case of LPG, the numbers of gas bottles that were used monthly were then converted into kWh. These energy resources and the floor size for residential and commercial purposes were collected and compared to investigate their pattern.

4.3. Building Density and Energy Consumption

The relationship between building density and energy consumption in housing commonly constructed in Bali¹, was established by Trimarianto (2003). He suggested that high-density houses needed more energy to improve the comfort of occupants. The houses need artificial lighting even on a sunny day because the sunlight is not enough to illuminate the rooms. The houses also used AC more often to provide the comfortable indoor temperatures.

In parallel to Trimarianto's arguments, this investigation found that the higher the density of a house, the higher the energy intensity. This phenomenon can be seen in Figure 3 that shows a comparison between BCR (Building Coverage Ratio) and monthly energy intensity. The monthly energy intensity in Sanur (4.47 kWh/m²) and Kuta (5.09 kWh/m²), which had higher BCR, was higher than Kamasan (2.65 kWh/m²) and Ubud (3.89 kWh/m²).

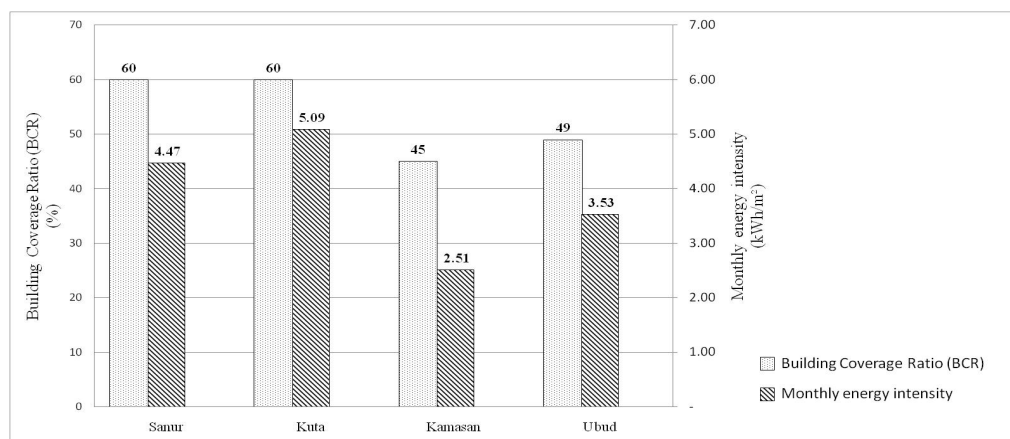


Figure 3. Monthly energy consumption and the average BCR in four villages

However, BCR is not the only factor that influences the energy usage in the house. The influence of building density on energy intensity and the other factors that influence the increase can be seen in Figure 4. In this figure, the level of building density based on the inventories and texture of the transformed houses that are explained in Chapter Five, is divided into four categories. The first category represents the house that still has an ideal *natah*, a family temple, traditional pavilions and a low transformation of *teba*. The second category represents the house that has an ideal *natah* and a family temple and has transformed pavilions and *teba*. The third category represents the house that has the original family temple but transformed *natah*, pavilions and *teba* and the fourth category represents those where there are changes in all parts of the house. The first category has the greatest open spaces and the lowest building density while the fourth has the smallest open spaces and the highest building density.

The scatter-plot within each category and the regression analysis (R^2) in Figure 4 indicate the extent to which energy intensity depends on the level of building density. The trend displayed in the figure confirms the trend of an increase of monthly energy intensity as the level of building density increases. However, the R^2 – value is weak (0.0194), and there are considerable variations of energy intensity pattern within the categories, therefore a clear dependence between these variables is not seen.

¹ Trimarianto examined two house models that are commonly constructed in urban area Bali. The models are the 36 m² dwelling type on a 108 m² plot and the 240 m² dwelling on 294 m² plot.

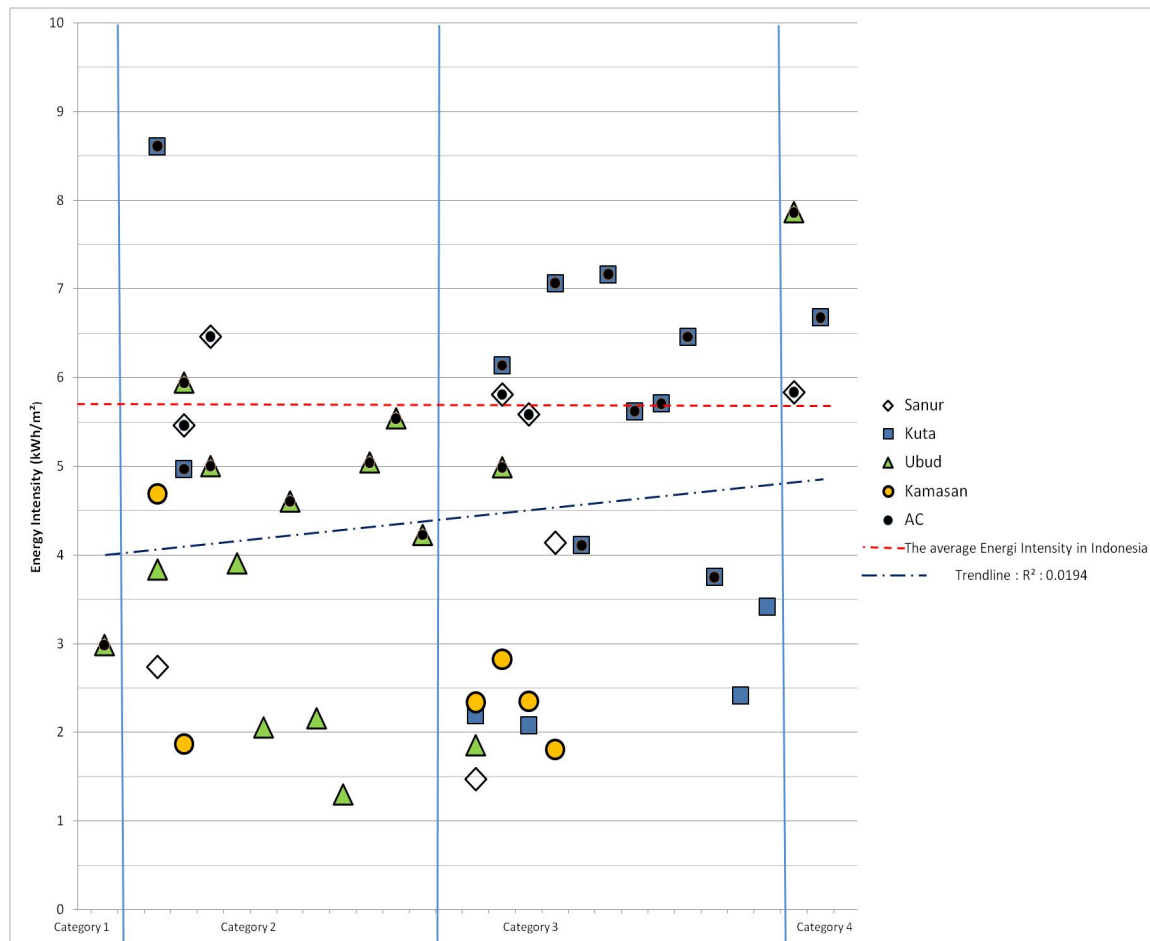


Figure 4: Energy consumption in the four villages

The clearer dependence in relation to energy consumption in the transformed house is displayed by the correlation between the installation of air conditioning (AC) and energy intensity (Figure 4). A different set of groupings, especially in the Category 2 and 4, emerges for monthly energy intensity, in which the houses equipped with AC show greater energy intensity than those without AC. This figure also shows that the houses without AC used less energy than the average energy intensity in Indonesia (5.8 kWh/m²) while the houses equipped with AC approached and were above the average energy intensity in Indonesia. This figure implies that the installation of AC significantly increases the energy intensity compared to the houses without AC.

As suggested by Trimariantio (2003), this device was installed in the house as a response to the increase of building density and reduction of open spaces. However, in the house transformed for tourist facilities, the installation of AC was distributed within the four house categories that represent various levels of building density. This phenomenon implies that there were additional variables, which govern the preference to install AC and lead to the increase of monthly energy intensity, other than level of building density. To demonstrate possible explanations for the additional variables, twelve transformed houses that are representative of each category in the four villages were explored by interviewing the owners. The house in Category 1, for example, which has low building density, ideal pavilions, and vegetation to create thermal comfort for its inhabitants, is also equipped with AC. In this house, AC is utilised to entice tourists. Three houses in Category 2 and 3 that have relative lower energy intensity (around 4 kWh/m²) amongst the houses equipped with AC use such a device not only for creating thermal comfort but also for attracting tourists, showing the prestige and luxury of their house and presenting the occupants' lifestyle. This figure indicates that in terms of the use of AC, creating a modern image is more important consideration than the density of the houses.

5. Conclusions

The energy and water consumption in the transformed house has been investigated. The investigation found that the tourist facilities increase the energy and water consumption especially in the facilities that use electrical devices and water to serve tourists such as home stays, cafes, restaurants, salons and laundries. The use of the advanced technologies is an attempt of people to provide a better service and to fulfil the demands of tourists for convenience in the transformed houses. The electrical devices are likely to be beneficial in terms of attracting tourists, and possibly even to create luxurious, prestigious and comfortable facilities.

The construction of tourist facilities and new structures for accommodating domestic activities has increased the building density in the houses. The high building density influences energy consumption used to increase the comfort of the occupants. Despite low correlation, building density represented by BCR tends to influence energy intensity in the transformed houses where the higher the BCR of the houses, the higher the energy intensity. The clearer correlation is displayed between installation of air conditioning (AC) and energy intensity. Transformed houses equipped with AC have greater energy intensity than those without AC.

Acknowledgments

My thanks are to homeowners as well as colleagues and friends from the Udayana University and elsewhere who have given a lively discussion and feedback. I am also very grateful for the students who helped me during fieldwork.

References

- Badan Standarnisasi Nasional (BSN). 2008, *SNI (Sandar Nasional Indonesia / Indonesian National Standard) no 3242 tentang Pengelolaan Sampah di Permukiman*, Jakarta: BSN.
- Badan Pusat Statistik (BPS) Bali. 2007-11, *Bali in Figure 2007-11*, Denpasar: BPS – The Bali Statistics Bureau.
- Badan Pusat Statistik (BPS) Bali. 2011, *Bali in Figure 2011*, Denpasar: BPS – The Bali Statistics Bureau.
- Covarrubias, M. 1974, *Island of Bali*, Kualalumpur: Oxford University Press.
- Geertz, H. and Geertz, C. 1975, *Kinship in Bali*, Chicago: the University of Chicago Press.
- Lefebvre, H. 2000, *Everyday Life in the Modern World* (translated by Sacha Rabinovitch), London: Continuum
- Gelebet, I N. 1986, *Arsitektur Tradisional Daerah Bali*. Denpasar: Departemen Pendidikan dan Kebudayaan, Proyek
- International Gas Union (IGU). 2012, *Natural Gas Conversion Pocketbook*, available at <http://agnatural.pt/documentos/ver/natural-gas-conversion-pocketbook>, accessed at 1 November 2013.
- Kementerian Energi dan Sumber Daya Mineral Republik Indonesia. 2011, *Konversi Minyak Tanah ke LPG Lebih Murah Lebih Bersih*, available at <http://www.esdm.go.id/berita/artikel/56-artikel/4122-konversi-minyak-tanah-ke-lpg-lebih-murah-lebih-bersih.html>, accessed at 1 November 2013.
- Lombard, L. P., Ortiz, J. and Pot, C. 2008, "A review on buildings energy consumption", *Energy and Building*, Vol. 40, pp. 394-398.
- Organikbali.com. 2013, *SIMANTRI Menuju System Pertanian Organik Terintegrasi*, available at <http://organikbali.com>, accessed on 28 November 2013.
- Permana, A.S. and Kumar, R.P.S. 2008, Understanding energy consumption pattern of households in different development forms: A comparative study in Bandung City, Indonesia.
- Poerbo, H. 1992, *Utilitas Bangunan: buku pintar untuk mahasiswa arsitektur –sipil*, Jakarta: Penerbit Djambatan.
- Powell, H. 1989, *the Last Paradise: an American's Discovery of Bali in the 1920s*, third impression, Singapore: Oxford University Press.
- Sardiana, et al. 2010, *Taman Gumi Banten: ensiklopedi tanaman upakara*, Denpasar: Udayana University Press.
- Silaban, F.1991, *Architect and his Works*, Bandung, Bandung Institute of Technology.
- Sueca, N. P. 2003, *Housing Transformation: Improving Environment and Developing Culture in Bali*, Unpublished PhD thesis. Newcastle: University of Newcastle upon Tyne
- Sueca, N. P. 2005, "Faktor - Faktor Determinan Transformasi Rumah di Bali", *Jurnal Permukiman Natak*, Vol. 3, No. 2 (Agustus 2005), pp. 62 - 101. Denpasar : Universitas Udayana Udayana
- Trimariato, C. 2003, *Thermal Efficient Dwelling Design: Bali, Indonesia*, Unpublished PhD thesis. Newcastle: University of Newcastle upon Tyne
- Widja, I M. 2004, "Eco House pada Perkembangan Rumah Tradisional Bali Studi Kasus: Desa Adat Mengwi, Badung," *Jurnal Permukiman Natak*, Vol. 2, No. 1 (February 2004), pp. 25 - 37

- Yeang, K. 1987, *Tropical Urban Regionalism: Building in a South – East Asian City*, Singapore: Concept Media.
- Yuan, L. J. 1987, *The Malay House: Rediscovering Malaysia's Indigenous Shelter System*. Malaysia: Institut Masyarakat Malaysia.

Assessment of the Scale of Artisanal Mining in Bangwe Township, Blantyre

Jabulani Matsimbe¹

¹ Department of Mining Engineering, Faculty of Engineering, The Polytechnic, University of Malawi, Blantyre, Malawi. Email: jmatzimbe@poly.ac.mw

Abstract

Even though mining contributes less than 1 % to Malawi's gross domestic product (GDP), it is central to the government's sustainable development goals strategy and spearheaded to be the backbone of Malawi's economy. Little is known about the scale of artisanal quarry mining production, mining methods used, capital requirements, its diversity and distribution across different areas in Malawi. Present study seeks to fill that gap by assessing the scale of artisanal and small scale quarry mining activities in Bangwe Township. With a population of 170, 350, it represents 21% of the total population of Blantyre city which has 809, 397 people. The township was chosen as it is the main hub and supplier of artisanal aggregates to surrounding areas in Blantyre. In addition, the township has many unemployed youth with a high potential to get involved in artisanal mining thereby improving their lives. Most youth have a negative perception about artisanal mining as it is viewed as a non-profit making and labour intensive business. There are no gemstone mining sites in Bangwe Township. It was also found that there are 7 artisanal quarry mining sites in the township comprising Ntopwa, Mpingwe, Mvula, Number One, Namatapa, Namiyango and Chikunda. On average, each quarry mining site produces 5 wheelbarrows per day and sells at US\$2.66 per wheelbarrow. As most builders require quarry for construction projects, the quarry miners sell at least 0.5 tonnes per day. The output of this study has created a database of artisanal quarry mining activities and the level of active youth involvement in artisanal mining in Bangwe Township. Policy makers will use the new knowledge to develop strategies that will foster the growth of artisanal quarry miners and empower the youth to join the artisanal mining business.

Keywords: Bangwe Hill, Mpingwe Hill, Mining Method, Quarrying, Small Scale Mining, Social Enhancement

1. Introduction

Despite limited technical knowledge, low productivity, dishonest buyers, lack of finance, equipment and cooperative groups, artisanal and small scale mining is an important entrepreneurial activity carried out in communities to make a living, support families and create employment. Little is known about the scale of artisanal mining production, mining methods used, capital requirements, its diversity and distribution across different areas in Malawi. The questions that arise are: "who is mining and for what purpose; what do different groups of artisanal miners require to improve their operating conditions and living conditions". Present study seeks to fill the artisanal mining technical information gap through the assessment of the scale of artisanal mining activities and level of active youth mining knowledge in Bangwe Township as it has an impact on socio-

economic development, environmental management, health and safety. Bangwe Township was chosen as it is the main hub and supplier of artisanal aggregates to surrounding areas in Blantyre, Malawi. In addition, the township has a lot of unemployed youth with a high potential to get involved in artisanal mining thereby improving their lives. Malawi youth unemployment rate for 2019 was 7.52%, a 0.04% increase from 2018.

According to Zvarivadza (2018), a research drive towards sustainable means of undertaking artisanal and small-scale mining (ASM) has to be developed to bring sanity and transparency in the minerals industry. Peaceful and all-encompassing approaches have to be devised in order to formalise ASM because ASM is a significant source of livelihood for mainly the poor and those who are unemployable due to lack of professional skills, a vivid fact governments cannot afford to ignore (Zvarivadza, 2018). In many developing countries such as Malawi, ASM is largely a poverty-driven activity which plays an important economic role (Hentschel, 2002). According to Hentschel (2002), many of the potential economic benefits of the ASM sector are lost through poor practice in mining, processing and marketing the target minerals; absence of adequate legal frameworks and secure rights for miners and communities; underdeveloped local governance structures and institutions.

According to Phoya (2015), artisanal mining is a livelihood strategy for between 13,500 to 40,000 people in Malawi and many continue to operate informally thus making it difficult to obtain statistics on their production and sales. Phoya (2015) further explains that Malawi's government must employ other strategies for managing and regulating ASM that go beyond legislation to ensure sustainable development outcomes. To effectively develop and deploy policy responses to reclaim ASM sites, an understanding of the locations and spatial distribution of the ASM sites is a necessary prerequisite (Kumi-Boateng & Stemn, 2020). Malawi was admitted as an Extractive Industries Transparency Initiative (EITI) candidate country in October 2015 and the MWEITI process covers three sectors: mining, oil and gas, as well as forestry (Stephens, 2015). Stephens (2015) further explains that ASM in Malawi is generally carried out through labour intensive methods for: limestone for lime production, terrazzo for the construction industry, rock aggregate crushing for quarry stone, river and dambo sand extraction for construction, clay for ceramics and pottery, extraction of saline soils for salt making gemstones and gold panning. ASM requires a Mineral Permit, Mining Claim Licence and Reserved Mineral Licence (Government of Malawi, 2014).

It is hoped that the output of this study will help create a comprehensive artisanal mining technical database, foster the growth of artisanal miners, and empower the youth to join the artisanal mining business.

2. Materials and Methodology

2.1. Study Area

Bangwe, a peri urban Township of Blantyre, Malawi is located at Latitude -15.813976 and Longitude 35.096475 to the east of Blantyre central business district. With a total area of 1020 hectares, Bangwe is one of the most populous townships in Blantyre city with a population of at least 170,350 people distributed in 33 villages and 41,456 households (Kaonga, Kambala, Mwendera & Mkandawire, 2013) representing more than 21% contribution to total population of Blantyre city which has 809, 397 people. Within its vicinity are Mpingwe Hill and Bangwe Hill. The study areas mainly comprise of biotite gneiss, granitic gneiss, feldspar gneiss and weathered gneiss. The granitic gneiss and biotite gneiss being stronger rocks are suitable for quarrying as compared to feldspar gneiss and weathered gneiss which are weaker. Table 1 shows the physical properties of rocks mined and processed by artisanal miners in Bangwe Township. These properties are a determining factor on what type of mining method to use for crushing the rock. The geology of Malawi is part of Kibaran orogeny formed through continental collision that constructed Rodinia as known in Africa (Malunga, 2018). Malawi is primarily composed of Archean and Paleoproterozoic (Ubendian) terrain which is dominated by the Basement Complex rocks later overlain by Karoo sedimentary rocks and intruded by basaltic/dolerite dykes and sills. The Permo-Triassic period was later followed by Upper Jurassic – Lower Cretaceous period which saw the intrusion of syeno-granitic and nepheline syenite rocks later intruded by volcanic rocks infilled by carbonatite and alkaline dykes. As shown in Figure 4, the Southern part of Malawi is dominated by these rocks and have been grouped as Chilwa Alkaline Province. The same period saw sedimentary deposition characterized by Dinosaur Beds. The above rocks have been overlain by Tertiary – Pleistocene rocks characterized by consolidated to semi

consolidated beds grouped into Timbiri, Chiwondo, Chitimwe and Alluvial. Minor volcanic activities have been witnessed through existence of Songwe Volcanics (Malunga, 2018).

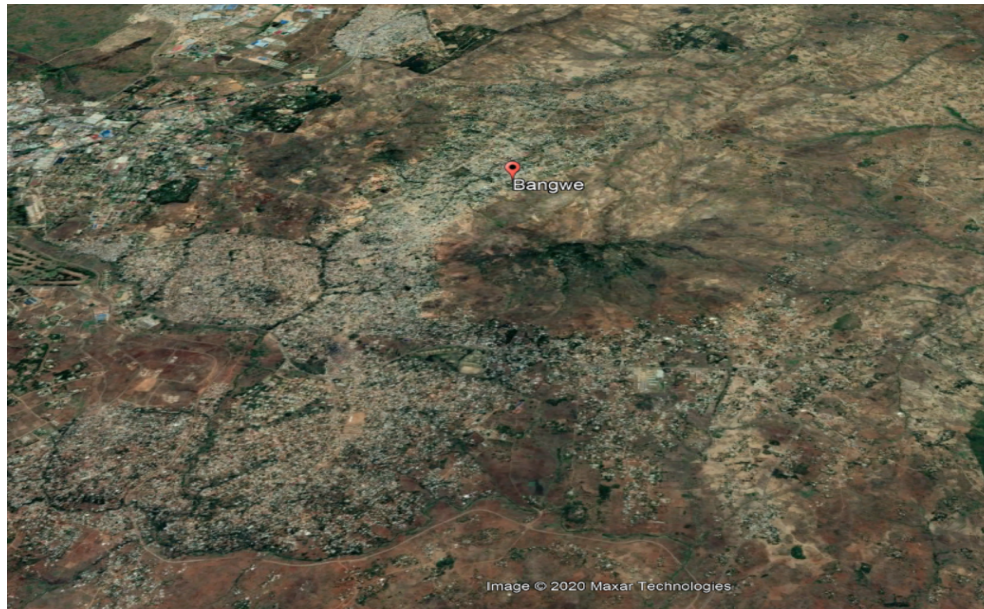


Figure 1. Aerial view of Bangwe Township (Google Earth 2020)

Table 1. Physical properties of rocks

Rock Type	Density [g/cm ³]	Abrasion Index [-]	Work Index [kWhr/ton]	Minerals
Limestone	2.69	0.0256	11.61	Calcite
Granite	2.68	0.3937	14.39	Quartz, Feldspar, Potassium Feldspar, Biotite, Muscovite, Amphibole
Sandstone	2.64	0.1831	12.77	Quartz
Basalt	2.94	0.2	19.72	Olivine, Pyroxene, Plagioclase Feldspar, Iron oxides
Gneiss	2.77	0.45	15	Feldspar, Quartz, Biotite, Muscovite, Amphibole

2.2. Procedure

The following steps were followed in the methodology:

- Conducting a scoping study to determine the scale of artisanal mining activities in the township and to design the reporting procedure
- Collection of data which provide basis for the present study. This involved visiting artisanal mining sites and collecting data comprising: equipment/tools used, quantity and quality of aggregates produced, customer base, capital invested, sales/earnings, labour requirements and mining methods
- Statistical analysis of production rates, cost expenditures and revenue generated

3. Results and Discussion

The researcher found that there are no gemstone mining sites in Bangwe Township. Approximately, 7 artisanal quarry mining sites are located in various areas of Ntopwa, Mpingwe, Mvula, Number One, Namatapa, Namiyango and Chikunda in Bangwe Township. The daily rate of productions, mining methods and equipment used are similar on all mining sites. The cost per wheelbarrow has a mean of US\$2.66 and a standard deviation of ± 0.01 . The daily rate of production has a mean of 5 wheelbarrows per 8 hour working day and a standard deviation of ± 1.00 . Therefore, to illustrate the scale of production in Bangwe, one mining site was used as a proxy because of its centrality to Limbe. The proxy mining site located in Ntopwa area at Latitude -15.820998° and Longitude 35.072593° (Figure 2) has a team of two miners that collect, heat and crush the stone. The work is

physically demanding and poses a lot of health and safety risks comprising bodily injury to fingers and eyes by hammers and flying stone chips respectively, and respiratory problems through inhaling of dust.

The mining tools are summarized in Table 2 and shown in Figure 3 where one of the miners at Ntopwa mining site is conducting preliminary works by following the rock vein using a chisel. Table 3 shows the cost of the tools and materials used for the artisanal mining activity. The mining method summarized in Table 2 involves digging/excavating around the rock to a depth of 1.5m, placing tyres, firewood and charcoal at the bottom of the exposed rock (Figure 4). A match/lighter is used to ignite the fire while ensuring proper coverage around the rock to minimize escape of heat or entering of air which would affect the loosening of the rock. The rock is left to burn for 24 hours and then the next day after it cools crushing takes place using chisel, 7 and 14 pound sledge hammer. The procedure is labour intensive and requires a lot of energy as well as safety precaution to hammer the rock using the 14 pound sledge hammer as it is heavy.

The mining site produces 5 wheelbarrows of rock aggregate (1 inch and $\frac{3}{4}$ inch sizes as shown in Figure 5) per day working 8 hours. The cost per wheelbarrow is US\$2.66. A 1 tonne lorry gets filled with 10 wheelbarrows (implying that 1 wheelbarrow equal 0.1 ton) equivalent to US\$26.20. Challenges faced comprise lack of equipment, lack of finance, unwillingness of the youth to work for the miner, few customers, competition from big quarry companies and lack of shelter from the sun/rain. Availability to work depends on demand and orders for the aggregate. The typical customers are home owners and private individuals. Large abandoned pits without reclamation leads to environment, health and safety concerns to the general public (Figure 6).

Table 2. Artisanal quarry mining tools used in Bangwe Township

Step	Mining Method	Mining Tool	Purpose
1	Demarcation	Hoe, crowbar, chisel	Marking the area to be excavated
2	Excavation	Hoe, pickaxe, crowbar, chisel	Excavate large rock boulders up to 1m in diameter. Penetrate deep rock joints and break apart.
3	Heat/fire setting	Wood, tyres, charcoal	Spalling. Crack and loosen large rocks to a depth of 1.3 m.
3	Pre-crushing	14 lb sledge hammer, chisel	Reducing large boulders of rock to $\frac{1}{4}$ - $\frac{1}{2}$ m diameter stones to be carried by buckets
4	Transportation	Buckets, trolleys, wheelbarrow	Carrying stones to crushing/selling point
5	Crushing	6-7 lb sledge hammer, Hammer	Crushing stones to final sizes: $\frac{1}{2}$ ", $\frac{3}{4}$ " or 1" diameter
6	Sieving	Metal screen, shovel	Removing fines from product

Table 3. Cost of mining tools and materials in Limbe hardware shops

Tool/Material	Cost (US\$)
Used tyres	2
Firewood	1
Charcoal	5
Chisel	6.63
14 lb sledge hammer	25.86
7 lb sledge hammer	19.23
6 lb sledge hammer	12.60
Hammer	7.89
Pick	7.82
Hoe	3.98
Shovel	7.89
Slashers	3.91
Wheelbarrow	52.38
Rake	9.95
Panga Knife	1.99

Spirit Level	5.24
Crowbar (locally known as 'Mgwala')	12.60

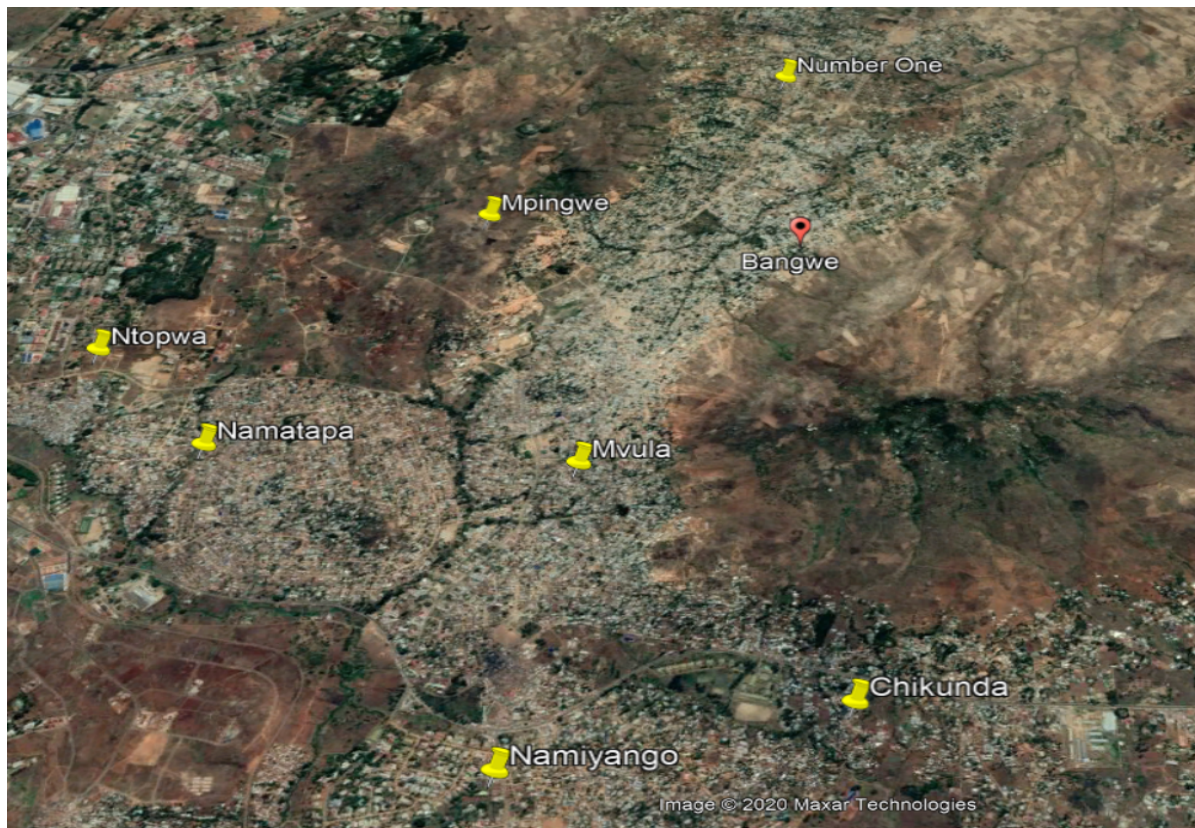


Figure 2. Location of quarry mining sites (Google Earth, 2020)



Figure 3. Artisanal quarry mining tools (14 lb sledge hammer, chisel, hoe and crowbar)



Figure 4. Excavation and heating procedure (Left: unburnt; Right: burnt)



Figure 5. Crushed rock aggregate sizes (6", 1" to ½ inch)



Figure 6. Pits left behind by ASM

4. Conclusion and Recommendation

In Bangwe Township, artisanal small-scale mining is characterized by limited capital investment, little to no technology, lack of personal protective equipment, high intensive manual labour, improvised/primitive mining methods, poor entrepreneurial and management skills, community employment opportunities, limited knowledge about legal procedures, lack of knowledge about tax payment and insurance, limited access to mining titles, seasonal alternation of mining with farming and piece jobs, and negative impact on environment, health and safety. According to World Bank (2019), a notable region-wide policy initiative that could act as a vehicle and impetus for data collection and sharing is the Africa Mining Vision (AMV) which was established in 2009 by the African Union in partnership with numerous international agencies to act as the blueprint for mineral led development in the region over the next 50 years. World Bank (2019) further explains that the AMV calls upon signatories to commit to “fostering the establishment of resilient artisanal and small-scale mining (ASM) communities” through formalization, and in order to do so underscores the need to “improve the understanding of ASM issues” through data collection.

Therefore, present study assessed the scale of production of artisanal rock aggregate miners in Bangwe Township. It was found that there are 7 artisanal quarry mining sites and no gemstone sites in the township. On average, each quarry mining site produces the equivalent of 5 wheelbarrows per day and sells at US\$2.66 per wheelbarrow. As most builders require quarry for construction projects, the quarry miners sell at least 0.5 tonnes per day. In Tanzania, artisanal aggregate quarrying is characterized by low productivity as it takes a man 3 weeks and a woman 4 weeks to produce a 7 ton lorry of limestone aggregates worth US\$80 less production costs (Elisante, 2009). In addition, Elisante (2009) estimates that more than 15,000 people in Tanzania earn a living through artisanal quarrying activities. Hentschel (2002) estimates 40,000 people working in the Malawian ASM sector. Despite limited technical knowledge, dishonest buyers, low productivity, lack of finance and equipment, the artisanal mining business is used to make a living, support families and create employment thereby impacting society development and social stability. Policy makers will have access to updated new knowledge on the welfare and scale of production of these artisanal miners which in turn will lead to strong government legislation, policy enforcement, easy licencing procedures and favourable business environment.

It is recommended that Government fully support the operations of artisanal miners by training them on necessary technical skills and technology, creating a repository and data sharing platform for the ASM sector, formalizing the sector through streamlined licensing, geological data & access to finance, and making it a centerpiece in economic and poverty alleviation plan. With good machines and technologies, these artisanal miners can grow big, increase their productivity and supply at both local & national level. There is also need to sensitize the nation on the importance and diversity of artisanal mining so as to encourage more youth and women to join the ASM sector. Future research work can look into the development of a business model which the artisanal and small scale miners can use to sustain their businesses, increase productivity, get better prices, cut down on costs and find better markets.

Conflict of Interest

The author has not declared any conflict of interests.

Acknowledgements

The author would like to thank University of Malawi, The Polytechnic for supporting the research.

References

- Elisante E. (2009). *Simplification of Jaw crusher for Artisanal Aggregates Miners*. Journal of Engineering and Technology Research Vol.1 (6), pp. 102-108.
- Government of Malawi. (2014). *Artisanal and Small Scale Mining Policy*. <https://mininginmalawi.files.wordpress.com/2014/11/2014>.
- Hentschel, T. (2002). *Global Report on Artisanal & Small-Scale Mining*. Minerals, Mining and Sustainable Development. <https://pubs.iied.org/pdfs/G00723>.
- Kaonga C, Kambala C, Mwendera C, Mkandawire T. (2013). *Water quality assessment in Bangwe Township, Blantyre City, Malawi*. African Journal of Environmental Science and Technology, <https://doi:10.5897/AJEST12.196>
- Kumi-Boateng, B. and Stemm, E. (2020). "Spatial Analysis of Artisanal and Small-Scale Mining in the Tarkwa-Nsuaem Municipality of Ghana", Ghana Mining Journal, Vol. 20, No. 1, pp. 66 - 74.
- Malunga G. (2018). *The Geology and Mineral Potential of Malawi*. Technical File, Mining and Trade Review.
- Phoya R.E. (2015). *Formalising for Development: Artisanal and Small-Scale Mining in Malawi's Draft Mining Legislation*. Assignment for module CP 50040 'International and Comparative Mineral Law and Policy CP 50040' Submitted towards LLM in Natural Resources Law and Policy (Centre for Energy, Petroleum and Mineral Law and Policy, University of Dundee). <https://mininginmalawi.files.wordpress.com/2018/07/r-etr>.
- Stephens M. (2015). *Malawi extractives industry transparent initiative report*. Aldersgate Street London. <https://eiti.org/document/malawi-eiti-report-20152016>.
- World Bank. (2019). *State of the Artisanal and Small-Scale Mining Sector*. Washington, D.C.: World Bank.
- Zvarivadza T. 2018. *Artisanal and Small-Scale Mining as a challenge and possible contributor to Sustainable Development*. Resources Policy 56 (2018) 49–58. <https://doi: 10.1016/j.resourpol.2018.01.009>.

OpenFOAM Based Approach for the Prediction of the Dam Break with an Obstacle

Syamsuri¹

¹ Department Mechanical Engineering, Institut Teknologi Adhi Tama Surabaya, Indonesia.
Email: syamsuri@itats.ac.id

Abstract

The phenomenon of the flow impact on a vertical wall resulting from a dam problem is simulated by using OpenFOAM. In this simulation, a dam break was also simulated with the addition of obstacles with various dimensions. The aim of this study is to assess the accuracy of the solver for problems in the impact wave category from the experimental results of previous researchers and other numerical solution techniques compared with the results of this solver. Different aspects of flow such as free surface elevation before and after the initial impact have been observed in depth. The method used in this research is numerical computation simulation with the OpenFOAM approach which has the advantage of being more accurate and fast simulation time. The variations in the dimensions of the obstacle in this study were $b/h = 0.25$, $b/h = 0.5$ and $b/h = 1.0$. From the simulation data, it is found that the numerical approach has been validated through quantitative comparisons with experimental measurements. The computational positions of the leading edge of the collapsed water column match the experimental data. The difference between the experiment and this numerical solution is below 2%.

Keywords: Dam Break, An Obstacle, Surface Profile, OpenFOAM

1. Introduction

Dam is a structural building that functions to accommodate and store a number of fluids (water), as well as channeling the needs for drinking water, electricity generation, and irrigation. Fluid movements (water) on dams such as heaving and rolling which trigger high pressure causes structural damage or what we know as dam break. This break damage causes considerable disasters such as floods or other natural damage. Numerical modeling studies so interesting to learn to understand the dynamics of fluid movement in this case.

Several studies with experimental methods on dam break have been carried out by previous researchers, among others: Verma *et al.* (2017) has conducted research on the experimental study of the soil dam breakthrough path using the fuse plug model. The different input parameters that help in understanding the phenomenon are the temporal variation of the initiation of the breakthrough, the breakthrough width, the breakthrough depth, the discharge intensity and the peak time. This paper provides the results of laboratory research conducted using wood fuse plugs and five different types of soil.

The behavior of the breakthrough depends on the dimensions of the fuse plug, type of fill material, reservoir capacity and inflow. Researchers on dam-break flow routing in confluent channels have been conducted by Chen *et al.* (2019). Experiments were carried out on smooth, transparent, rectangular prismatic channels to study the flow of dam break under four different confluent angles. Based on the variation in water level and flow rate, as the confluent angle increases, the effect of retardation and reduction in flooding has increased. Specifically, the arrival time of the floods was delayed by about 0.91% to 21.18%, and the peak flood discharge was reduced by about 9.05% to 58.36% flow. Kocaman *et al.* (2020) conducted a study on experimental and numerical analysis of a dam-break flow through different contraction geometries of the channel. Laboratory testing was performed on a smooth rectangular duct with a horizontal dry bed for three different lateral contraction geometries. The free surface profile and time variation of the water level in the selected area, obtained directly from three synchronized CCD video cameras, record via a virtual wave probe. The experimental results were compared with numerical solutions of volume of fluid based on shallow water equations and reynolds-averaged navier-stokes (RANS) with the k- ϵ turbulence model. A good agreement is obtained between the computed results and the measurement results. The new experimental data presented can be used to validate numerical models for simulating dam flows over irregular topography.

Numerical modeling is an option because it is effective, safe and cost-effective. Various methods for the study of numerical modeling of fluid motion dam break has been applied. By using a method LS/IB, Yu *et al.* (2017) able to show similar results between the experimental and numerical modeling of fluid motion at any given time. On a different method, Issakhov *et al.* (2019) were able to show the movement of fluid turbulence at any particular time and a different angle obstacle by using VOF method. Other than that, Yu *et al.* (2019) using the CLSVOF / IB method to simulate the movements fluid that are affected by Reynold's number. With increasing numbers of Reynolds, fluid movements tend to be unstable or turbulent. Zhao *et al.* (2017) have conducted research on numerical simulations of dam breaker floods with MPM. Dam-break flows with different initial aspect ratios are simulated in the material point method and shallow water equation models which are extensively verified. So to test the accuracy and stability of the point method material, a dam-break flow simulation is performed and the results are in accordance with the validation of other numerical methods and experimental data. The material point method shows its potential to tackle the hydrodynamics like this case.

OpenFOAM software is a type of software development from CFD. This software is widely used in industry because it is open source and can be modified. For modeling, this software is able to simulate the movement of two-phase fluids with a specific turbulence model by Higuera *et al.* (2013). So that in this study the authors used software OpenFOAM 2.2.2. to simulate the dam break with variation ratio of obstacle, because this topic is still not widely discussed.

2. Method

In this study using the application of breaking of dam. The geometry is shown in Figure 1 where the boundaries are the walls with the top open. Pressure on the surface is set at 1 ATM. The fluid used in this simulation is water with kinematic viscosity of $1.0 \times 10^{-6} \text{ m}^2 \cdot \text{s}^{-1}$ and a density of $1.0 \times 10^3 \text{ kg} \cdot \text{m}^{-3}$. The fluid was dropped naturally, so that the fluid moves due to the acceleration of gravity at $9.81 \text{ m} \cdot \text{s}^{-2}$ which leads down. At the bottom of the middle side as shown in Figure 1 there is an obstacle, which in this simulation will be varied with the ratio of width and height of the obstacle. The width of the obstacle in the set remains at 0.024 m while the height of the obstacle is varied by b/h ratio of 0.25, 0.5, and 1. The movement of this water flow will later be monitored at certain times including 17 s where this condition represents the time the fluid starts to flow, 47 s represents the state of the fluid when it hits the obstacle, 58 s represents the state of the fluid some time after hitting the obstacle, and 152 s when the fluid has passed through the obstacle and hit the back wall. From the four monitoring times, flow characteristics will be analyzed at each height variation from the obstacle. In this simulation using the free surface modeling method or commonly known as the Volume of Fluid Method (VOF). Where this method in this simulation is used to calculate the motion of flux, which must be settled separately.

Mathematic Model of Flow

Laminar flow is a fluid that has a certain viscosity and it is an incompressible flow can be described by the Navier-Stokes equations in an Eulerian reference frame [Ferziger & Peric, 2002],

$$\rho \left(\frac{\partial u_i}{\partial t} + u_j \cdot \frac{\partial u_i}{\partial x_j} \right) = \rho F_i + \frac{\partial \sigma_{ij}}{\partial x_j} \quad (1)$$

$$\frac{\partial u_i}{\partial x_j} = 0 \quad (2)$$

where,

u_i is a velocity component

ρ is a density

F_i is a gravity component

σ_{ij} is a stress tensor

While the equation for stress tensor can be seen in the following equation:

$$\sigma_{ij} = -P\delta_{ij} + \mu \left(\frac{\partial u_i}{\partial x_j} + \frac{\partial u_j}{\partial x_i} \right) \quad (3)$$

Where,

μ is a dynamics viscosity

p is a pressure

δ_{ij} is a cronecker delta

The method is based on the use of a fractional function C . Derivative of the fractional function must be equal to zero [10]:

$$\frac{\partial C}{\partial t} = V \cdot \nabla C + \nabla \cdot [C(1 - C)U_r] = 0 \quad (4)$$

where:

C = Fractional Function ($C = 0$ If the cell is empty, $C = 1$ If the cell is full)

V = fluid velocity

U_r = an artificial force that “compresses” the region under consideration

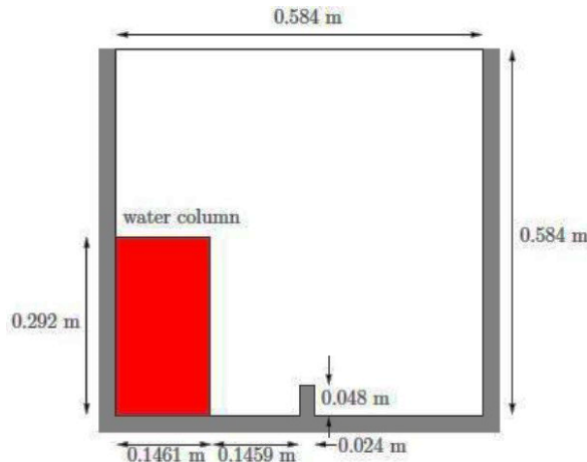


Figure 1: Dam break geometry

3. Results & Discussion

3.1 Validation for Surface Profile

Comparison of the surface profile of the time evolution of dam break between numerical and experimental studies by Kaceniauskas, 2005 when $t = 0.275$ sec is shown in Figure 2. This figure shows that the numerical results are in a good agreement with the experimental study results. In general, the results show that the mean error between numerical and experimental data is less than 2 %.

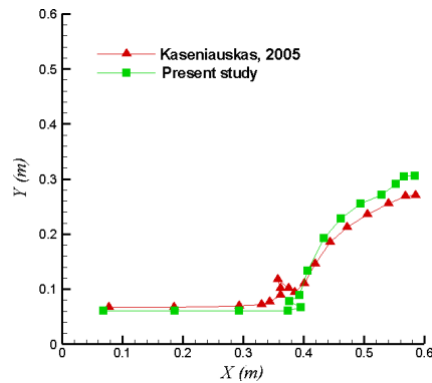


Figure 2: Surface profile of dam break with $t = 0.275$ sec

3.2 The phenomenon of flow characteristics of obstacle with ratio $b/h = 0.25$ at 17 s, 47 s, 58 s, and 152 s

The characteristic of the dam break flow phenomenon which is affected by time changes is shown in Figure 3. When the floodgate is opened, the water will flow. This happens when $t = 17$ s shows the flow of water moves to fill the empty space on the left bottom wall of the obstacle (figure 3a) caused by the existence of gravity. Then when $t = 47$ s shows the flow of water completely hits the barrier wall and moves in the vertical direction with the formation of a curve on the surface (figure 3b). The curvature on the surface occurs because water experiences an inertia force [Zhainakov & Kurbanaliev, 2013]. Furthermore, when $t = 58$ s shows the formation of a bubble at the end of the flow (figure 3c). When the gravitational force is greater than the inertia force, the vertical flow moves downward and hits the bottom right bottom wall of the obstacle ([Biscarini *et al.*(2010)] , [Oertel & Bung, 2012]). Furthermore, the flow will move upwards and there will be bubbles around the wall (figure 3d). This bubble formation caused by interactions between water and air ([Hansch *et al.* (2014)], [Ryu *et al.*(2007)]).

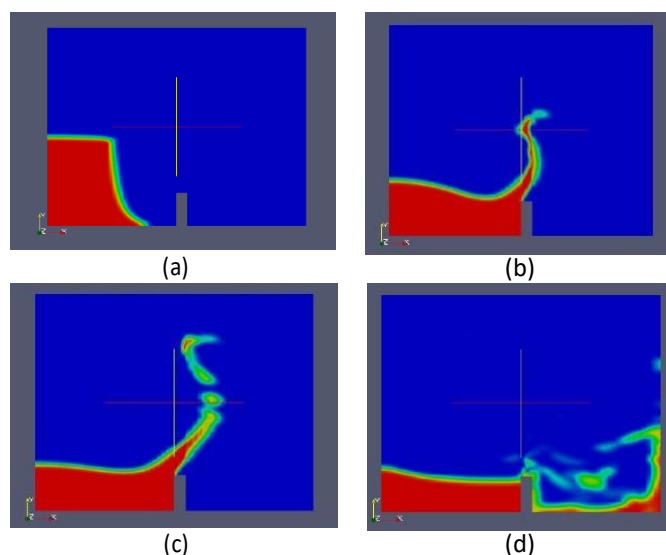


Figure 3: The phenomenon of flow characteristics of obstacle with ratio $b/h = 0.25$ at (a) 17 s, (b) 47 s, (c) 58 s, and (d) 152 s

3.3 The flow characteristic phenomenon at 17 s with ratio of obstacle $b/h = 0.25, 0.5$, dan 1

The effect of the obstacle ratio b/h on dam break flow at 17 s is shown in Figure 4. This phenomenon shows that when the water gate is opened, the flow of dam break is almost the same, namely the flow of water moves to fill the empty space on the bottom left wall of the obstacle. That is because the dam break flow has not hit the obstacle and the speed at which the fluid falls in all obstacle variations only utilizes the acceleration of gravity. So that all contours produced show the same conditions.

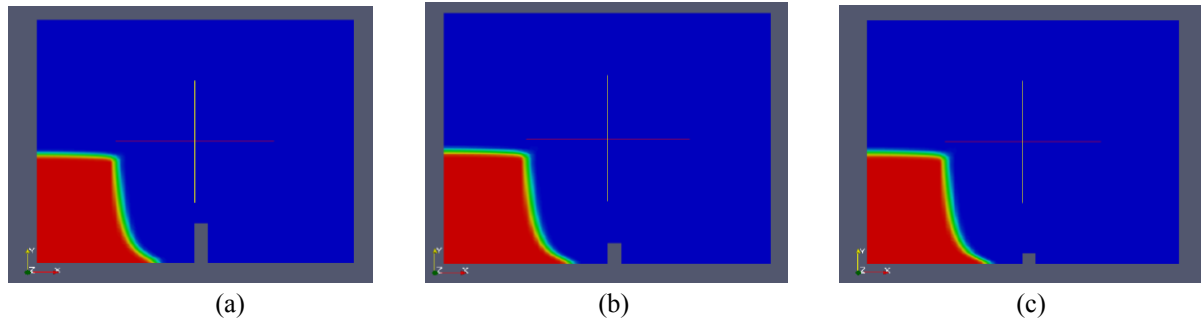


Figure 4: The flow characteristic phenomenon at 17 s with a ratio of obstacle
(a) $b/h = 0.25$, (b) $b/h = 0.5$, and (c) $b/h = 1$

3.4 The flow characteristic phenomenon at 47 s with ratio of obstacle $b/h = 0.25, 0.5$, dan 1

Figure 5 shows the effect of the ratio b/h to the dam break flow at 47 s. This phenomenon shows that when the obstacle b/h ratio is getting bigger it is seen that the end of the flow tends towards horizontal and when the obstacle ratio b/h gets smaller then it appears that the end of the flow tends towards the vertical. This happens because the smaller the ratio b/h obstacle produces collision pressure that occurs in the flow dam break is greater, conversely the greater the ratio b/h obstacle produces greater gravity the flow of dam break ([Issakhov & Imanberdiyeva (2019)] , [Issakhov *et al.*(2018)]).

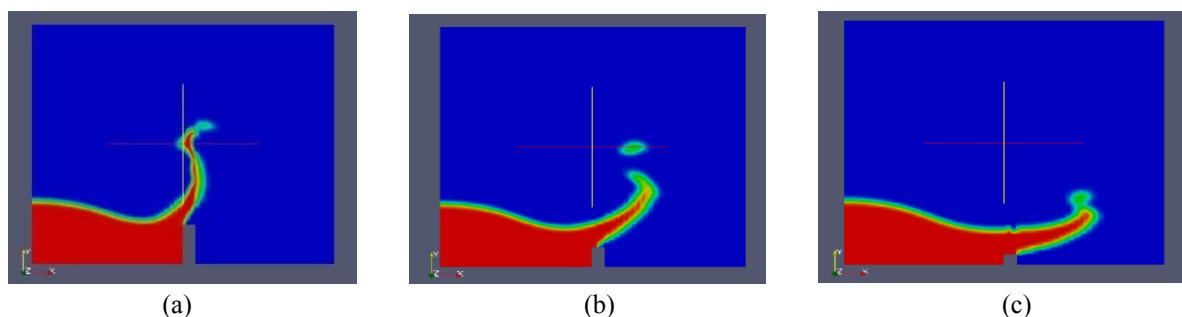


Figure 5: The flow characteristic phenomenon at 47 s with a ratio of obstacle
(a) $b/h = 0.25$, (b) $b/h = 0.5$, and (c) $b/h = 1$

3.5 The flow characteristic phenomenon at 58 s with ratio of obstacle $b/h = 0.25, 0.5$, dan 1

The effect of the obstacle b/h ratio on dam break flow at 58 s is shown in Figure 6. From this phenomenon when the obstacle b/h ratio is getting bigger it is seen that the end of the flow has tended towards horizontal and when the obstacle b/h ratio is getting smaller then it appears that the end of the flow tends towards the vertical ([Issakhov & Imanberdiyeva, 2019] , [ssakhov *et al.*(2018)]). The bubble at the end of the flow is caused by air trapped in the dam break flow ([Hansch *et al.* (2014)], [Ryu *et al.*(2007)]).

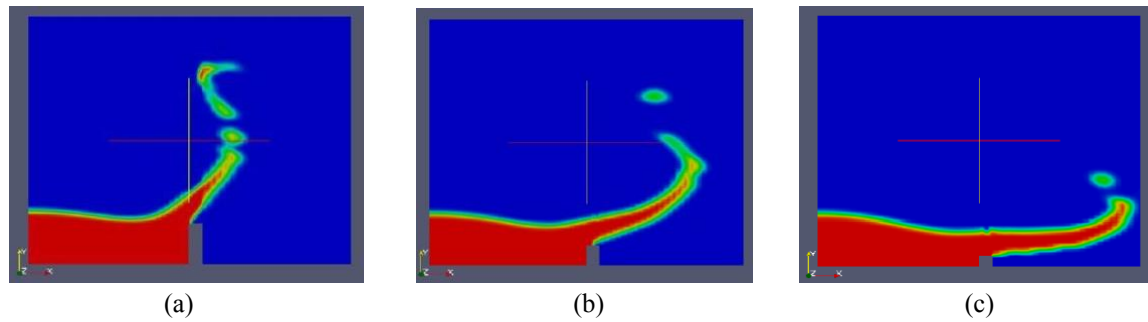


Figure 6: The flow characteristic phenomenon at 58 s with a ratio of obstacle
(a) $b/h = 0.25$, (b) $b/h = 0.5$, and (c) $b/h = 1$

3.6 The flow characteristic phenomenon at 152 s with ratio of obstacle $b/h = 0.25, 0.5$, dan 1

The effect of the obstacle b/h ratio to the dam break flow at 152 s is shown in Figure 7. From this phenomenon, it can be seen that the flow of dam break when passing through the obstacle $b/h = 0.25$, there is still a lot of water retained by the obstacle compared to other b/h ratios, this is caused by the obstacle with the ratio $b/h = 0.25$ having a higher height than another. So that the ability to hold water can be more than others, but the obstacle must receive a greater impact than the others. The smaller the ratio b/h obstacle causes the flow formed tends to be more turbulent [Ozmen-Cagatay & Kocaman, 2011].

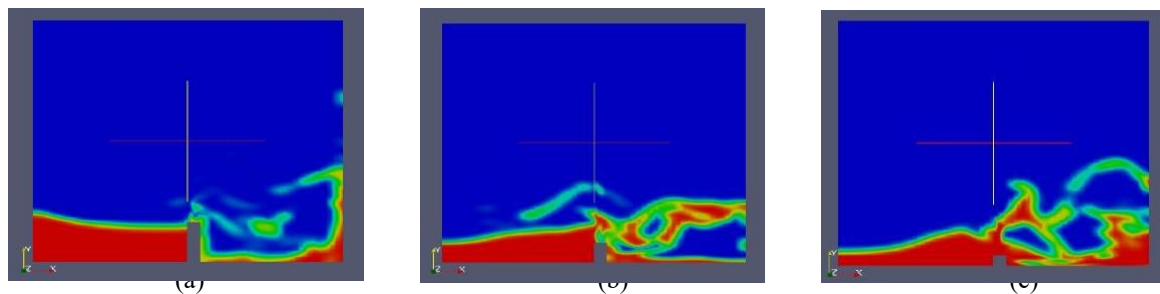


Figure 7: The flow characteristic phenomenon at 152 s with a ratio of obstacle
(a) $b/h = 0.25$, (b) $b/h = 0.5$, and (c) $b/h = 1$

3.7 Comparison of characteristics of a water column

The effect of time on the height of the water movement on the variation of the ratio b/h is shown in Figure 8. From the three graphs, when the time is longer the height of the water movement is lower. The ratio $b/h = 0.25$ has a higher water movement height than the other b/h ratio. This indicates that the high ratio of b/h will inhibit the flow of fluid.

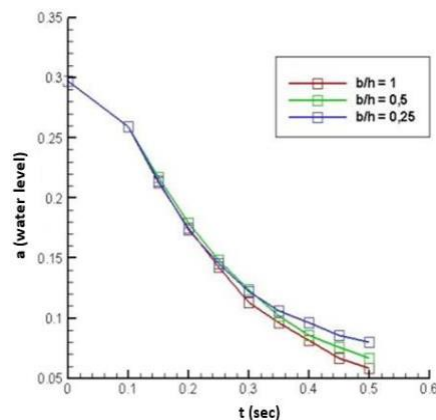


Figure 8. Effect of time on height of water movement on obstacle ratios $b/h = 0.25$, $b/h = 0.5$ and $b/h = 1$

5. Conclusions

Validation has been carried out with previous studies using experimental methods compared with OpenFOAM simulation results. The validation results show that, there are similarities of the surface profiles for the dam break when $t = 0.275$ sec. For case 3 with obstacle $b/h = 1.0$, when $t = 17$ sec the phenomenon of water flow near the lower wall has moved to the front wall but has not yet hit the obstacle, the same was the case for cases 1 & 2. At $t = 47$ sec the flow has hit the obstacle and the water follows the contour of the obstacle then the water moves vertically. Meanwhile, at $t = 58$ sec, it was seen that bubbles formed and water began to separation from the main stream. However, when $t = 152$ sec, it was seen that the fluid flow passing through the obstacle had hit the front wall, and the bubble was also getting bigger. The fluid flow formed at this time tends to be more turbulent.

Acknowledgments

We would like to thank to ITATS for funding this research. Special thank's to Prof. Ming Jyh CHERN and Assistant Prof. Nima Vaziri for very useful discussions.

References

- Biscarini, C., Di Francesco, S. & Manciola, P. 2010. CFD modeling approach for dam break flow studies,” *Hydrology and Earth System Sciences*, 14, pp.705-718.
- Chen, S., Li, Y., Tian, Z. & Fan, Q. 2019. On dam-break flow routing in confluent channels. *Int. J. Environ. Res. Public Health*, 16, 4384, pp.1-23.
- Ferziger, J.H. & Peric, M. 2002. *Computational methods for fluid dynamics*, Springer 3rd Ed., Springer-Verlag Berlin Heidelberg.
- Hänsch, S., Lucas, D., Höhne, T & Krepper, E. 2014. Application of a new concept for multi-scale interfacial structures to the dam-break case with an obstacle. *Nuclear Engineering and Design*, 279, pp.171- 181.
- Higuera, P. Lara, J.L. & Losada, I.J. 2013. Realistic wave generation and active wave absorption for Navier–Stokes models: Application to OpenFOAM. *Coastal Engineering*, 71, pp. 102-118.
- Issakhov, A. & Imanberdiyeva, M. 2019. Numerical simulation of the movement of water surface of dam break flow by VOF methods for various obstacles. *International Journal of Heat and Mass*, Vol.136, pp. 1030-1051.
- Issakhov, A., Zhandaulet, Y. & Nogaeva, A. 2018. Numerical simulation of dam break flow for various forms of the obstacle by VOF method. *International Journal of Multiphase Flow*, 109, pp. 191-206.
- Kocaman, S., Güzel, H., Evangelista, S., Ozmen-Cagatay, H. & Viccione, G. 2020. Experimental and numerical analysis of a dam-break flow through different contraction geometries of the Channel. *Water*, 12, 1124, pp.1-22.
- Oertel, M. & Bung, D.B. 2012. Initial stage of two- dimensional dam-break waves: laboratory versus VOF,” *Journal of Hydraulic Research*, 50(1), pp.89-97.
- Ozmen-Cagatay, H. & Kocaman, S. 2011. Dam-break flow in the presence of obstacle: experiment and CFD simulation. *Engineering Applications of Computational Fluid Mechanics*, 5(4), pp. 541-552.
- Ryu, Y., Chang, K.A. & Mercier, R. 2007. Application of dam-break flow to green water prediction,” *Applied Ocean Research*, 29 (3), pp. 128-136.
- Verma, D. K., Setia, B & Arora, V. K. (2017). Experimental study of breaching of an earthen dam using a fuse plug model. *IJE TRANSACTIONS A: Basics*, Vol. 30, No. 4, pp.479-485.
- Yu, C.H. & Sheu, T.W.H. 2017. Development of a coupled level set and immersed boundary method for predicting dam break flows. *Computer Physics Communications*, Vol. 221, pp.1-18.
- Yu, C.H. Wen, H.L., Gu, Z.H. & An, R. D. 2019. Numerical simulation of dam-break flow impacting a stationary obstacle by a CLSVOF/IB method. *Communications in Nonlinear Science and Numerical Simulation*, Vol.79, 104934, pp.1-14.
- Zhainakov, A.Z. & Kurbanaliev, A.Y. 2013. Verification of the open package OpenFOAM on dam break problems. *Thermophysics and Aeromechanics*, Vol.20, pp. 451-461.
- Zhao, X., Liang, D. & Martinelli, M. 2017. Numerical simulations of dam-break floods with MPM *Procedia Engineering*, 175, pp.133 – 140.

Forced Outage Analysis of Brazilian Thermal Power Plants using the Kruskal-Wallis Test

Leonardo dos Santos e Santos¹

¹ Reliability Engineer, Itaquí Power Plant, Eneva, Brazil

Correspondence: Tel: +55 98 3334 7163. E-mail address: leonardo.santos@eneva.com.br (L. dos Santos e Santos). Current address: Av. dos Portugueses s/n, Módulo G, São Luís, Maranhão, Brasil, 65085-582.
ORCID: 0000 0002 2038 1184.

Abstract

In this paper, the forced outage data from the Brazilian National Interconnected System (SIN) is provided and the statistics from the thermal power plants are computed. The SIN is characterized by a marked seasonality in electricity supply. In addition, the expansion pattern of the Brazilian electric sector shows signs of exhaustion, and the demand for flexible thermal power plants, based on availability, requires outage management as a reliability-centered maintenance (RCM) strategy. In this work, the non-parametric Kruskal-Wallis test and Dunn's pairwise-comparisons were chosen for evaluating the mean forced outage duration (MFOD) and the forced outage factor (FOF) using the data from the national electricity system operator (ONS) with R Software. The distribution fitting was provided using Weibull++ software from Reliasoft. Based on the MFOD and unit failure rate data, the FOF for Brazilian thermal power plants is 3.33% with a 90% probability and 95% confidence level. Finally, Brazilian thermal power plants were benchmarked against North American power plants.

Keywords: Kruskal-Wallis Test, Forced Outage, Thermal Power Plant

1. Introduction

1.1 The Brazilian power grid and its thermal power plants

The Brazilian power grid, known as the national interconnected system (SIN), currently has an installed capacity of 162 GW, of which hydroelectric power plants account for 101.9 GW (62.9%), thermal and nuclear plants account for 22.9 GW (14.1%), and smaller-scale hydropower plant, biomass, wind, and solar plants account for the remaining 37.3 GW (23.0%), as shown in Figure 1 (Nacional do Sistema, 2020a). The recent revision of the long-term load forecasting of the SIN due the socioeconomic impacts caused by the new corona virus, indicates an average power rating of 65.774 GW in 2020 with a progressive increase to 76.612 GW by 2024 (Nacional do Sistema, 2020a). Figure 2 shows the long-term load forecasting.

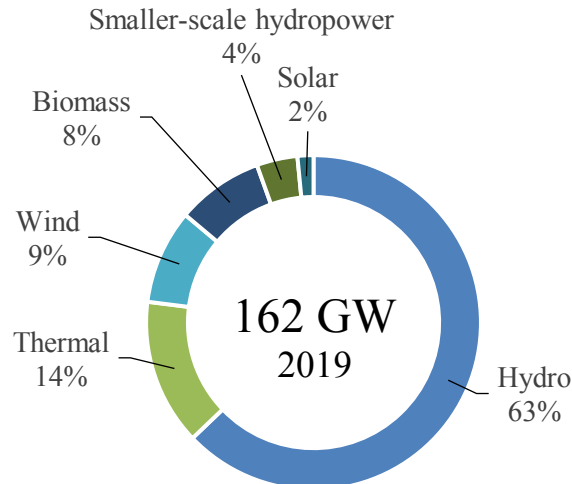


Figure 1: The Brazilian power grid installed capacity by 2019 (Nacional do Sistema, 2020a).

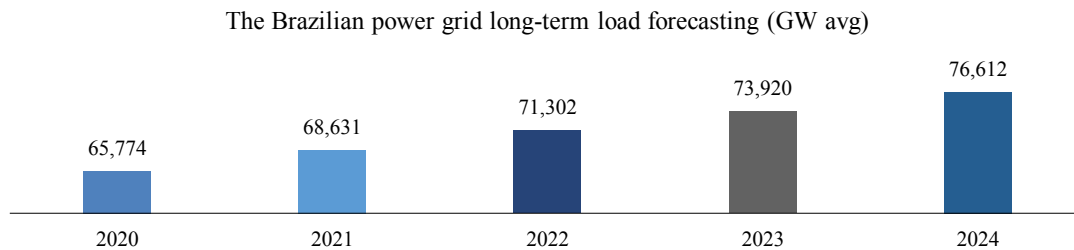


Figure 2: The Brazilian power grid long-term load forecasting (Nacional do Sistema, 2020a).

The Brazilian power grid is characterized by a marked seasonality in electricity supply due to the large production capacity during the rainy season and the run-of-river (ROR) operation of the Madeira complex and Belo Monte hydroelectric plants, thus, there is a constant recovery of the water reservoirs and displacement of the depletion period. However, during the dry season, electricity production is shifted to thermal power plants (Nacional do Sistema, 2020a).

According to the national electricity system operator (ONS), the SIN would have gone through a second critical period (90 months) from the summer of 2011/2012 to the end of 2019, as that of the historic critical period from June 1948 to November 1955 (Nacional do Sistema, 2020a).

Due to the predominance of hydraulic-powered electricity generation in the SIN, the contracting of thermal power plants is based on availability. This is because the cost merit, economic benefit, and security risk mitigation needed to supply the national power demand need to be evaluated before considering the use of contracted energy. These factors are evaluated based on the remuneration for the availability of the thermal generator and the reimbursement of operating costs incurred with the actual plant dispatch (Center for Regulatory and Infrastructure Studies, 2017). Figure 3 presents the load in the SIN from 2016 to 2020.

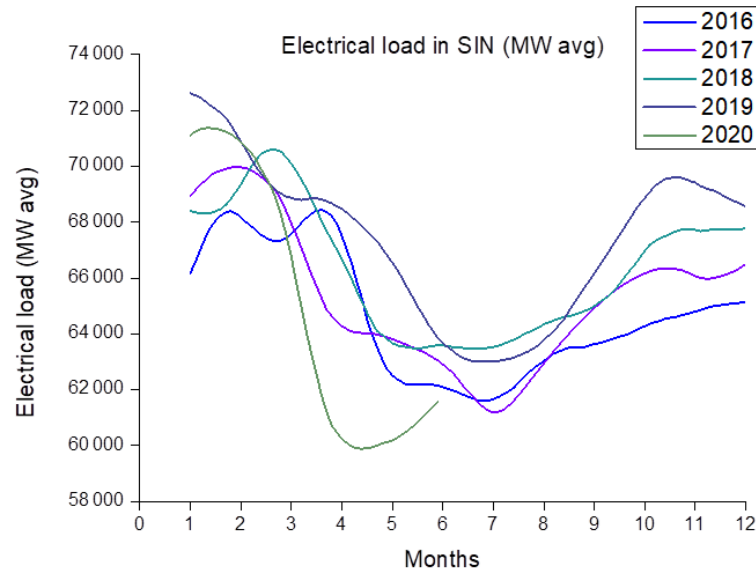


Figure 3: Electrical load in SIN from 2016 to 2020 (MW avg). Adapted from (Nacional do Sistema, 2017, 2018, 2019a, 2020b).

Currently, thermal power generation in Brazil has a high variable unit cost (CVU), with 40% of the installed capacity having a CVU of over 250 BRL/MWh (~47 USD/MWh). This indicates that thermal power plants are used for electrical dispatch only in extremely unfavorable hydrological conditions, thus, increasing the challenges for maintaining the water level in reservoirs (Nacional do Sistema, 2020a).

The ONS, a private entity created in 1998, coordinates and controls the operations of the power generation and transmission facilities integrated in the SIN. In addition, the ONS evaluates the future and short-term conditions of these facilities (Sousa, 2009).

The decision-making process of the ONS is regulated by the grid procedures and approved by the Brazilian Electricity Regulatory Agency (ANEEL) through public hearings. In addition, the ONS provides ANEEL with input data and optimization models, to enable the reproduction of the method used for determining the plants' dispatch (Sousa, 2009).

In summary, the ONS functions to minimize the service cost, thus, decreasing the risk of insufficient power supply in each subsystem that composes the SIN. Thermal power stations operation provides efficiency gains during the dry and low-pour period, thus, increasing the firm energy of the system (Sousa, 2009).

According to the National Confederation of Industry, the national thermoelectric system of Brazil was originally contracted as a reserve for sporadic electrical performance during unfavorable hydrological periods. However, the data presented by Chamber of Electric Energy Commercialization (CCEE) show that the percentage of thermal power plants in the SIN load is approximately 16.5% (De Comercialização de Energia Elétrica, 2020) at most times in the base operation (National Confederation of Industry, 2018).

The base operation is aimed at complementing electrical generation at all load levels. In addition to this, there is also the peak operation, which occurs in periods of fluctuating demand, and the operation aimed at performing ancillary services such as (Ribeiro, 2019): controlling (i) primary frequency, (ii) secondary frequency, (iii) reactive support, (iv) self-restoration, (v) special protection system (SEP), and (vi) complementary dispatch for maintaining the operational power reserve (Nacional do Sistema, 2019b).

However, the expansion pattern of the Brazilian electric sector shows signs of exhaustion, with the inclusion of the ROR and intermittent renewable sources (wind and solar). Consequently, there is a growing demand for flexible thermal power plants operated in an electric dispatch mode (National Confederation of Industry, 2018).

The structural trend in the SIN involves the gradual reduction in the capacity of country's reservoirs regularization. Therefore, to recover water storage, thermal power complementation needs to be carried out more frequently and for longer periods, even during hydrological periods close to the long-term average (National Confederation of Industry, 2018).

In a study carried out by (Nogueira et al., 2019), they reported that 50% of Brazilian hydroelectric plants are over 20 years old and 32% are over 40 years old. The aging of these plants is the major cause for the increasing frequency and duration of maintenance interventions, whether as scheduled or due to forced shutdowns.

ANEEL calculates the unavailability of hydroelectric plants based on two key performance indicators (KPI): scheduled unavailability rate (IP) and equivalent rate of forced unavailability (TEIF). The IP quantifies the percentage of hours that the turbo-generator was turned off to carry out scheduled maintenance, while the TEIF quantifies the percentage of hours that the equipment remained in forced shutdown (Ministério de Minas e Energias, 2014). The reference values of the KPI are shown in Table 1.

Table 1: Reference values of the forced outages of hydroelectric plants (Ministério de Minas e Energias, 2014).

Hydroelectric MW Trb/Gen	TEIF (%) ¹
001–029	2.068
030–059	1.982
060–199	1.638
200–699	2.133
700–1300	3.115

¹ TEIF is harmonized with Forced Outage Factor (FOF) indicator from IEEE Std 762™-2006 (IEEE, 2007)

The Brazilian electrical system (SEB) contracts are based on physical guarantee through energy guaranty contracts certified by the Ministry of Mines and Energy (MME) (Castro et al., 2016). One of the main performance risks for power plants is related to the decreasing physical guarantee due to unavailability, thus, leading to a reduction in the revenue of the commercialization of Electric Energy in Regulated Environments (CCEAR) and an increase in the additional costs for the acquisition of ballast in the Short-Term Market (MCP) (Martins, 2013).

The unavailability of each plant is computed by the ONS using the IP and TEIF. These values are calculated monthly, based on the moving average of the previous 60 months. If the verified unavailability KPIs are higher than those declared, there will be a reduction in the physical guarantee (Martins, 2013).

Therefore, to minimize the risk of not supplying the national power demand, the combination of these variables is important: (i) basis operation, (ii) aging of hydroelectric plants, and (iii) flexible dispatch requirements: and demands from thermal power plants, high availability, and reliability standards.

1.2 Maintenance at Thermal Power Plants

Maintenance Management at the generating units is important for an economically optimized electrical dispatch in hydrothermal generation systems. However, it is challenging to choose the best schedule for preventive maintenance to minimize the operating cost of the generating agency, maximize the reliability of the system, and extend the units' operational life. In addition, with an increase in the size of the generating unit, the challenges also increase (Balaji et al., 2016). The maintenance costs of thermal power plants are greatly influenced by: (i) the type of starting, (ii) the frequency of starting, and (iii) the loading pattern (Dipak, 2015a). Figures 4 and 5 show examples of the effect of these factors on a gas turbine.

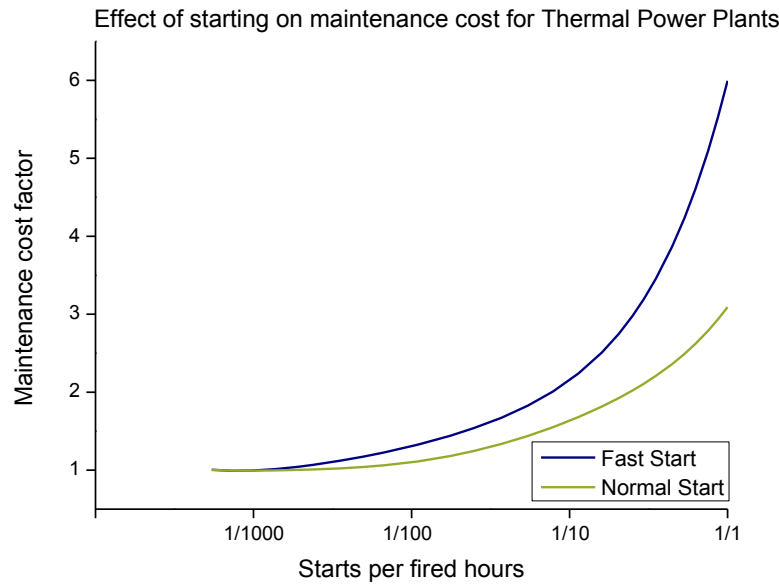


Figure 4: Effect of starting on maintenance cost. Adapted from (Dipak, 2015a).

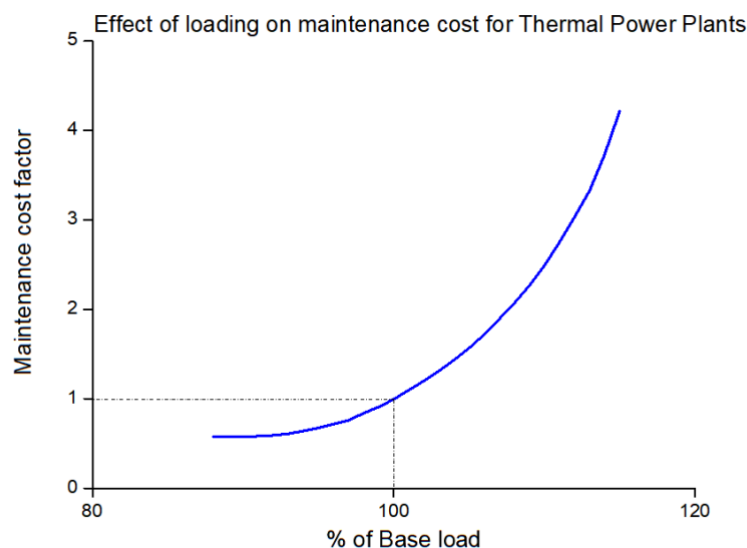


Figure 5: Effect of loading on maintenance cost. Adapted from (Dipak, 2015a).

Currently, the steam thermal power plants have larger sizes with a high steam-generating capacity and highly sophisticated firing system. However, with an increase in the unit size and capacity of thermal plants, forced outages have greater significance not only on the larger loss of revenue, but also greater risk of injury and damage to the plants (Dipak, 2015b).

To effectively manage these challenges, the reliability-centered Maintenance (RCM) process is carried out. The RCM process is a common-sense procedure for creating maintenance strategies to preserve assets' functions. The standard SAE JA1011, published in 1999, sets the criteria that any process must comply with to be considered an RCM. It establishes that for a process to be acknowledged as RCM, it must follow these seven steps (Sifonte and Reyes-Picknell, 2017):

- i. Delineate the operational context and the functions, and associated desired standards of assets performance (operational context and functions)
- ii. Determine how an asset can fail to fulfill its functions (functional failures)
- iii. Define the causes of each functional failure (failure modes)

- iv. Describe what happens when each failure occurs (failure effects)
- v. Classify the consequences of failure (failure consequences)
- vi. Determine what should be performed to predict or prevent each failure (tasks and intervals)
- vii. Decide whether other failure management strategies may be more effective (one-time changes).

Some uncertainties in thermal power plant dispatch can cause deviations from the system balance, which sometimes require inefficient and costly last-minute solutions in the near real-time time frame (Makarov et al., 2017). These uncertainties include: (i) uninstructed deviations of conventional generators from their dispatch set points, (ii) generator forced outages, (iii) generator failures to start up, (iv) load drops, (v) losses of major transmission lines, and (vi) frequency variation (Makarov et al., 2017).

Outage management organization and administration ensures the safe and effective implementation and control of the maintenance activities during planned and forced outages. Outage planning and performance takes into consideration the safety, quality, and schedule in this order. Thus, the maintenance planning and scheduling process should reflect this (Lipár, 2012).

The objective of this study is to perform a multiple pairwise-comparisons of the annual forced shutdown statistics by ONS using the Kruskal-Wallis non-parametric test to verify if the populations' distributions have changed over the years. This allows for the computing of the reliability analysis for the forced outage data and to analyze the availability of thermal power plants and comparing it to benchmarks.

2. Materials and Methods

2.1 Thermal power plants: forced shutdown statistics

Forced shutdown involves the unscheduled removal of a component out of service due to failure or emergency shutdown. Forced shutdown requires the manual or automatic switching off of an equipment to avoid risks to the physical integrity of the people or the environment, or damage to the equipment, or other consequences to the electrical system. It includes accidental shutdown (without disturbance in the SIN), incorrect shutdown (with disturbance in the SIN), and shutdown resulting from SEP or configuration actions (Nacional do Sistema, 2019 c).

The ONS provides performance and statistical reports issued from the generating units belonging to the SIN. Therefore, to apply the methodology used in this work, the report ONS DPL-REL-0099/2020: *Relatório de Análise Estatística de Desligamentos Forçados de Equipamentos Referente ao ano de 2019* (Statistical Analysis Report on Forced Equipment Shutdowns for 2019) was analyzed (Nacional do Sistema, 2019 c).

The ONS reported that the occurrence of the unsatisfactory operational performance of a thermal power plant directly impacts the security and reliability of electricity supply and energy tariffs, given that its unavailability causes the generation of another power unit with a higher CVU (Agência Nacional de Energia Elétrica, 2020).

The consolidated data of the forced shutdowns of thermal generators are presented using the indicators: Mean Forced Shutdown Duration for Transmission and Generation Functions (DMDF) and Forced Shutdown Rate for Transmission and Generation Functions (TDFF) (Nacional do Sistema, 2019c).

The DMDF indicator aims to manage the performance of the transmission, transformation, reactive control, and the generation functions, regarding the mean duration of the forced shutdowns during the period considered. The DMDF is calculated as follows (Nacional do Sistema, 2019d):

$$DMDF = \frac{\text{Forced outage hours (FOH)}}{\text{Numbers of unplanned outages from in service state}} \quad \text{Eq. 1}$$

The TDFF indicator aims to manage the rate of forced shutdowns on the transmission and generation functions during service hours at the period considered. The TDFF is calculated as follows (Nacional do Sistema, 2019d):

$$TDFF = \frac{\text{Numbers of unplanned outages from in service state}}{\text{Service Hours (SH)}} \times 8760 \quad \text{Eq. 2}$$

Where:

The constant value 8760 is the annualization factor – 24 h for 365 d.

The TEIF, DMDFF, and TDFF indicators may be harmonized with the IEEE Standard Definitions for use in Reporting Electric Generating Unit Reliability, Availability, and Productivity, IEEE Std 762TM-2006 as follows (IEEE, 2007):

$$MFOD = DMDFF \quad \text{Eq. 3}$$

$$\text{Unit Failure Rate} = \frac{1}{MSTFO} = TDFF \quad \text{Eq. 4}$$

$$FOF = \left(\frac{FOH}{PH} \right) \times 100 = TEIF = \frac{\text{Unit Failure Rate} \times MFOD}{PH} \times 100 \quad \text{Eq. 5}$$

Where MFOD is the mean forced outage duration and MSTFO is the mean service time to forced. PH is the period hours or active hours and it represents the number of hours a unit was in the active state, FOF is the forced outage factor, i.e., the fraction of a given operating period in which a generating unit was not available due to forced outages. The IEEE nomenclature was adopted to present the consolidated data in this work.

2.2 Kruskal-Wallis test and Multiple pairwise-comparisons

The data from the statistic report provided by ONS presents the information grouping over a 5 years interval (2015 to 2019). In this study, the Kruskal-Wallis (KW) test was performed to test the null hypothesis (H_0) that the annual probability distributions of the Brazilian thermal generators are equal. The KW test is a well-known non-parametric test applied in a wide range of disciplines such as engineering and manufacturing applications, medicine, biology, psychology, and education (Ostertagová et al., 2014).

The KW test, named in honor of the American statisticians William Kruskal and W. Allen Wallis, was created in 1952 and is a non-parametric test used to compare three or more populations. The test does not make assumptions about normality. However, it assumes that the populations have the same distribution, and that the samples are random and independent (Ostertagová et al., 2014; Ronald et al., 2007; Moreno et al., 2019).

The KW test requires that the data come from continuous probability distributions. The H_0 being tested by the KW statistic assumes that all the population distributions are equal, and the alternative hypothesis (H_1) assumes that at least two population distributions differ from each other (Ostertagová et al., 2014; Ronald et al., 2007). Data are pooled across groups and ranked from the lowest value of the dependent variable to the highest value. In case of a tie, the average rank is attributed to the tied experimental values (Andrew, 1998).

According to McDonald, , the KW test also assumes that the variation within the groups is equal (homoscedasticity), however, groups with different standard deviations have different distributions. Thus, if different groups have different shapes, the KW test may give inaccurate results (McDonald, 2007; Fagerland and Sandvik, 2009).

Since the KW test assumes that different groups have similar distribution, and groups with different standard deviations have different distributions, if the data are heteroscedastic, KW is no better than the one-way ANOVA and may be worse. For heteroscedastic data, the Welch's ANOVA is preferred (McDonald, 2007).

The H_0 of KW assumes that the distribution for all k populations are similar, while the H_1 assumes that the distribution of at least two population differs. H_0 and H_1 can be expressed as follows (Andrew, 1998):

$$H_0: F_1(x) = F_2(x) = \dots = F_k(x) \quad \text{Eq. 6}$$

$$H_1: \exists 1 \leq i, l \leq k: F_i(x) \neq F_l(x) \quad \text{Eq. 7}$$

The sum of the ranks R_i is calculated for each group i ($i = 1, 2, \dots, k$) of size n_i , then the test statistic H is calculated, which represents the variance of the ranks among all groups, with an adjustment for the number of ties (Hecke, 2010).

$$H = \left(\frac{12}{N(N+1)} \sum_{i=1}^k \frac{R_i^2}{n_i} \right) - 3(N+1), \quad N = \sum_{i=1}^k n_i \quad \text{Eq. 8}$$

Where n_i is the sample size for the i^{th} group, R_i is the rank-sum for the i^{th} group, N is the total sample size, and k is the number of groups.

If there are many ties in the samples, a correction factor must be applied, and the test statistic corrected for the ties will be (Ostertagová et al., 2014; Hollander et al., 2013):

$$H^* = \frac{H}{f^*}, \quad f^* = 1 - \left(\frac{\sum_{i=1}^m (t_i^3 - t_i)}{N^3 - N} \right) \quad \text{Eq. 9}$$

Where t_i is the number of ties in the i^{th} group of the m ties groups, f^* is the correction factor, H is the KW statistic, and H^* is the KW statistic corrected for ties.

Whenever H_0 is true and either (Ostertagová et al., 2014):

$$\begin{cases} k = 3, n_i \geq 6 \text{ for } i = 1, 2, 3 \\ k > 3, n_i \geq 5 \text{ for } i = 1, 2, \dots, k \end{cases} \quad \text{Eq. 10}$$

The distribution of the test statistic, H , is approximated using the chi-square distribution with $(k-1)$ degrees of freedom. The H_0 is rejected on the right-hand tail of the chi-square distribution (Ostertagová et al., 2014)

After the test statistic is calculated, the p-value is then calculated. The p-value is defined as the probability of observing the given value of the test statistic, or greater, under the H_0 (Ferreira and Patino, 2015).

That is, the H_0 is rejected on a significance level α , when a one-sided p-value is less than the significance level (Ferreira and Patino, 2015):

$$P[\chi^2(k) > H] < \alpha \quad \text{Eq. 11}$$

Where α is the significance level, i.e., the probability of making the wrong decision when the H_0 is true, χ^2 is the quantile of the chi-square distribution, and H is the statistic from the KW test.

2.3 Effect size for the Kruskal–Wallis test

The statistics of the effect size for the KW test provide the degree to which the data of one group has higher ranks than that of another group. The effect size is related to the probability that the value from one group will be greater than the value from another group (Mangiafico, 2016).

The eta-squared coefficient can be calculated as the measure of the KW test effect size. According to Prajapati et al., eta is a measure of association and is the proportion of the total variance that is attributed to an effect (Prajapati et al., 2010). Eta-squared ranges from 0 to 1, and as a rule, 0.01 is a small effect, 0.06 is a moderate effect, and 0.14 is a large effect (Laerd Statistics, 2020).

$$E_R^2 = \frac{H}{(N^2 - 1)/(N + 1)}, \quad \begin{cases} 0.01 \text{ to } 0.06, \text{ small effect} \\ 0.06 \text{ to } 0.14, \text{ moderate effect} \\ \text{from } 0.14 \text{ on, large effect} \end{cases} \quad \text{Eq. 12}$$

Where H is the statistic from the KW Test, k is the number of groups, and N is the total number of observations. According to Ferreira and Patino, there is a misconception that a very small p-value indicates a highly relevant difference between groups. However, it is necessary to consider the effect size, as it may indicate that the sample size should be increased. The authors recommend preferably reporting the mean values for each group, the difference, and the 95% confidence interval, and then the p-value (Ferreira and Patino, 2015).

This significant result in a KW test indicates that there are group differences, however it does not indicate which groups. Thus, a *post hoc* procedure can be used to determine which groups are different from each other (Andrew, 1998).

According to Laerd Statistics, if the populations distributions have similar shapes, then, the medians can be compared to evaluate the distribution differences (Laerd Statistics, 2020). However, when the distribution shapes are different, the mean rank from the KW test should be considered. This is because with an increase in the group's mean rank, the observation values in that group increases in comparison to those of the other groups (Minitab 19 Support, 2020). The concept is shown in Figure 6.

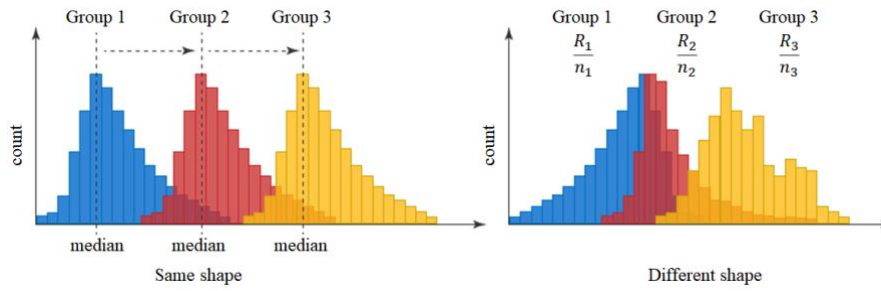


Figure 6: Evaluation criteria for the populations shape in KW test. Adapted from (Laerd Statistics, 2020).

The KW test does not assume normality but assumes that the shapes of the distributions in different groups are similar. This suggests that non-parametric tests are not a good solution for heteroscedastic data (McDonald, 2007).

According to Dinno, in the case of a rejected H_0 , the Dunn's test should be performed after the KW test (Dinno, 2015). The Dunn's test is based on the normal distribution with Bonferroni correction, where n_c is the possible number of two-to-two comparisons that will be made between the k groups (Moreno et al., 2019).

$$n_c = C_2^k = \frac{k!}{2!(k-2)!} = \frac{k(k-1)}{2} \quad \text{Eq. 13}$$

The test involves the comparison of the module of the differences between the means of the ranks for two groups $|\bar{R}_i - \bar{R}_j|$ with the least significant difference (LSD) (Moreno et al., 2019).

$$LSD = Z_{(\alpha_c)} \sqrt{\left[\frac{N(N+1)}{12} \left(\frac{1}{n_i} + \frac{1}{n_j} \right) \right]}, \quad \alpha_c = \frac{\alpha}{k(k-1)/2} \quad \text{Eq. 14}$$

Where:

LSD is the least significant difference, α_c is the Bonferroni's correction, α is the significance level, n_i and n_j are the sample sizes of two compared populations, N is the total sample size, and Z_{α_c} comes from negative Z score table for α_c (Moreno et al., 2019).

When $|\bar{R}_i - \bar{R}_j| \geq LSD$, H_0 is rejected, and the pairwise comparison shows that two compared populations are significantly different (Moreno et al., 2019).

2.4 Reliability analysis for the forced outage data

The analysis method proposed in this work considers all the thermal generators dispatched centrally and belonging to the selected facilities according to the ONS's criteria (see Table 2) (Nacional do Sistema, 2019c):

- i. Thermal power plants with an effective power equal to or greater than 300 MW.
- ii. Thermal power plants with $200 \text{ MW} \leq \text{effective power} < 300 \text{ MW}$, with a transformation equal to or greater than 230 kV.
- iii. Thermal power plants powered by natural gas, coal, and nuclear sources.

Table 2: Centrally dispatched thermal power plants according to the ONS's criteria for statistical analysis (Nacional do Sistema, 2019c).

Number of centrally dispatched Thermal Power Plants				
2015	2016	2017	2018	2019
106	108	109	111	112

The MFO and unit failure rate indicators from the thermal power plants are presented for 2015 to 2019, as shown in Table 3 and Appendix 1. While the causes of the forced outages are shown in Figure 7 (Nacional do Sistema, 2019c):

Table 3: Centrally dispatched Thermal Power Plants KPIs according to ONS's criteria (Nacional do Sistema, 2019c).

Centrally dispatched Thermal Power Plants KPIs					
KPI/Year	2015	2016	2017	2018	2019
Mean Forced Outage Duration	7.103	7.346	5.383	6.312	11.631
Unit Failure Rate	8.852	4.761	5.452	3.976	5.112

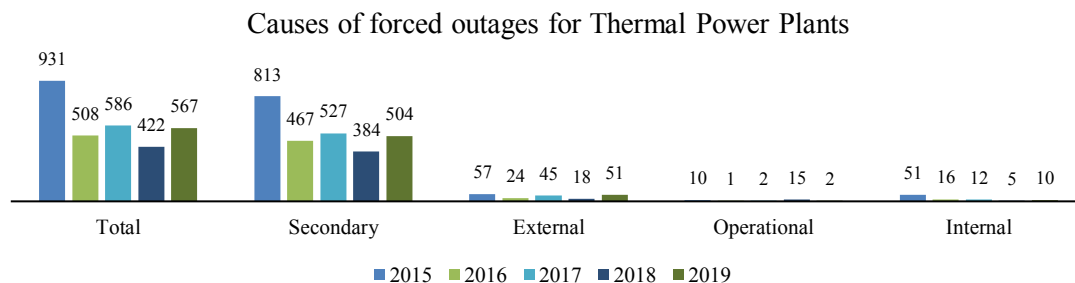


Figure 7: Causes of forced outages for the thermal power plants. Adapted from (Nacional do Sistema, 2019c).

Based on the criteria by ONS, there are four major reasons for the forced power outage of power plants in SIN (Nacional do Sistema, 2019c):

- i. **Internal outage**, which is related to the main parts of the power plant such as the insulators, the primary winding from transformers, stator, bearing and generator shaft, circuit breakers, and others.
- ii. **Secondary outage**, which is related to the complementary or auxiliary equipment of the power plants such as wiring, protection, control, command, auxiliary services, ventilation, and cooling system. In addition, it also includes outages due to the incorrect performance from the protection system in case of external failures.
- iii. **External outage**, which is related to the outage due to the correct performance of the protection system due to failures (acting as a back-up protection) or due to overload caused by outage from a third party. In addition, it also includes the outage caused by system configuration.
- iv. **Operational outage**, which is related to systemic electrical conditions such as oscillations, overvoltage, over-frequency, overload, and other systemic causes.

3. Results

The KW non-parametric test was computed using R software. The R software is a free software used for statistical computing and for the construction of graphics that can be downloaded and distributed free of charge under the GNU license (Landeiro, 2011; R Development Core Team, 2011).

The prerequisites for computing the KW test using R software require the R packages: (i) *tidverse* for data manipulation and visualization (Wickham et al., 2019), (ii) *ggpubr* for creating ready to publish plots (Alboukadel, 2020a), and (iii) *rstatix*, which provides R functions for statistical analyses (Alboukadel, 2020b).

The available data from the ONS were prepared using comma-separated values (CSV) grouped into two columns: weight (KPI value) and group (year).

```
library(tidyverse)
library(ggpubr)
library(rstatix)
mfod <- read.csv2("dmdff.csv")
rate <- read.csv2("tdff.csv")
```

Subsequently, the summary statistics was computed by groups using the *kruskal_test* function from the *rstatix* package (DataNovia, 2020). Since the number of groups used in this study was greater than 3 and the sample size was greater than 5 for all groups, according to Eq. 10, the distribution of the test statistic, H , was well approximated using the chi-square distribution with $(5 - 1)$ degrees of freedom. The significance level chosen was $\alpha = 0.05$. Manual calculations were performed to determine the mean ranks (R_i/n_i), and the results are shown in Tables 4 and 5.

Table 4: KW test mean rank for the mean forced outage duration.

Year	Sample size	Rank-sum	(Rank-sum) ² /sample size	Mean rank
2015	94	20 699.00	4 557 963.84	220.20
2016	80	16 304.50	3 322 959.00	203.81
2017	86	16 222.50	3 060 110.54	188.63
2018	86	18 561.00	4 005 938.62	215.83
2019	86	21 741.00	5 496 175.36	252.80
Total	432	93 524.00	20 443 147.36	-

Table 5: KW test mean rank for the unit failure rate.

Year	Sample size	Rank-sum	(Rank-sum) ² /sample size	Mean rank
2015	97	28 123.00	8 153 640.51	289.93
2016	82	17 365.00	3 677 356.40	211.77
2017	89	20 415.50	4 683 063.37	229.39
2018	88	16 236.00	2 995 542.00	184.50
2019	93	18 885.50	3 835 076.45	203.07
Total	449	101 025.00	23 344 678.74	-

Mean forced outage duration statistics:

```
mfod %>% group_by(group) %>% get_summary_stats(weight, type = "common")
# A tibble: 5 x 11
  group variable      n  min  max median  iqr  mean   sd   se   ci
  <int> <chr>      <dbl> <dbl> <dbl> <dbl> <dbl> <dbl> <dbl> <dbl>
1  2015 weight      94 0.283 51.8   5.44 5.12  6.91  6.33 0.653 1.30
2  2016 weight      80 0.175 64.7   5.41 5.16  7.14  8.50 0.95  1.89
3  2017 weight      86 0.508 28.2   4.38 4.72  5.74  4.89 0.527 1.05
4  2018 weight      86 0.267 20.2   5.49 5.30  6.29  4.12 0.444 0.883
5  2019 weight      86 0.467 72.0   6.36 7.85 12.1 15.1  1.63  3.24
```

Unit failure rate statistics:

```
rate %>% group_by(group) %>% get_summary_stats(weight, type = "common")
```

```
# A tibble: 5 x 11
  group variable     n  min  max median  iqr mean   sd   se   ci
  <int> <chr>      <dbl> <dbl> <dbl> <dbl> <dbl> <dbl> <dbl> <dbl> <dbl>
1  2015 weight    97  1.00  27.4   8.02  9.01  9.10  5.87  0.596  1.18
2  2016 weight    82  1    18.2   5.00  4.02  5.90  4.27  0.472  0.938
3  2017 weight    89  1    20.2   5.02  4.02  6.18  3.79  0.402  0.799
4  2018 weight    88  1    80.3   4.51  4.04  5.64  8.78  0.936  1.86
5  2019 weight    93  1    38.8   4.07  4.04  5.94  5.90  0.612  1.22
```

Where N is the number of individuals, min is the minimum value, max is maximum value, $median$ is the median, $mean$ is the mean, sd is the standard deviation of the mean, se is the standard error of the mean, and ci is the 95% confidence interval of the mean (Kassambara, 2020a).

Mean forced outage duration Kruskal-Wallis test:

```
res.krskal <- mfod %>% kruskal_test(weight ~ group)
res.krskal
# A tibble: 1 x 6
  .y.      n statistic    df      p method
* <chr> <int>      <dbl> <int>  <dbl> <chr>
1 weight  432      12.5     4 0.0142 Kruskal-Wallis
```

Unit failure rate Kruskal-Wallis test:

```
res.krskal <- rate %>% kruskal_test(weight ~ group)
res.krskal
# A tibble: 1 x 6
  .y.      n statistic    df      p method
* <chr> <int>      <dbl> <int>  <dbl> <chr>
1 weight  449      36.5     4 0.000000231 Kruskal-Wallis
```

Where $.y.$ is the y variable used in the test, n is the sample count, $statistic$ is the Kruskal-Wallis rank-sum statistic used to compute the p -value, df is the degree of freedom, p is the computed p -value, and $method$ is the statistical test used to compare groups (Kassambara, 2020b).

The p -values of the computed KW test was less than a 0.05 significance level, thus, rejecting the H_0 for both KPIs, indicating that at least two population distributions differ from each other.

After computing the KW p -values and plotting the boxplots, the statistics of effect size for the test was verified by computing the eta-squared from the `kruskal_effsize` function:

Mean forced outage duration effect size:

```
mfod %>% kruskal_effsize(weight ~ group)
# A tibble: 1 x 5
  .y.      n effsize method magnitude
* <chr> <int>      <dbl> <chr>  <ord>
1 weight  432  0.0198 eta2[H] small
```

Unit failure rate effect size:

```
rate %>% kruskal_effsize(weight ~ group)
# A tibble: 1 x 5
  .y.      n effsize method magnitude
```



```
* <chr> <int> <dbl> <chr> <ord>
1 weight 449 0.0732 eta2[H] moderate
```

Where *.y.* is the y variable used in the test, *n* is the sample counts, *effsize* is the estimate of the effect size, *method* is the eta-squared, and *magnitude* is the magnitude of effect size (Kassambara, 2020c).

This significant results in the KW tests indicate that there were group differences, however it does not indicate which groups. Thus, a Dunn test procedure was used to determine which groups were different from each other.

Mean forced outage duration Dunn test:

```
# Pairwise comparisons
pwc <- mford %>%
  dunn_test(weight ~ group, p.adjust.method = "bonferroni")
pwc
# A tibble: 10 x 9
  .y.    group1 group2   n1    n2 statistic      p    p.adj p.adj.signif
* <chr> <chr> <chr> <int> <int> <dbl> <dbl> <dbl> <chr>
1 weight 2015 2016    94    80  -0.863 0.388    1      ns
2 weight 2015 2017    94    86  -1.69  0.0902  0.902    ns
3 weight 2015 2018    94    86  -0.235 0.814    1      ns
4 weight 2015 2019    94    86   1.75  0.0801  0.801    ns
5 weight 2016 2017    80    86  -0.782 0.434    1      ns
6 weight 2016 2018    80    86   0.620 0.535    1      ns
7 weight 2016 2019    80    86   2.53  0.0115  0.115    ns
8 weight 2017 2018    86    86   1.43  0.153    1      ns
9 weight 2017 2019    86    86   3.37  0.000751 0.00751 **
10 weight 2018 2019    86    86   1.94  0.0521  0.521    ns
```

Unit failure rate dunn test:

```
# Pairwise comparisons
pwc <- rate %>%
  dunn_test(weight ~ group, p.adjust.method = "bonferroni")
pwc
# A tibble: 10 x 9
  .y.    group1 group2   n1    n2 statistic      p    p.adj p.adj.signif
* <chr> <chr> <chr> <int> <int> <dbl> <dbl> <dbl> <chr>
1 weight 2015 2016    97    82  -4.02 0.0000593 0.000593 ***
2 weight 2015 2017    97    89  -3.18 0.00148 0.0148 *
3 weight 2015 2018    97    88  -5.52 0.0000000340 0.000000340 ****
4 weight 2015 2019    97    93  -4.61 0.00000397 0.0000397 ****
5 weight 2016 2017    82    89   0.887 0.375    1      ns
6 weight 2016 2018    82    88  -1.37 0.171    1      ns
7 weight 2016 2019    82    93  -0.443 0.658    1      ns
8 weight 2017 2018    89    88  -2.30 0.0214 0.214    ns
9 weight 2017 2019    89    93  -1.37 0.171    1      ns
10 weight 2018 2019    88    93   0.962 0.336    1      ns
```

Where *.y.* is the y variable used in the test, *group1* and *group2* are the compared groups in the pairwise tests, *n1* and *n2* are the sample counts, *statistic* is the test statistic (z-value) used to compute the p-value, *p* is the p-value, *p.adj* is the adjusted p-value, and *p.adj.signif* is the significance level of the p- adjusted p-values, respectively (Kassambara, 2020d).

The following convention for symbols indicates statistical significance (STHDA, 2017): *ns* means $p > 0.05$, * means $p \leq 0.05$, ** means $p \leq 0.01$, *** means $p \leq 0.001$, and **** means $p \leq 0.0001$.

To identify the differences between the consolidated annual values, boxplot graphs were plotted, as shown in figures 8 and 9.

Mean forced outage duration boxplot:

```
# Visualization: box plots with p-values
pwc <- pwc %>% add_xy_position(x = "group")
ggboxplot(mfod, x = "group", y = "weight",
          color = "group", palette = c("#00AFBB", "#E7B800", "#FC4E07", "#3CB371", "#BA55D3"),
          order = c("2015", "2016", "2017", "2018", "2019"),
          ylab = "Mean Forced Outage Duration", xlab = "Year"
) +
  stat_pvalue_manual(pwc, hide.ns = TRUE) +
  labs(
    subtitle = get_test_label(res.kruskal, detailed = TRUE),
    caption = get_pwc_label(pwc)
  )
```

Unit failure rate boxplot:

```
# Visualization: box plots with p-values
pwc <- pwc %>% add_xy_position(x = "group")
ggboxplot(rate, x = "group", y = "weight",
          color = "group", palette = c("#00AFBB", "#E7B800", "#FC4E07", "#3CB371", "#BA55D3"),
          order = c("2015", "2016", "2017", "2018", "2019"),
          ylab = "Unit Failure Rate", xlab = "Year"
) +
  stat_pvalue_manual(pwc, hide.ns = TRUE) +
  labs(
    subtitle = get_test_label(res.kruskal, detailed = TRUE),
    caption = get_pwc_label(pwc)
  )
```

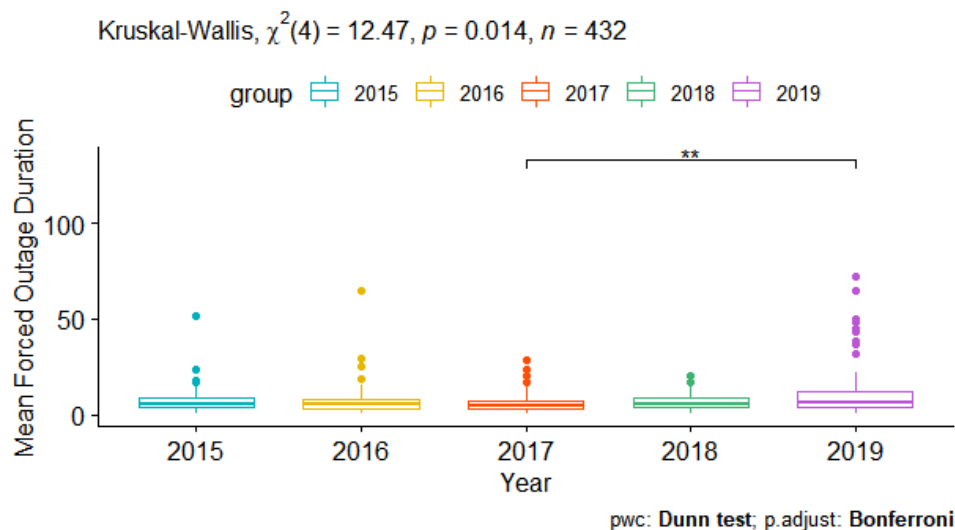


Figure 8: Mean forced outage duration boxplot.

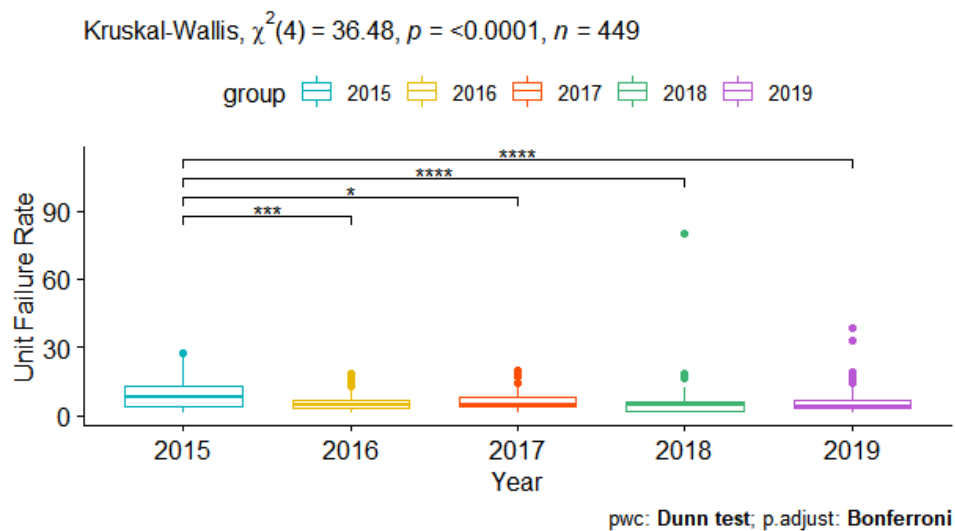


Figure 9: Unit failure rate boxplot.

To verify the distribution fitting for the annual data from the MFOD and the unit failure rate, the data was fitted using the distribution wizard from software Weibull++ (version 19.0.2.1075, from Reliasoft). According to Reliasoft, the distribution wizard performs multiple goodness of fit tests to determine the best distribution for a data set based on the chosen parameter estimation method. In addition, it performs three goodness of fit tests to determine the rank of the distributions (Reliasoft, 2017):

- The Kolmogorov-Smirnov test (Goodness of fit – GOF) tests used to determine the statistical difference (the difference between the expected and obtained results). Default weighted in 40% for the Maximum likelihood (MLE) analysis method.
- The Correlation coefficient test (Plot fit – PLOT) measures how well the plotted points fit a straight line. Default weighted in 10% for the MLE analysis method.
- The Likelihood value test (Likelihood Ratio – LKV) computes the value of the log-likelihood function, given the parameters of the distribution. Default weighted in 50% for the MLE analysis method.

Tables 6 and 7 show the distribution fitting for the MFOD and unit failure rate. The top ranked distributions implemented for each year and KPI.

Table 6: Mean forced outage duration distribution fitting.

Mean forced outage duration distribution fitting									
2015		2016		2017		2018		2019	
Distribution/ Ranking		Distribution/ Ranking		Distribution/ Ranking		Distribution/ Ranking		Distribution/ Ranking	
Loglogistic	1	Loglogistic	1	G-Gamma	1	G-Gamma	1	Loglogistic	1
G-Gamma	2	G-Gamma	2	3P-Weibull	2	3P-Weibull	2	G-Gamma	2
Gamma	3	Lognormal	3	Gamma	3	2P-Weibull	3	Lognormal	3
Lognormal	3	2P-Exponential	4	Lognormal	4	Gamma	4	3P-Weibull	4
2P-Weibull	4	3P-Weibull	5	2P-Exponential	5	Loglogistic	5	2P-Weibull	5
3P-Weibull	5	Gamma	6	Loglogistic	6	Logistic	6	2P-Exponential	6
2P-Exponential	6	1P-Exponential	7	2P-Weibull	7	Lognormal	7	1P-Exponential	7
Logistic	7	2P-Weibull	8	Logistic	8	2P-Exponential	8	Gamma	7
1P-Exponential	8	Logistic	9	1P-Exponential	9	Normal	9	Logistic	8
Normal	9	Normal	10	Normal	10	Gumbel	10	Normal	9

Gumbel 10 Gumbel 11 Gumbel 11 1P-Exponential 11 Gumbel 10

Table 7: Unit failure rate distribution fitting.

Unit failure rate distribution fitting									
2015		2016		2017		2018		2019	
Distribution/ Ranking		Distribution/ Ranking		Distribution/ Ranking		Distribution/ Ranking		Distribution/ Ranking	
3P-Weibull	1	3P-Weibull	1	G-Gamma	1	Lognormal	1	G-Gamma	1
G-Gamma	2	Gamma	2	3P-Weibull	2	G-Gamma	2	Lognormal	1
Gamma	3	G-Gamma	3	Gamma	3	3P-Weibull	3	Loglogistic	2
2P-Weibull	4	2P-Exponential	4	2P-Weibull	4	Loglogistic	4	2P-Exponential	3
Lognormal	5	2P-Weibull	5	Loglogistic	5	Gamma	5	3P-Weibull	4
Loglogistic	6	Lognormal	6	Logistic	6	2P-Exponential	6	2P-Weibull	5
Logistic	7	Loglogistic	6	Lognormal	7	2P-Weibull	7	Gamma	6
2P-Exponential	8	Logistic	7	2P-Exponential	8	1P-Exponential	8	1P-Exponential	7
Normal	9	1P-Exponential	8	Normal	9	Logistic	9	Logistic	8
1P-Exponential	10	Normal	9	1P-Exponential	10	Normal	10	Normal	9
Gumbel	10	Gumbel	10	Gumbel	10	Gumbel	11	Gumbel	10

The distribution shapes were plotted to evaluate the scale and skewness within the groups, as an indication of heteroscedasticity, as shown in Figures 10 and 11.

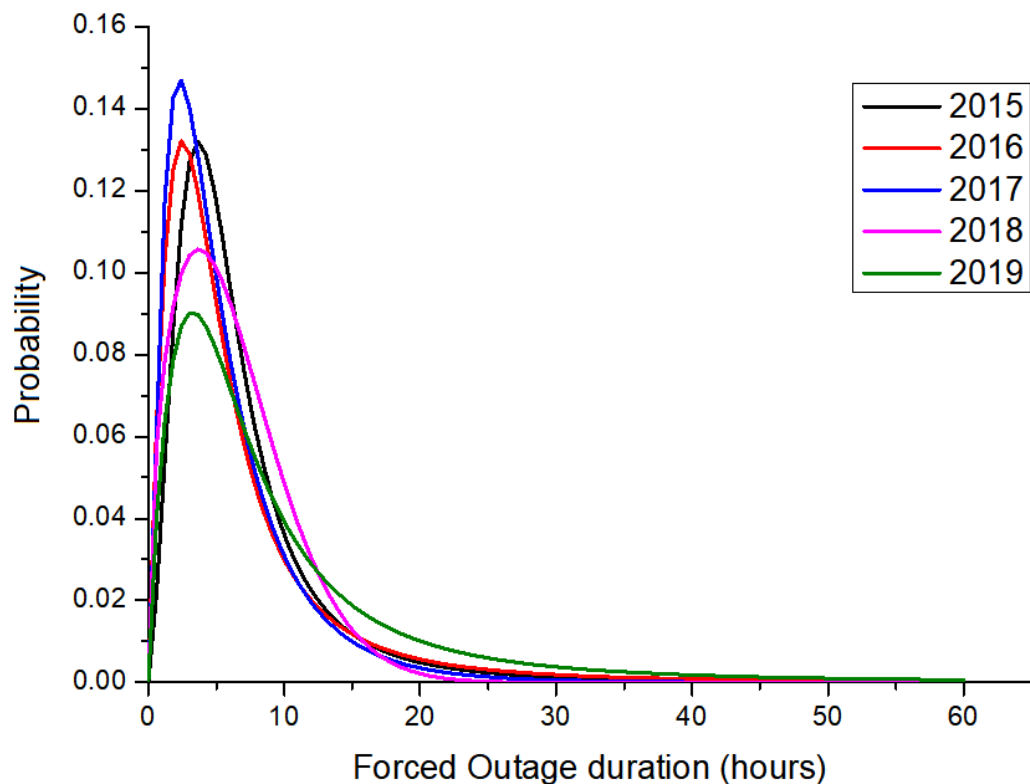


Figure 10: Probability density functions for Mean Forced Outage Duration data.

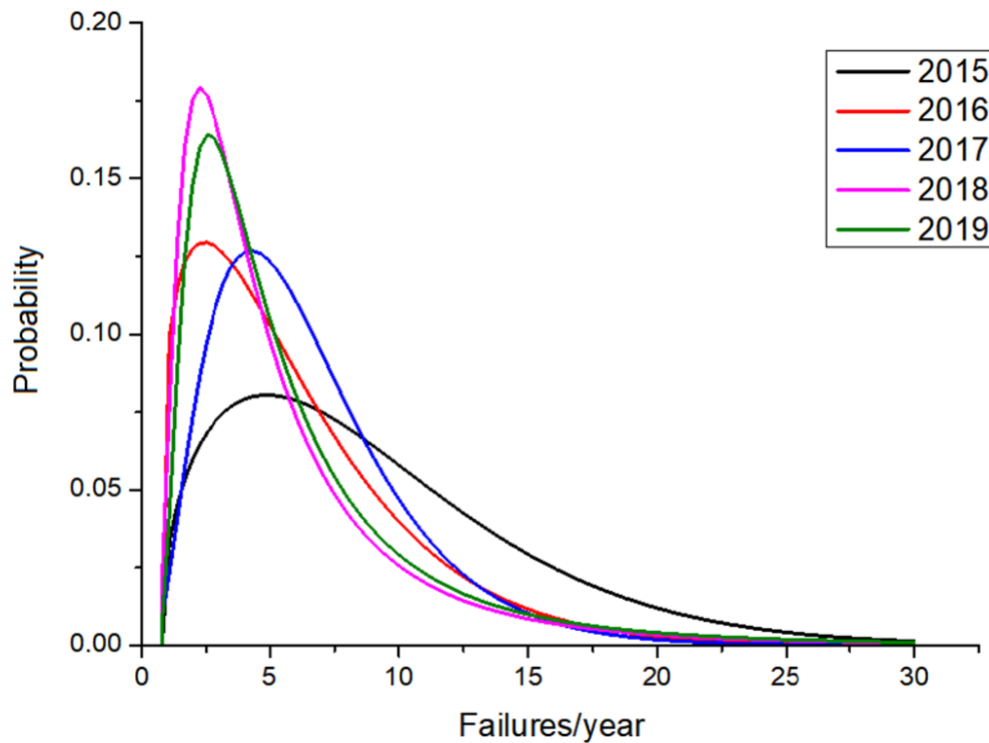


Figure 11: Probability density functions for Unit Failure Rate data.

Then, the distribution locations were computed considering the B50% life, assuming the groups had equal variation (homoscedasticity). The median is the value that the variable has a 50% probability of exceeding (Camarillo et al., 2017). Tables 8 and 9 show the B50% life as per computed using the Quick Calculation Pad from Weibull++ Software. The Two-sided Confidence Level of 95% was considered, which is the measure of the imprecision of the true effect size in the population of interest estimated in the study population (Patino and Ferreira, 2015).

Table 8: Median of the mean forced outage duration pdf (hours).

Median of mean forced outage duration pdf (hours)			
Year	Upper Bound (0.975)	B50% Life	Lower Bound (0.025)
2015	6.239337	5.383541	4.645127
2016	5.851687	4.769084	3.886769
2017	5.286304	4.391294	3.647816
2018	6.611890	5.571840	4.695390
2019	8.435479	6.846163	5.556288

Table 9: Median of unit failure rate pdf (outages/year).

Median of unit failure rate pdf (outages/year)			
Year	Upper Bound (0.975)	B50% Life	Lower Bound (0.025)
2015	9.165611	7.913893	6.848868
2016	5.821421	4.868818	4.089926
2017	6.286079	5.437703	4.703824
2018	4.483247	3.752409	3.140709
2019	4.985610	4.207730	3.551219

3.1 Availability analysis of the thermal power plants

Using the implemented distribution fitting, the B90% life was calculated for both the MFOD and the unit failure rate with a 95% Confidence Level. The aim of the distribution fitting was to evaluate with a 90% probability, the expected time needed to recover the functions of the thermal power plants and the average number of outages. Data from the KW test and distribution fitting indicates that the MFOD increased for 2019 and the unit failure rate has been stable since 2016. Accordingly, the data from 2019 were chosen for the analysis. Tables 10 and 11 show the B90% life as computed using the quick calculation pad from Weibull++ Software. The Two-sided confidence level of 95% was also considered. Figures 12 and 13 show the probability of restoring the power plant function and the failure rate.

Table 10: Mean forced outage duration distribution B90% life.

Mean forced outage duration distribution B90% life (hours)			
Year	Upper Bound (0.975)	B90% Life	Lower Bound (0.025)
2015	16.890513	13.643275	11.020325
2016	20.920577	15.590435	11.618306
2017	14.310876	11.632169	9.454861
2018	13.705005	11.928806	10.382807
2019	32.871988	24.089521	17.65348

Table 11: Unit failure rate distribution B90% life.

Unit failure rate distribution B90% life (outages/year)			
Year	Upper Bound (0.975)	B90% Life	Lower Bound (0.025)
2015	19.650076	17.116064	14.922217
2016	13.809283	11.638246	9.823966
2017	12.954111	11.233481	9.741394
2018	14.224801	11.177519	8.783036
2019	15.237316	12.101755	9.611436

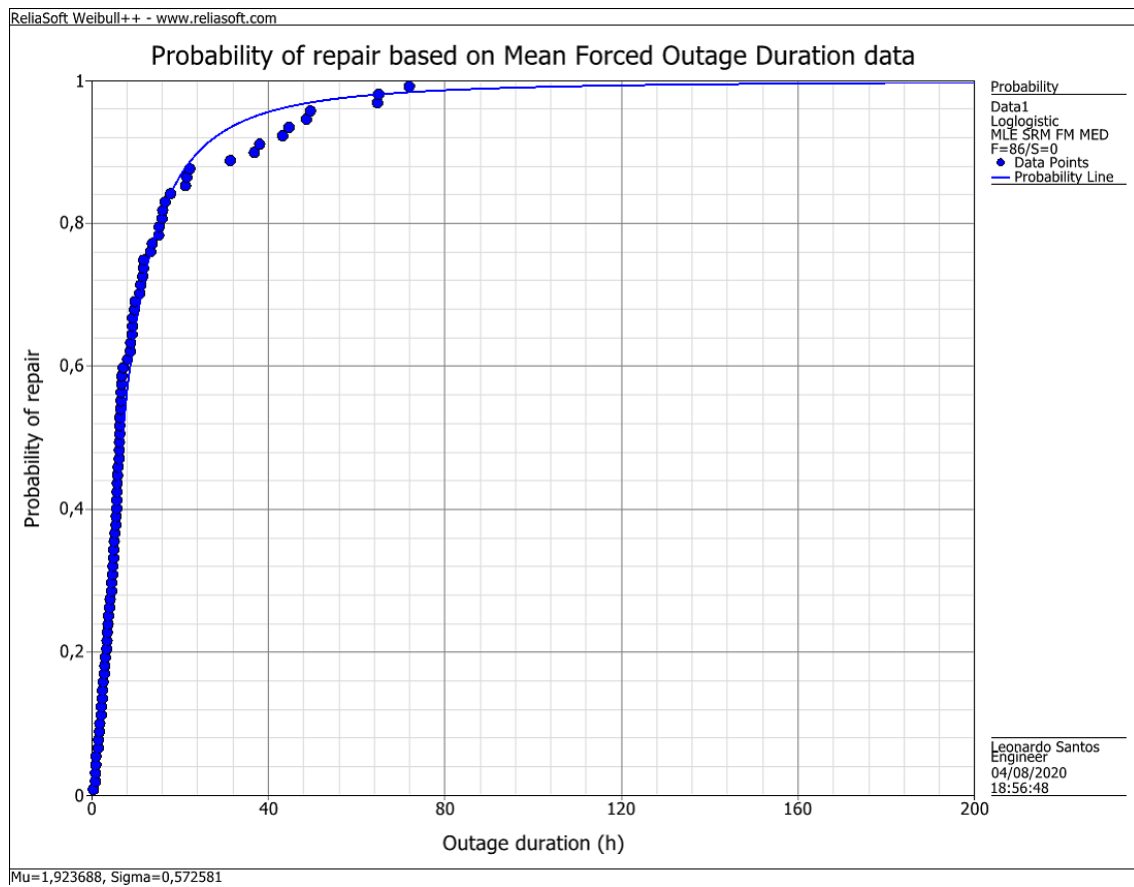


Figure 12: Probability of repair based on the mean forced outage duration data.

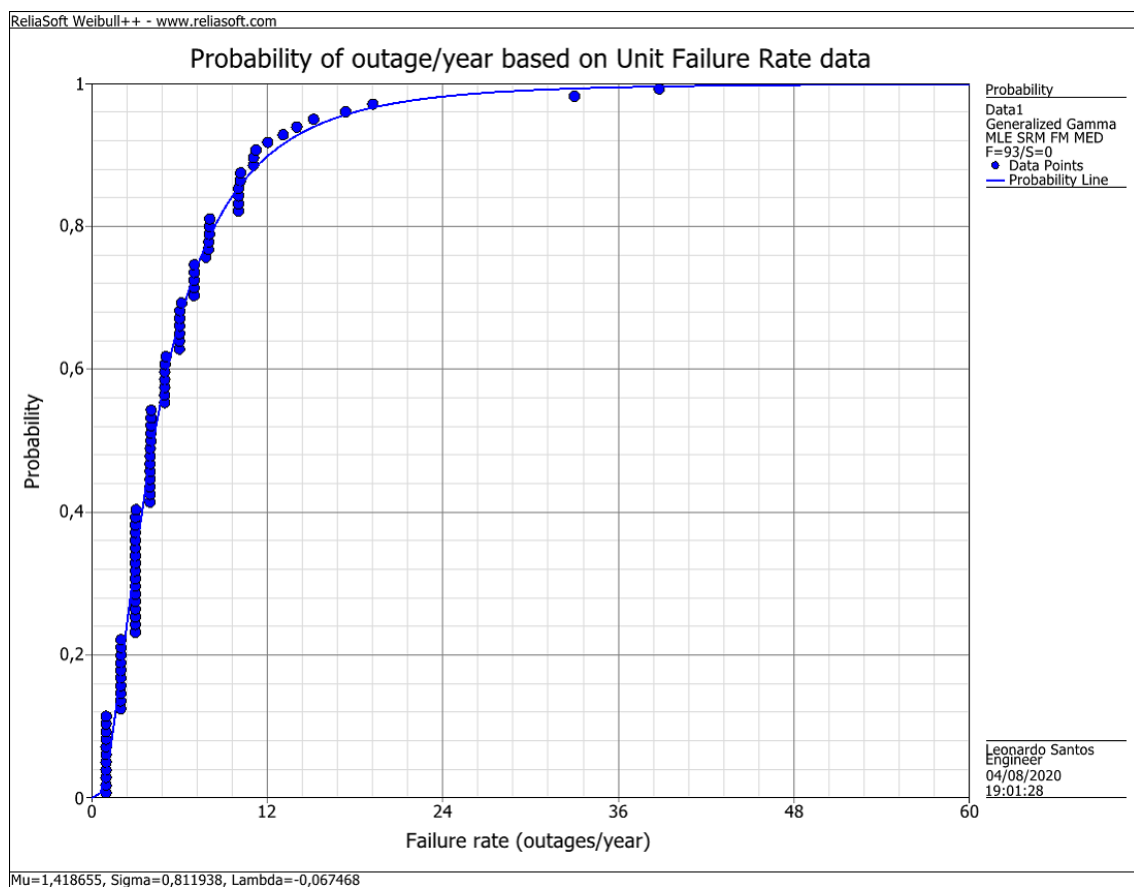


Figure 13: Probability of outages based on the unit failure rate data.

Using the Eq. 5 and the consolidated data from Tables 10 and 11, the FOF for 2019 was calculated, as shown in Table 12:

Table 12: Forced Outage Factor (FOF) for Brazilian thermal power plants.

Forced Outage Factor (%)			
Year	Upper Bound (0.975)	FOF	Lower Bound (0.025)
2019	5.72	3.33	1.94

The FOF was compared to the data from the North American Electric Reliability Corporation (NERC). NERC is a not-for-profit international regulatory authority: the Electric Reliability Organization (ERO) for North America, subject to oversight by the Federal Energy Regulatory Commission (FERC) and governmental authorities in Canada (NERC, 2020). The consolidated statistics are shown in Table 13, using data from Generating unit statistical brochure (2018), containing data on units reporting events only.

Table 13: Forced Outage Factor (FOF) for North America thermal power plants (NERC, 2018).

Unit Type	MW Trb/Gen	# of Units	FOF
Fossil (all fuel types)	All Sizes	1018	5.59
Gas turbine	All Sizes	660	4.94
Multi-boiler/multi-turbine	All Sizes	18	4.31
Jet engine	All Sizes	218	2.86
Combined cycle	All Sizes	281	2.19
Diesel	All Sizes	142	2.13
Nuclear (all types)	All Sizes	99	1.25

4. Discussion

In this study, the computed KW test p-values was less than a 0.05 significance level, thus, rejecting the H_0 for both KPIs, indicating that at least two population distributions differ from each other. In addition, the pairwise comparisons using the Dunn test show that:

- i. The computed KW for the MFOD indicator rejected the H_0 , indicating that at least two population distributions differ from each other ($P[\chi^2(4) > 12.5] = 0.0142 < 0.05$). In addition, based on the eta-squared computing and the pairwise analysis by the Dunn test for the 0.05 significance level ($p \leq 0.05$ for pairwise comparison 2017-2019), there was a difference between the population distributions from 2017 and 2019 with a small size effect. Furthermore, the KW test mean rank was 188.63 and 252.80 for 2017 and 2019, respectively.
- ii. The computed KW for the unit failure rate indicator rejected the H_0 , indicating that at least two population distributions differ from each other ($P[\chi^2(4) > 36.5] = 0.000000231 < 0.05$). In addition, based on the eta-squared computing and the pairwise analysis by the Dunn test for the 0.05 significance level ($p \leq 0.001$ for pairwise comparison 2015-2016, $p \leq 0.05$ for pairwise comparison 2015-2017, and $p \leq 0.0001$ for pairwise comparisons 2015-2018 and 2015-2019), there was a difference between the population distribution from 2015 and that from the other years with a moderate size effect. The KW test mean rank was 289.93 for 2015 and varied from 184.50 to 229.39 for 2016-2020 data.

This significant result in the KW test indicated that there are differences between the groups, however it does not indicate which groups (Andrew, 1998). In addition, it does not indicate whether the difference is meaningful, nor does it specify how many of the groups are different from each other (Chan and Walmsley, 1997). If the result indicated no differences for the 0.05 significance level ($p > 0.05$), the stability system scenario could be verified by considering the five-years timeframe. Since the result showed significant differences, a multiple comparison

between treatments was performed to construct pair-wise multiple comparisons to identify the source of the significance (Chan and Walmsley, 1997).

According to McDonald, the KW test does not assume normality, but that the shapes of the distributions in different groups are similar (McDonald and John, 2007). This indicates that non-parametric tests are not a good solution for heteroscedastic data. According to Laerd Statistics, the mean rank from the KW test should be considered for different shapes. With an increase in the group's mean rank, the observation values increase in comparison to those of the other groups (Minitab 19 Support, 2020). In addition, as reported by (McDonald, 2007), the standard deviations of the measurements of different groups should always be compared to evaluate their differences.

Based on the eta-squared computing, the computed KW for the MFOD indicator indicates a difference between the population distributions from 2017 and 2019 with a small size effect. The KW test mean rank for 2017 and 2019 was 188.63 and 252.80, respectively, While the standard deviation for 2017 and 2019 was 4.89 and 15.1 hours, respectively.

These results indicate that the observation values from 2019 are higher than those from 2017. In addition, it also indicates differences in the group distributions. Therefore, it is necessary to investigate for signs of skewness and variance, as proposed by (Fagerland and Sandvik, 2009).

The effect size of the KW test was computed to verify the degree to which one group has data with higher ranks than another group. This test is related to the probability that a value from one group will be greater than that from another group (Mangiafico, 2016). According to Prajapati et al., the eta-squared is a measure of association, and the proportion of the total variance attributed to an effect (Prajapati et al., 2010). Eta-squared ranges from 0 to 1, and as a rule, 0.01 is a small effect, 0.06 is a moderate effect, and 0.14 is a large effect (Tomczak et al., 2014).

Based on the eta-squared ($E_R^2 = 0.0198 \leq 0.06$), the effect size for the MFOD KW test indicated that there is a difference between the population distributions with a small size effect. In addition, based on the eta-squared ($0.06 < E_R^2 = 0.0732 \leq 0.14$), the effect size for the unit failure rate KW test indicated that there is a difference between the population distributions with a moderate size effect.

A *post hoc* procedure was performed to determine which groups are different from each other (Ribeiro, 2019.; Andrew, 1998). According to Dinno, when the H_0 is rejected, the Dunn's test should follow the KW test (Dinno, 2015). The computed Dunn test for the 0.05 significance level of the MFOD KW test indicated a difference between the population distributions from 2017 and 2019 ($p \leq 0.05$ for pairwise comparison 2017–2019). In addition, the computed Dunn test for the 0.05 significance level for the unit failure rate KW test indicated a difference between the population distributions from 2015 and that of the other years ($p \leq 0.001$ for pairwise comparison 2015-2016, $p \leq 0.05$ for pairwise comparison 2015-2017, and $p \leq 0.0001$ for pairwise comparisons 2015-2018 and 2015-2019).

The computed distribution fitting and the distribution locations analysis show that:

- i. When the groups had equal variation (homoscedasticity), the distribution fitting for the MFOD indicator confirmed a small size effect based on the computed eta-squared ($E_R^2 = 0.0198 \leq 0.06$) and the pairwise analysis by the Dunn test for the 0.05 significance level. In addition, the distribution location (B50% life) slightly increased for the 2019 data (4.39 in 2017 and 6.84 in 2019), indicating a higher forced outage duration.
- ii. When the groups had equal variation (homoscedasticity), the distribution fitting for the unit failure rate indicator confirmed the moderate size effect based on the computed eta-squared ($0.06 < E_R^2 = 0.0732 \leq 0.14$) and the pairwise analysis by the Dunn test for the 0.05 significance level. In addition, the

distribution location (B50% life) decreased from the 2016 data on, indicating an overall lower unit failure rate (7.91 in 2015, 4.86 in 2016, 5.43 in 2017, 3.75 in 2018, and 4.20 in 2019).

- iii. The distribution fitting for both the MFOD and unit failure rate indicated that the data have a non-normal distribution, thus, ranking the distributions loglogistic and generalized gama for the MFOD data and 3-parameters Weibull, and generalized gama and lognormal distributions for the unit failure rate.
- iv. The graphical analysis of MFOD pdf indicates a right-skewed behavior with an increased shifting in the 2019's location parameter, and a slightly higher scale-parameter compared to the other years.
- v. The graphical analysis of unit failure rate pdf indicates a right-skewed behavior with an increased shifting in the 2015's location-parameter and a higher scale-parameter compared to the other years.

However, there are some limitations with using the KW test. According to McDonald, the KW test cannot detect the differences between symmetrical distributions with similar location, and very different scale-parameter have different distributions. Sometimes, the KW test is considered a median test for the H_0 . This is because it assumes that the distributions in each group have similar shape, and the KW test can reject the null hypothesis even for same medians (McDonald, 2007). Another situation in which the median test for the H_0 is violated is when the distributions have different degrees of skewness, which affects both type I error, rejecting the null hypothesis when it is true (Fagerland and Sandvik, 2009).

In addition, according to McDonald, there is no consensus about heteroscedastic data for applying a test that assumes homoscedasticity (McDonald, 2007). The graphical analysis of the MFOD probability and unit failure rate pdfs indicate a right-skewed behavior for all the available groups, and the medians were considered for the complementary evaluation of the computed data.

The Distribution Wizard from Weibull++ Software used in this study is a valuable tool for fitting distribution models. According to Reliasoft, the MLE analysis is an appropriate method for data sets with many observed failures, however, the MLE tends to be statistically distorted for small sample sizes. Therefore, the default weighted composition of three goodness of fit tests were applied to determine the rank of the distributions: (i) 40% for the Kolmogorov-Smirnov test, (ii) 10% for the Correlation coefficient test, and (iii) 50% for the Likelihood value test (Reliasoft, 2017).

By combining the analytical and graphical tools, it was possible to verify which data pack to choose for applying the B90% life analysis: in this case, the 2019 data from the MFOD and unit failure rate reports provided by ONS was used. The BX% life is the lifetime metric, in which X% of the units in a population fail, when considering the reliability analysis (Woo, 2017). Applying B90% life calculation for the MFOD data indicates a lifetime metric, in which 90% of the power units would recover to available state. Likewise, applying the B90% if calculation for the unit failure rate data indicates the failure/year metric which 90% of the power units would achieve. The choice of the year 2019 to process the availability analysis considers the following scenarios: (i) the atypical rise in the MFOD for 2019 and (ii) the stability of the unit failure rate over the past 4 years.

The B90% life and unavailability computing show that:

- i. The FOF of the Brazilian thermal power plants is 3.33% with a 90% probability and a 95% confidence level, based on the data from the MFOD and unit failure rate data.
- ii. This value is slightly higher than the upper limit applied by ANEEL for hydroelectric plants (higher value is 3.115%).
- iii. The FOF of the Brazilian thermal power plants is also lower than 70% of North America thermal power plants (Fossil, Gas turbine, and Multi-boiler/multi-turbine types), based solely on the evaluated statistics.

The analysis of the operating scenario indicates that the combination of: (i) the historical second critical period in SIN (Nacional do Sistema, 2020 a) and (ii) the higher power demand in the first quarter of 2019 (Nacional do Sistema, 2020 a) (Figure 3), have contributed to the increase in the MFOD. Furthermore, there has been no significant difference in the annual unit failure rate since 2016, assuming that the groups had equal variation (homoscedasticity) and applying the KW test ($p > 0.05$). In addition, the FOF of the Brazilian thermal power plants (3.33% at 90% probability and 95% confidence level) is comparable to that from 2436 power plants from the NERC (NERC, 2018), indicating that the Brazilian thermal generation is a reliable system regardless of the challenges due to (i) the type of starting, (ii) the frequency of starting, and (iii) the loading pattern (Dipak, 2015a).

5. Conclusion

Brazil is a continental-size country and its SIN is characterized by a marked seasonality in its electricity supply. The expansion pattern of the Brazilian electric sector shows signs of exhaustion, with the inclusion of the ROR and intermittent renewable sources. In addition, 50% of the Brazilian hydroelectric plants are over 20 years old and 32% are over 40 years old. Therefore, there is an increase in the demand for flexible thermal power plants based on availability that can be operated in electric dispatch mode. Therefore, the knowledge acquired from the statistical analysis of forced outages is fundamental to understand the availability of Brazilian thermal power plants, to ensure the security risk mitigation to supplying the national power demand.

Assuming the homoscedasticity, the KW test and Dunn's pairwise-comparisons are valuable non-parametric approaches for evaluating the differences in the population's distributions for forced outage data. The tests were applied for available forced outage data provided by ONS and the results indicated that the forced outage statistics of the Brazilian thermal plants are favorable and comparable to the North America's benchmarks.

Furthermore, the distribution fitting indicated right-skewed (therefore, non-normal) distributions for the available data from ONS and the KW test fits properly for this type of data, based on the distribution rank from the computed data. However, the limitations to this study are the assumption of homoscedasticity and the effect size for the KW test, which indicates a small effect (Eta-squared ≤ 0.06) for the MFOD data. This may indicate that the sample size should be increased or separated by outage causes for applying normality tests: internal, secondary, external, and operational causes.

The inflexible power generation corresponds to 75% of the Brazilian load in 2020, however, the thermal power generation accounts for 7% only. Therefore, strategies for including flexible thermal power units in the SIN, the logistics expansion to explore onshore natural gas in the Northern Brazil and generating power nearby reservoir (the Reservoir-to-wire – R2W) can increase national energy security, thus, creating a virtual reservoir in the SIN that is safe and reliable for the country's development.

Declaration of competing interests

The author declares that he has no known competing financial interests or personal relationships that could have appeared to influence the work reported in this paper.

Acknowledgement

The author sincerely thanks the Brazilian National Electricity System Operator – ONS – (www.ons.org.br) for making public valuable information about the performance of the Brazilian National Interconnected System (SIN). This research did not receive any specific grant from funding agencies in the public, commercial, or not-for-profit sectors. The author would like to thank Editage (www.editage.com) for English language editing.

References

- Alboukadel, K., 2020 a. ggpubr: “ggplot2” Based Publication Ready Plots. R package version 0.4.0. Available online: <https://CRAN.R-project.org/package=ggpubr> (accessed 12 August 2020).
- Alboukadel, K., 2020 b. rstatix: Pipe-Friendly Framework for Basic Statistical Tests. R package version 0.6.0. Available online: <https://CRAN.R-project.org/package=rstatix> (accessed 12 August 2020).
- Andrew, C., 1998. Descriptive and inferential statistics, in: Leon. Alan, S.B., Michel, H. (Eds), *Comprehensive Clinical Psychology*. Pergamon, ISBN 9780080427072 3.12, 243–285. [https://doi.org/10.1016/B0080-4270\(73\)00264-9](https://doi.org/10.1016/B0080-4270(73)00264-9).
- Balaji, G., Balamurugan, R., Lakshminarasimman, L., 2016. Fuzzy clustered multi objective differential evolution for thermal generator maintenance scheduling. *Int. J. Intell. Eng. Syst.* 9, 1–13. <https://doi.org/10.22266/ijies2016.0331.01>.
- Camarillo, T., Mathur, V., Mitchell, Tyler, Ratra, B., 2017. Median statistics estimate of the distance to the galactic center. *Publ. Astron. Soc. Pac.* 130. <https://doi.org/10.1088/1538-3873/aa9b26>.
- Castro, N., Brandão, R., Rosental, R. Dorado, P., 2016. Background, current status and perspectives. *Energy Procedia. Brazil and the Int. Electr. Integr.* 106, 204–214. [10.1016/j.egypro.2016.12.116](https://doi.org/10.1016/j.egypro.2016.12.116), <https://doi.org/10.1016/j.egypro.2016.12.116>.
- Chan, Y., Walmsley, R.P., 1997. Learning and understanding the Kruskal-Wallis one-way analysis-of-variance-by-ranks test for differences among three or more independent groups (3), 322. *Phys. Ther.* 77, 1755–1762. <https://doi.org/10.1093/ptj/77.12.1755>.
- De Comercialização de Energia Elétrica, C., 2020 d. Info Mercado Mensal, nº 155 – Contabilização de Maio de 2020. Available online: <http://www.ccee.org.br/> (accessed 12 August 2020).
- Dinno, A., 2015. Nonparametric pairwise multiple comparisons in independent groups using Dunn’s test. *STATA J.* 15, 292–300. <https://doi.org/10.1177/1536867X1501500117>.
- Dipak, K.S., 2015 a. Gas turbine and heat recovery steam generator, in: Dipak, K.S. (ed.), *Thermal Power Plant*. Elsevier, pp. 239–283. <https://doi.org/10.1016/B978-0-12-801575-9.00007-X>.
- Dipak, K.S., 2015 b. Interlock and protection, in: Dipak, K.S. (ed.), *Thermal Power Plant*. Elsevier, pp. 387–405. <https://doi.org/10.1016/B978-0-12-801575-9.00011-1>.
- Fagerland, M.W., Sandvik, L., 2009. The Wilcoxon-Mann-Whitney test under scrutiny. *Stat. Med.* 28, 1487–1497. <https://doi.org/10.1002/sim.3561>.
- Ferreira, J.C., Patino, C.M., 2015. What does the p value really mean? *J. bras. pneumol.* 41, 485–485. Available online: http://www.scielo.br/scielo.php?script=sci_arttext&pid=S1806-37132015000500485&lng=en&nrm=iso. ISSN 1806-3756 (accessed 12 August 2020). <https://doi.org/10.1590/S1806-37132015000000215>.
- Statistical tools for high-throughput data analysis (STHDA), 2017 b. Ggpubr: Publication Ready Plots. Available online: <http://www.sthda.com/english/articles/> (accessed 12 August 2020).
- Geração termelétrica a gás natural: Comprovação de disponibilidade de combustível, 2017 a. Available online: <http://hdl.handle.net/10438/19056> (accessed 12 August 2020). Center for Regulatory and Infrastructure Studies Y3
- Hollander, M., Wolfe, D.A., Chicken, E., 2013. *Nonparametric Statistical Methods*, 3rd ed. John Wiley & Sons.
- IEEE-SA Standards Board, 2007. IEEE standard definitions for use in reporting electric generating Unit Reliability, Availability, and Productivity. IEEE std 762 2006 (Revision of IEEE Std 762-1987), C1–66.
- Laerd statistics. Kruskal-Wallis H test using SPSS statistics, 2020 Available online: <https://statistics.laerd.com/spss-tutorials/kruskal-wallis-h-test-using-spss-statistics.php> (accessed 12 August 2020).
- Landeiro, V.L., 2011. *Introdução ao uso do programa R*. Instituto Nacional de Pesquisas Da Amazônia, Brazil.
- Lipár, M., 2012. Operational Safety of Nuclear Power Plants. [10.1533/9780857093776.3.773](https://doi.org/10.1533/9780857093776.3.773), <https://doi.org/10.1533/9780857093776.3.773>.
- Makarov, Y., Etingov, P., Ma, J., 2017. Incorporating Forecast Uncertainty in Utility Control Center. [10.1016/B978-0-12-809592-8.00011-1](https://doi.org/10.1016/B978-0-12-809592-8.00011-1), <https://doi.org/10.1016/B978-0-12-809592-8.00011-1>.
- Mangiafico, S.S., 2016. Summary and Analysis of Extension Program Evaluation in R 1. Available online: <http://rcompanion.org/handbook/> (accessed 12 August 2020). Rutgers, New Brunswick, NJ Cooperative Extension.
- Martins, A.S., 2013. *Project finance aplicado ao setor de geração de energia elétrica Brasileiro – Fontes alternativas: Análise dos riscos e mitigadores em projetos de energia eólica*. 161 p. Available online: <https://www.maxwell.vrac.puc-rio.br/> (accessed 12 August 2020). Departamento de Administração, Pontifícia Universidade Católica do Rio de Janeiro, Rio de Janeiro.
- McDonald, J.H., 2007. *The handbook of biological statistics*. Available online: <http://www.uni-koeln.de> (accessed 12 August 2020).
- Ministério de Minas e Energias, 2014. Portaria No 484, de 11 de setembro de. Available online: <http://www.mme.gov.br> (accessed 12 August 2020).

- Minitab 19 Support. Interpret all statistics for Kruskal-Wallis test, 2020. Available online: <https://support.minitab.com/en-us/minitab/19/help-and-how-to/statistics/nonparametrics/how-to/kruskal-wallis-test/interpret-the-results/all-statistics/> (accessed 12 August 2020).
- Moreno, L., Morcillo, A., 2019. Comparação de três ou mais grupos independentes Teste de Kruskal-Wallis. 10.13140/RG.2.2.12990.43846.
- Nacional do Sistema, O., 2017. Boletim de Carga Mensal dezembro. Available online: <http://www.ons.org.br/paginas/conhecimento/acervo-digital/documentos-e-publicacoes?categoria=Boletim+Mensal+de+Carga> (accessed 12 August 2020).
- Nacional do Sistema, O., 2018. Boletim de Carga Mensal dezembro. Available online: <http://www.ons.org.br/paginas/conhecimento/acervo-digital/documentos-e-publicacoes?categoria=Boletim+Mensal+de+Carga> (accessed 12 August 2020).
- Nacional do Sistema, O., 2019 a. Boletim de Carga Mensal dezembro. Available online: <http://www.ons.org.br/paginas/conhecimento/acervo-digital/documentos-e-publicacoes?categoria=Boletim+Mensal+de+Carga> (accessed 12 August 2020).
- Nacional do Sistema, O., 2019 b. Submódulo 14.2 Arranjos comerciais para os serviços ancillaries. Available online: <http://www.ons.org.br/> (accessed 12 August 2020).
- Nacional do Sistema, O., 2019 c. DPL-REL-0099/2020 Relatório de Análise Estatística de Desligamentos Forçados de Equipamentos referente ao ano de 2019.
- Nacional do Sistema, O., 2019 d. Indicadores de desempenho de equipamentos e linhas de transmissão e das funções transmissão e geração. Available online: <http://www.ons.org.br/> (accessed 12 August 2020).
- Nacional do Sistema, O., 2020 a. PEN sumário executivo plano da operação energética 2020/2024. Available online: <http://www.ons.org.br/paginas/energia-no-futuro/suprimento-energetico> (accessed 12 August 2020).
- Nacional do Sistema, O., 2020 b. Boletim de Carga Mensal junho. Available online: <http://www.ons.org.br/paginas/conhecimento/acervo-digital/documentos-e-publicacoes?categoria=Boletim+Mensal+de+Carga> (accessed 12 August 2020).
- Nogueira, F.M.M., Alarcon, R., Arturo, D., 2019. Impacto das interrupções na geração hidrelétrica do Brasil. Available online: <https://publications.iadb.org/pt/impacto-das-interruptoes-na-geracao-hidreletrica-do-brasil> (accessed 12 August 2020). Inter-American Development Bank. 50p.
- North American Electric Reliability Corporation. 2020. About NERC. Available online: <https://www.nerc.com/AboutNERC/Pages/default.aspx> (accessed 12 August 2020).
- North American Electric Reliability Corporation, 2018. Generating Unit Statistical Brochure – Units reporting events. Available online: <https://www.nerc.com/pa/RAPA/gads/Pages/Reports.aspx> (accessed 12 August 2020).
- Agência Nacional de Energia Elétrica, 2020. Nota Tec.-SFG/ANEEL. Available online: <https://www.aneel.gov.br/> (accessed 12 August 2020).
- DataNovia, 2020 Kruskal-Wallis test in R. Available online: <https://www.datanovia.com/en/lessons/kruskal-wallis-test-in-r/> (accessed 12 August 2020).
- Ostertagová, E., Ostertag, O., Kováč, J., 2014. Methodology and application of the Kruskal-Wallis test. Appl. Mech. Mater. 611, 115–120.
- Kassambara, A., 2020d. The comprehensive R Archive Network. Package ‘rstatix’. Available online: <https://cran.r-project.org/web/packages/rstatix/> (accessed 12 August 2020).
- Patino, C.M., Ferreira, J.C., 2015. Confidence intervals: A useful statistical tool to estimate effect sizes in the real world. J. bras. pneumol. 41 (Cited 2020.8.11), 565–566. Available online: http://www.scielo.br/scielo.php?script=sci_arttext&pid=S1806-37132015000600565&lng=en&nrm=iso (accessed 12 August 2020). ISSN 1806-3756. <https://doi.org/10.1590/S1806-37562015000000314>.
- Prajapati, B. Mark, D., Richard, A.A., 2010. Sample Size Estimation and Statistical Power Analyses.
- R Development Core Team, 2011. A: A language and environment for statistical computing. Available online: <http://www.R-project.org/>. R Foundation for Statistical Computing, Vienna, Austria. ISBN 3-900051-07-0 (accessed 12 August 2020).
- Kassambara, A., 2020a. Rdocumentation. rstatix v0.6.0. Available online: https://www.rdocumentation.org/packages/rstatix/versions/0.6.0/topics/get_summary_stats (accessed 12 August 2020).
- Kassambara, A., 2020b. Rdocumentation. kruskal_test. Available online: https://www.rdocumentation.org/packages/rstatix/versions/0.6.0/topics/kruskal_test (accessed 12 August 2020).
- Kassambara, A., 2020c. Rdocumentation. kruskal_effsize. Available online: https://www.rdocumentation.org/packages/rstatix/versions/0.6.0/topics/kruskal_effsize (accessed 12 August 2020).
- Reliasoft, 2017. Weibull++/Alta. User’s Guide. Available online: http://www.synthesisplatform.net/WeibullALTA/en/UG_WeibullALTA11.pdf 11 (accessed 12 August 2020).

- Ribeiro, H.F., 2019. Behavior analysis of thermal power stations in the national interconnected system. Available online: <http://monografias.poli.ufjf.br/> (accessed 12 August 2020). Universidade Federal do Rio de Janeiro, Escola Politécnica, Rio de Janeiro, RJ. 77p.
- Ronald, N., Forthofer, Eun, S.L., Mike, H., 2007. Nonparametric tests, in: Forthofer, R.N., Eun, S.L., Mike, H. (Eds), Biostatistics, 2nd ed. Academic Press, pp. 249–268. <https://doi.org/10.1016/B978-0-12-369492-8.50014-5>.
- Sifonte, J.R., Reyes-Picknell, J.V., 2017. Reliability Centered Maintenance-Reengineered: Practical Optimization of the RCM Process with RCM-R.
- Sousa, J.R.F., 2009. A geração termelétrica: A contribuição das térmicas a gás natural liquefeito. Available online: <http://www.repositorio.unicamp.br/handle/REPOSIP/264491> (accessed 12 August 2020). Universidade Estadual de Campinas, Faculdade de Engenharia Mecânica, Campinas, SP. 131p.
- National Confederation of Industry, Brazil, 2018. Thermal Power Plants: The Inevitable Choice. Available online: <https://www.portaldaindustria.com.br/cni/canais/industry-proposals-2018-elections/> (accessed 12 August 2020).
- Tomczak, Maciej, Tomczak, Ewa, 2014. The need to report effect size estimates revisited. An Overview Some Recommended Meas. Eff. Size 21, 19–25.
- Hecke, T.V., 2010. Power study of ANOVA versus Kruskal-Wallis test. J. Stat. Manag. Syst. 15. <https://doi.org/10.1080/09720510.2012.10701623>.
- Wickham, H., Averick, M., Bryan, J., Chang, W., McGowan, L., François, R., Grolemond, G., Hayes, A., Henry, L., Hester, J., Kuhn, M., Pedersen, T., Miller, E., Bache, S., Müller, K., Ooms, J., Robinson, D., Seidel, D., Spinu, V., Takahashi, K., Vaughan, D., Wilke, C., Woo, K., Yutani, H., 2019. Welcome to the tidyverse. J. Open Source Softw. 4, 1686. <https://doi.org/10.21105/joss.01686>.
- Woo, S., 2017. Reliability Design of Mechanical Systems: A Guide for Mechanical and Civil Engineers. <https://doi.org/10.1007/978-3-319-50829-0>

Appendix

Appendix 1: Mean Forced Outage Duration and Units Failure Rate
(Nacional do Sistema, 2019 c).

Thermal Power Plant	Mean Forced Outage Duration (hours)					Unit Failure Rate (outage/year)				
Unit	2015	2016	2017	2018	2019	2015	2016	2017	2018	2019
1	5,59	14,20	12,80	9,53	6,40	12,05	16,32	4,01	9,07	8,03
2	-	-	-	-	-	3,00	-	-	-	-
3	6,64	-	-	-	-	5,01	-	-	-	-
4	2,22	-	-	-	-	6,01	-	-	-	-
5	-	-	6,69	6,98	6,07	-	-	14,15	16,19	19,24
6	-	-	-	-	4,85	-	-	-	8,11	38,82
7	-	-	-	10,88	9,33	-	-	-	80,28	33,02
8	5,07	13,36	3,52	-	5,75	5,01	2,01	3,00	-	2,00
9	4,97	5,45	4,97	-	4,13	9,05	1,00	6,02	-	3,00
10	6,85	14,48	4,76	-	13,40	5,02	3,02	5,01	-	2,01
11	6,25	-	-	-	6,62	2,00	-	-	-	1,00
12	0,67	-	-	-	-	3,00	-	-	-	-
13	-	-	-	-	-	2,00	-	-	-	-
14	11,11	4,72	5,77	9,30	16,14	13,15	4,01	7,01	5,02	8,06
15	9,57	6,31	28,23	12,94	11,18	18,24	3,00	5,02	3,01	7,05
16	3,18	-	3,55	4,05	4,23	7,02	1,00	2,00	1,00	3,00
17	4,98	2,11	1,40	1,36	-	4,01	3,00	1,00	3,00	1,00
18	6,07	3,47	6,73	4,12	1,00	6,03	2,00	2,00	1,00	1,00
19	8,00	-	8,90	6,30	-	1,00	-	2,00	1,00	2,00
20	17,33	25,03	-	8,57	9,32	7,07	1,00	-	1,00	3,00
21	4,21	-	6,24	6,74	3,14	5,01	1,00	3,01	5,02	5,01
22	4,85	5,37	-	6,08	9,92	4,01	4,01	-	4,01	5,03
23	7,01	3,06	7,59	10,62	5,85	6,02	5,00	5,01	3,01	3,00
24	-	6,83	0,51	0,71	5,35	-	6,02	7,00	6,00	7,02
25	16,59	0,82	-	1,98	22,26	8,08	6,00	-	11,00	6,05
26	4,20	3,14	11,06	3,31	9,20	2,00	7,02	4,02	5,00	8,07
27	5,69	6,02	7,24	13,60	1,01	3,01	3,01	7,02	6,04	8,01
28	3,31	1,54	0,93	-	8,88	8,02	5,00	3,00	-	15,19
29	9,21	3,73	-	1,69	6,68	8,07	3,00	-	4,00	10,05
30	8,57	5,48	11,39	6,12	5,61	20,28	15,07	5,03	5,01	6,02
31	7,21	15,68	14,26	2,72	-	4,01	2,01	3,02	8,02	-
32	4,22	-	2,74	4,65	-	2,00	-	2,00	2,00	-
33	-	4,09	1,32	3,92	-	-	3,00	2,00	2,00	1,00
34	-	13,88	3,58	7,97	-	2,00	4,03	3,00	4,01	-
35	-	-	-	-	4,56	-	-	-	-	7,82
36	-	5,01	6,14	5,63	7,19	-	14,04	12,09	18,21	7,04
37	-	5,57	7,76	7,17	6,32	-	14,01	8,04	10,08	10,07

38	11,38	3,29	2,52	1,33	2,63	11,15	10,04	5,01	4,00	2,00
39	0,28	1,07	1,28	2,22	1,62	4,00	13,02	4,00	7,01	3,00
40	2,02	2,30	1,26	1,03	2,25	5,01	4,00	5,00	2,00	1,00
41	0,74	1,43	3,73	1,50	1,85	5,00	5,00	4,01	3,00	5,01
42	3,81	6,82	5,89	5,45	6,30	16,06	9,06	11,07	8,04	11,07
43	2,75	6,10	8,55	6,54	1,56	12,03	5,02	7,03	6,01	3,00
44	11,80	2,79	5,38	4,86	6,86	4,02	4,00	4,01	7,02	11,08
45	8,93	1,87	1,43	10,14	5,16	4,01	4,00	5,00	5,02	6,01
46	2,87	6,02	1,20	2,11	5,76	7,02	3,00	4,00	6,01	6,02
47	5,29	4,60	2,63	4,58	6,89	7,03	2,00	6,00	4,01	4,01
48	13,01	0,55	4,64	9,86	5,90	2,01	3,00	9,01	3,01	10,05
49	11,00	1,69	1,53	1,52	3,54	8,07	6,01	2,00	9,01	7,02
50	8,34	10,35	2,51	5,53	5,81	7,03	6,03	2,00	6,02	7,03
51	2,44	-	3,08	5,22	0,47	16,05	-	6,01	7,03	1,00
52	8,26	10,82	2,90	9,33	3,57	2,00	5,03	3,00	1,00	4,01
53	3,33	6,20	4,42	20,18	4,55	4,01	7,03	7,02	1,00	5,01
54	3,69	-	9,97	4,14	0,92	3,00	-	1,00	10,02	3,00
55	12,05	3,25	-	4,97	5,08	15,23	17,07	1,00	2,00	12,05
56	7,62	3,50	6,98	7,22	3,77	16,17	7,01	5,01	2,00	14,04
57	9,94	5,63	-	1,80	21,60	25,09	7,02	1,00	5,00	17,39
58	4,04	0,18	0,55	10,43	-	10,05	2,00	1,00	4,01	2,03
59	6,49	10,20	7,47	5,12	21,30	14,15	1,00	6,01	7,03	10,20
60	17,98	6,30	8,34	6,91	43,28	19,60	10,06	8,05	7,03	4,08
61	0,93	1,54	-	1,10	31,45	20,04	4,00	2,00	1,00	5,09
62	2,70	13,65	3,41	-	36,89	17,07	5,03	5,01	-	4,07
63	4,89	3,94	3,12	4,11	17,92	11,06	6,01	9,02	4,01	11,25
64	9,01	6,53	3,70	3,65	11,62	8,05	4,01	10,03	6,01	3,01
65	4,24	18,64	1,57	-	11,83	16,13	5,03	4,00	-	5,01
66	3,75	14,38	1,23	7,77	71,97	8,03	1,00	7,00	1,00	2,03
67	2,13	2,88	3,82	7,71	49,58	7,01	2,00	7,02	5,01	4,07
68	3,45	29,45	7,73	4,89	64,77	11,04	6,08	12,08	3,00	4,09
69	3,91	7,40	3,98	0,48	16,71	12,06	4,01	7,01	1,00	8,09
70	51,77	6,09	4,35	1,41	3,50	9,45	10,04	10,04	2,00	3,00
71	4,16	1,12	3,25	1,28	65,06	13,07	1,00	5,01	3,00	2,03
72	3,80	14,21	3,45	4,63	38,10	9,04	2,01	8,02	2,00	4,07
73	7,87	-	3,38	-	9,73	14,15	-	7,01	-	6,03
74	3,84	-	7,76	11,08	48,69	12,06	-	5,02	1,00	3,05
75	7,32	1,93	1,33	0,27	-	5,02	10,02	5,00	3,00	1,00
76	7,35	14,04	20,53	2,33	5,58	12,10	11,16	5,01	5,00	3,00
77	23,64	6,39	9,59	16,90	5,08	6,10	5,01	9,07	1,00	1,00
78	3,83	3,62	5,34	5,73	15,24	7,02	6,01	9,03	5,01	10,18
79	4,57	64,66	9,38	2,90	-	13,08	6,28	3,01	1,00	1,02
80	5,94	3,90	1,21	6,12	-	5,01	2,00	6,00	5,01	1,00
81	2,29	13,33	5,60	8,56	6,31	4,00	4,02	7,01	5,03	3,00
82	6,12	1,05	2,08	4,18	44,74	4,01	6,00	5,00	2,00	6,16
83	2,04	4,77	9,71	15,83	2,25	13,03	4,00	11,07	6,07	4,00

84	8,61	4,44	16,78	3,44	8,81	11,10	4,01	4,02	12,04	3,01
85	2,00	0,78	0,83	-	-	2,00	2,00	3,00	1,00	-
86	2,72	3,32	5,26	4,10	6,42	27,19	8,01	20,21	3,00	6,02
87	8,36	2,58	2,67	3,56	4,88	3,01	4,00	11,03	7,01	5,01
88	5,82	-	3,68	3,39	2,49	8,04	-	11,05	3,00	3,00
89	4,51	1,34	4,24	3,72	0,93	27,35	10,01	9,03	6,02	2,00
90	3,38	-	4,80	7,77	3,93	6,01	-	2,00	1,00	2,00
91	7,98	-	4,33	7,77	2,97	8,04	-	5,01	2,00	2,00
92	14,54	-	1,61	15,68	1,91	12,22	-	7,01	9,10	3,00
93	2,79	2,19	3,49	4,25	3,04	6,01	4,00	5,01	1,00	4,01
94	3,14	-	5,30	10,87	2,52	4,99	-	10,05	6,03	1,00
95	4,64	2,76	2,26	4,78	16,02	15,11	6,01	7,01	3,00	4,02
96	14,19	6,15	6,78	9,03	13,80	13,24	18,15	11,07	2,00	4,03
97	10,50	11,25	12,43	8,89	6,43	15,20	4,02	7,02	5,03	3,01
98	8,59	9,07	23,97	12,85	15,36	13,16	10,08	6,02	1,00	3,01
99	7,89	5,85	6,68	7,19	8,18	20,26	10,05	5,01	16,20	13,11
100	7,44	8,83	4,14	12,34	6,76	14,12	18,18	10,03	7,04	10,06
101	2,09	-	-	-	-	3,00	-	-	-	-
102	3,14	0,75	-	-	-	8,02	1,00	-	-	-
103	0,82	-	-	-	-	4,00	-	-	-	-
104	10,05	6,21	6,45	8,83	10,94	12,08	7,04	18,17	5,02	4,02
105	15,60	7,65	8,02	12,48	11,79	12,11	13,13	17,16	5,02	4,02

Application of the BowTie Method in Accident Analysis: Case of Kaziwiziwi Coal Mine

Jabulani Matsimbe¹, Steven Ghambi¹, Abdul Samson¹

¹ Department of Mining Engineering, Faculty of Engineering, The Polytechnic, University of Malawi, Blantyre, Malawi.

Correspondence: Jabulani Matsimbe. Email: jmatsimbe@poly.ac.mw

Abstract

A BowTie is a diagram illustrating proactive and reactive risk management at any working environment. This case study applied the bowtie method to provide a simple visual analysis of the hazards that caused fatal accidents at Kaziwiziwi coal mine on 2nd November 2012 and 15th November 2019. Two coal miners were killed on the spot and others injured due to failure of a bucket hoisting system and hanging rock fall. The authors demonstrated that the bowtie method is an effective visualization tool that can be used to analyze the hazard, top event, threats, consequences, barriers and escalation factors of mining accidents; and therefore give an overview of everything not wanted around a certain hazard. Mining companies in Malawi will apply this new knowledge to proactively conduct situational audits of unwanted scenarios, and identify barriers to prevent accidents from happening so far as is reasonably practicable. In addition, the Department of Mines will find this bowtie visualization tool useful when carrying out accident analyses in the future which in turn will promote safety awareness and policy development in the mining industry, and suggest ways on how to keep the normal but hazardous aspects from turning into something unwanted.

Keywords: Bowtie Method, Incident Investigation, Malawi Mining Industry

1. Introduction

Malawi is a landlocked country whose main export is tobacco and its economy mostly relies on agriculture. Mining is still a budding sector in the country with a high potential to positively impact the economy. Most mining projects are still in the exploration phase and yet to start bankable feasibility studies. There is coal exploitation in the Northern region of Malawi done by Kaziwiziwi, Mchenga and Rukuru underground coal mines. These are the major producing coal mining companies, and supply coal at national and international level. Malawi has over 22 million tons of proven coal reserves in a number of coal fields across the country (Annual Economic Report 2012). The largest coal field is the Livingstonia coal field with probable reserves of over 2-5 million tonnes and proven reserves of 4 million tons of coal with ash content of 17 %, a sulphur of 0.5 % and a calorific value of 6,800 kcal /kg. Livingstonia coal field is a 90 km² stretch in Rumphi district in the Northern Region of Malawi (Annual Economic Report 2012). Mining sites are high hazard environments due to the nature

of the work being carried out. Present study focused on Kaziwiziwi coal mine because it recorded the most mining accidents in the past decade. On 2nd November 2012, Face of Malawi reported that a “hanging rock was ejected from the wall of the mine as the miners were digging around it and it crashed the miner and killed him on the spot”. On 15th November 2019, sources at the mine said that “a coal miner was killed on the spot and others injured when a bucket filled with coal at a 75m deep hoisting system fell from above ground to the depth of the shaft where the men were. The men couldn't escape since the drive at the bottom was filled with a stockpile”.

Malema (2017) established that the working conditions experienced at the two mining companies of Mchenga and Kaziwiziwi in Rumphi district are generally poor but did not research on how mining companies in Malawi can effectively carry out risk analysis to prevent or mitigate mining accidents and lost time due to injury. Yasidu (2019) only reported on the influences of water vapor on roof fall accidents at Mchenga and Kaziwiziwi underground coal mines in Malawi and they found that tensile failure at weak sedimentary planes due to the seasonal decrease in tensile strength by the vapor migration into the rock mass leads to roof falls at Malawian coal mines. Mining Safety Regulations (1982) states that “A manager or foreman or person in any similar supervisory capacity shall not, by his instruction, default or negligence, cause or permit to exist any state of affairs which is reasonably calculated to endanger the safety of persons or property”. Therefore, there is a research gap on how coal mining companies can proactively identify hazards, assess risks and prevent accidents or ‘any state of affairs’ at mining sites. This in turn will help companies save compensation money, develop a safety & risk management culture, minimize lost time due to injury or deaths, and increase mineral production. The bowtie method has been used within the oil and gas, petrochemical, aviation and mining domains (Achield & Weaver, 2012; Burgess-Limerick, Horberry, & Steiner, 2014; Pitblado & Weijand, 2014; Saud, Israni, & Goddard, 2014; Dodshon, & Limerick, 2015). In Australia, the use of bowties is an accepted way to graphically demonstrate whether organisation controls have reduced the risk of a major incident so far as is reasonability practicable (Safe Work Australia, 2012; Dodshon, & Limerick, 2015).

It is hoped that the knowledge gained from this research will promote risk and incident analysis by mining companies in Malawi thereby improving mineral production and safety culture. The most critical hazards at Kaziwiziwi coal mine comprise lifting/hoisting operations, working at height, driving machinery, drilling, blasting, coal processing, toxic contaminant, ventilation, coal dust, hanging rock, noise, and fire. This research focused on lifting/hoisting operations, working at height, driving machinery, and hanging rock as they are the most common hazards that lead to top events at the mining site. The bowtie method was applied to determine if it could help investigators or supervisors identify the risk controls that could have prevented the severity of the top event outcomes to an acceptable level of risk.

2. Materials and Methodology

2.1. Study Area

Kaziwiziwi coal mine is located at Latitude -10.626465 and Longitude 34.106333 within the Livingstonia coal field in Rumphi district, northern Malawi (Fig. 1). The mine covers an approximate area of 17.5 km². Overall, the whole livingstonia coal field has probable reserves of 2-5 million tons and proven reserves of 4 million tons of coal with ash content of 17 %, sulphur content of 0.5 % and calorific value of 6.800 kcal/kg (Annual Economic Report 2012; Maneya 2012). Kaziwiziwi coal mining company started with four underground labour intensive long-wall faces (the mine bases) from where coal was loaded directly into trucks for transportation to customers. During that period, there were no facilities to clean and size the coal until 1987, when screening and sizing facilities were installed. Kaziwiziwi coal mine currently produces on average 65.45 metric tons of coal per month. With this current production, there is a 162 % increase in coal production compared to an average monthly production of 25 metric tons during the first 5 years of its operations. At full capacity, the mining company can produce an average of 2,100 metric tons of coal per month (Malema 2017).



Figure 1: Aerial view of Kaziwiziwi coal mine (Google Earth 2020)

2.2. Procedure

Present study applied the bowtie method (Fig. 2) to provide a simple visual explanation of the hazards that caused fatal accidents at Kaziwiziwi coal mine on 2nd November 2012 and 15th November 2019. A bowtie representation was created for each hazard. Each bowtie model contained the following components of an accident/incident: threats, preventative risk barriers, top events, mitigation risk barriers, consequences and escalation factors.

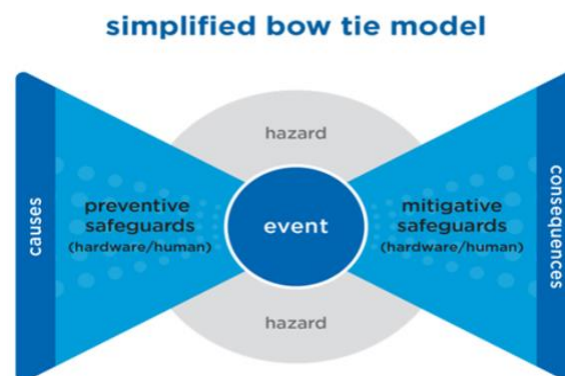


Figure 2. Simplified bowtie model

3. Results and Discussion

Observation was made between risk barriers present at the time of the accident/incident and those that were not. The authors based their research information on current and past mine workers; online articles & media reports; author's site visit experience and safety questions to site personnel. The collected risk components data in Table 1 is presented diagrammatically in Fig. 3 to Fig. 6 using the bowtie method. This gives a simple visual representation of proactive and reactive risk management controls that could have prevented or mitigated the mining accidents at Kaziwiziwi coal mine as far as is reasonably practicable. Results from the bowtie method indicate its usefulness as a communication tool to elicit further information and uncover holes in a company's

risk management; and identify the preventative & mitigatory risk barriers even before the start of a mining operation.

3.1. Preventative Risk Barriers

The most frequently identified preventative risk barriers comprised risk management, training, safety culture, procedures, auditing, supervision, maintenance, lighting and warning or proximity detection systems.

3.2. Mitigatory Risk Barriers

The most frequently identified mitigatory risk barriers comprised berms/escape ramps, emergency response, rescue teams, seatbelts, rockfall barriers, and rockbolts.

Table 1: Examples of components that form the BowTie model

Threat	Preventative barrier	Hazard Top event	Mitigation barrier	Consequence
1. Load too heavy 2. Incorrect loading 3. Strong winds 4. Snagging of gear/load 5. Operator overextends load 6. New mine worker 7. Lack of operating procedures 8. Lack of maintenance 9. Poor lighting 10. Non-compliance due to minimal supervision 11. Structural failure of mine hoisting system 12. Power failure	1. Check safe working load manifest; Check inspection status of hoist/bucket; Mine hoist system design 2. Limited lift stability check 3. Monitor and adhere to weather criteria-stop lift if exceeded 4. Use lifting plan; Use camera/CCTV monitoring for blind angles; Use a banksman for blind lifts 5. Check that operator is competent enough for the operation of hoist plant; Use camera/CCTV monitoring. 6. Induction training; Restrict access to hoisting area 7. Management operating procedures to ensure pre-operational checks. Safety culture 8. Adequate maintenance to identify safety defects. Regular replacement of old ropes with new ones 9. Hazard lights to be used under all low light conditions 10. Presence of supervisor at every hoisting operation 11. Check inspection status of hoist; Pre-lift hoist check; Proper mine shaft design 12. Back-up generator (Escalation Factor: No fuel in generator); Inspection/maintenance of electrical systems	Underground Mine Hoisting Operation Failure of hoist rope carrying bucket/skip	1. Restrict access to hoisting area 2. Every hoist to have an emergency escape route/ramp 3. Coal stockpile & waste rock not to be too close to escape routes/ramps. 4. Emergency response plan 5. Mine rescue teams 6. Emergency repair of primary bleeder	1. Mine worker hit by bucket leading to fatality or injury. 2. Bucket impacts ground. 3. Production losses. 4. Damage equipment. 5. Damage ventilation mechanisms
1. Lack of reinforcement/ground control design 2. Improper rock support installation 3. Loose wedges/rocks 4. Minimal inspection and monitoring of working environment/personnel 5. Lack of	1. Mine design; Install rockbolts/support 2. Only trained technicians to install rock support 3. Roof testing (sound the rock & listen for the drummy sounds that signal loose rock) & scaling of loose rock 4. Regular inspection/monitoring of roof and side walls; Provide sufficient lighting in working area; Watch out for support/rock cracking sound; Provide signposts in rockfall risky areas; Report unsafe condition to supervisor 5. Install warning devices; Use of photogrammetry, total station or LIDAR	Underground Mine Hanging rock Rockfall	1. Rockfall protection barriers e.g. high tensile steel wire. 2. Restrict entry to rockfall affected area 3. Warning devices e.g. microseismic monitoring systems	1. Killing or injuring miner. 2. Damage equipment 3. Disrupt ventilation system. 4. Blockage of installed emergency escape routes 5. Production losses

monitoring equipment/technology 6. Presence of fault zones/discontinuities 7. Sudden change in geologic structures 8. Influx of groundwater	to monitor movement of rocks 6. Dewatering techniques			
1. Slippery surface 2. Unstable surface 3. Material obstructing surface	1. Anti slip coating on surface 2. Adequate condition of scaffold/ladder 3. No excessive equipment on workflow	Working at height Slips and trips on height	1. PPE worn 2. First aid and stabilization 3. Emergency lifting equipment	1. Cuts and bruises due to impact 2. Fractures due to impact 3. Person stuck at height
1. Poor haul road condition 2. Poor machine maintenance 3. Faulty machine 4. Poor visibility 5. Learner operator 6. Driver loss of attention (due to phone, fatigue, eating, chatting) 7. Intoxicated driving	1. ABS, regular road inspection and maintenance 2. Daily machine inspection and scheduled maintenance 3. Dispose machine at end of its life; Purchase new machinery; Maintenance 4. Listen to weather report and adjust driving schedule accordingly 5. Experienced operator; Defensive operation 6. Regular refreshment breaks, all gadgets to be kept by supervisor 7. Breathalyzer	Driving machinery Losing control over the machinery	1. Forward collision warning system, airbag, wearing seatbelt 2. Designated walkways for miners with barricades 3. Rollover protection	1. Crash into other machine 2. Hitting a mine worker 3. Machine rollover

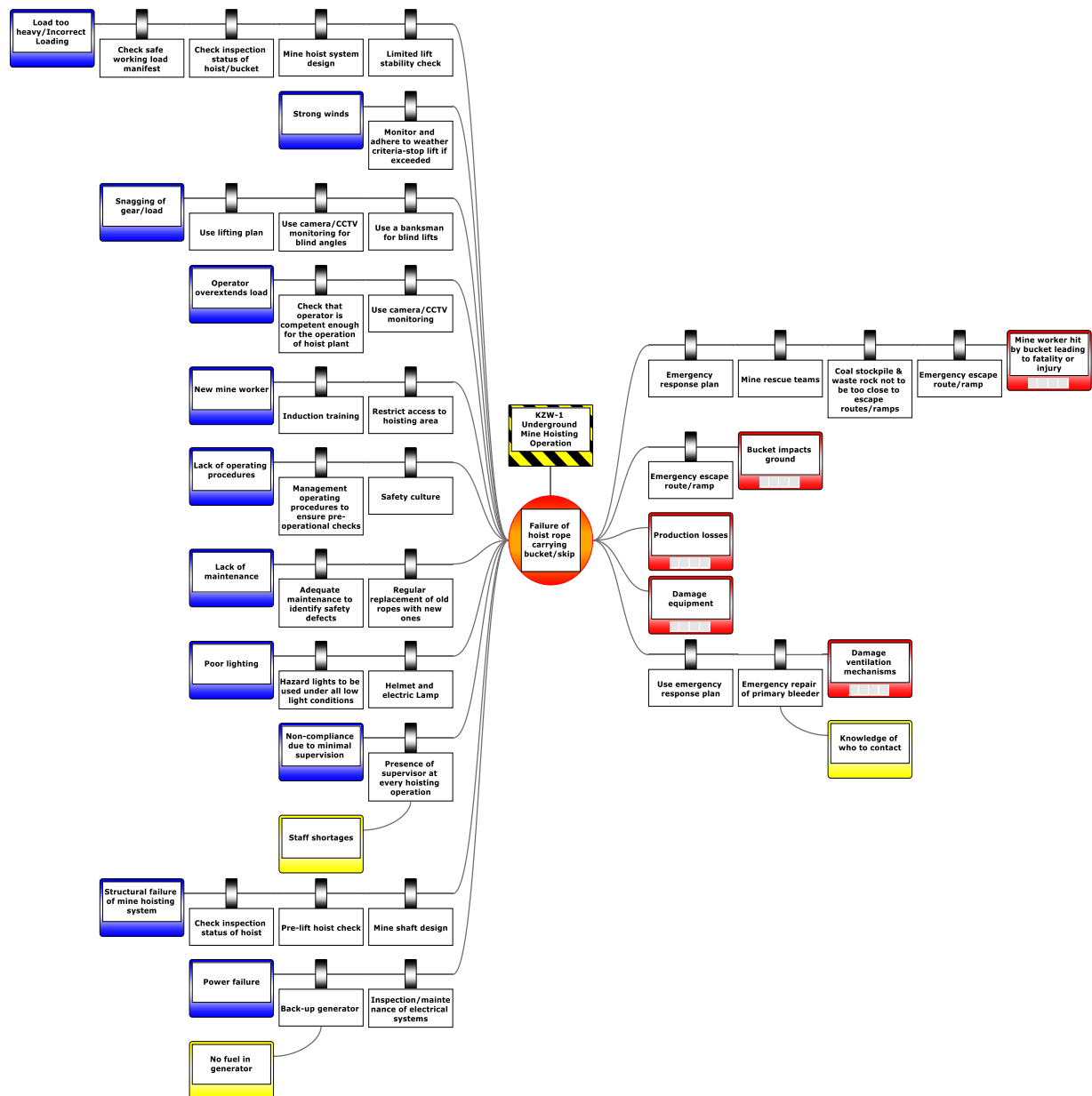


Figure 3: An illustrative BowTie risk model for a hoisting operation at Kaziwiziwi coal mine

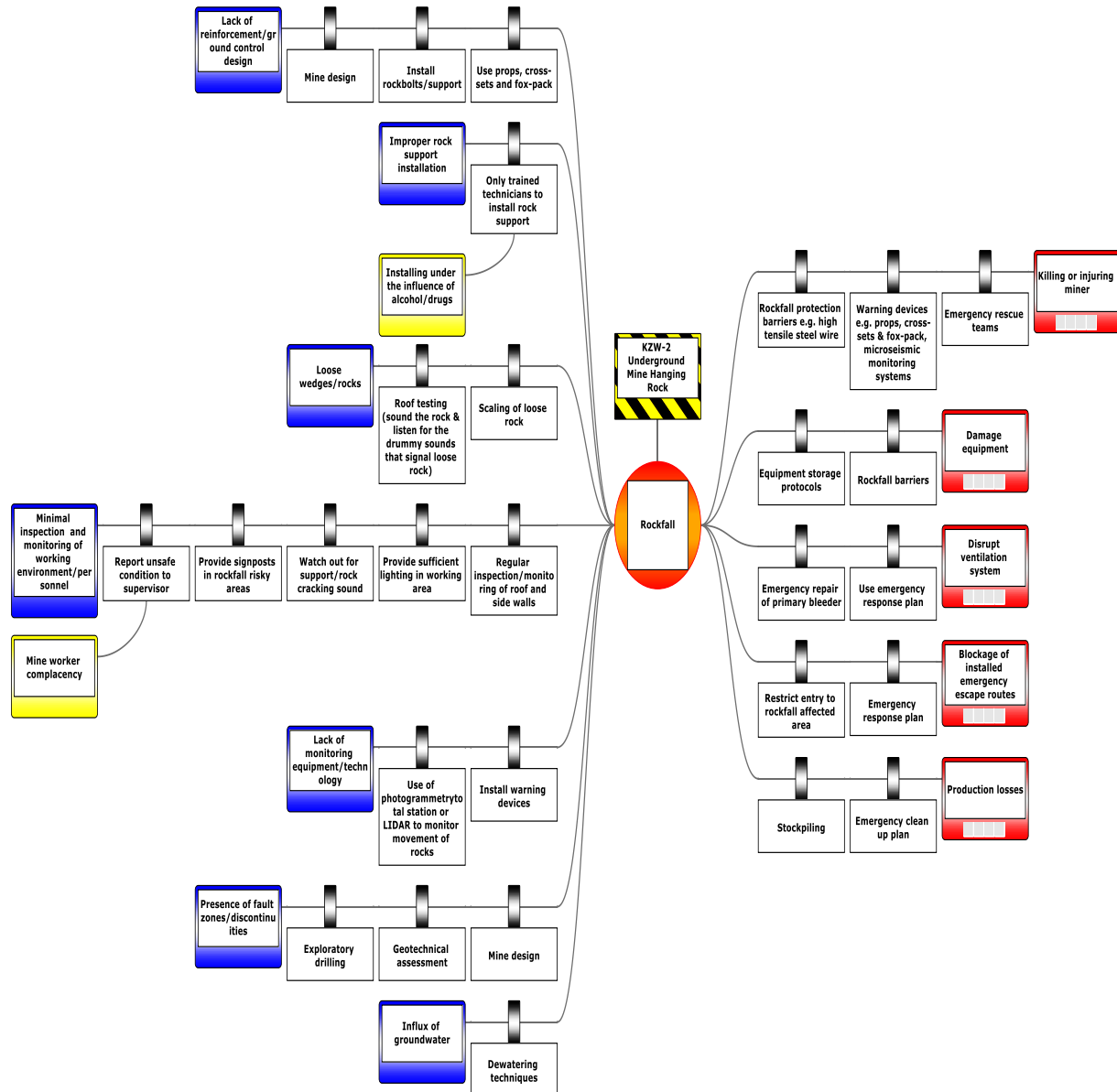


Figure 4: An illustrative BowTie risk model for hanging rock at Kaziwiziwi coal mine

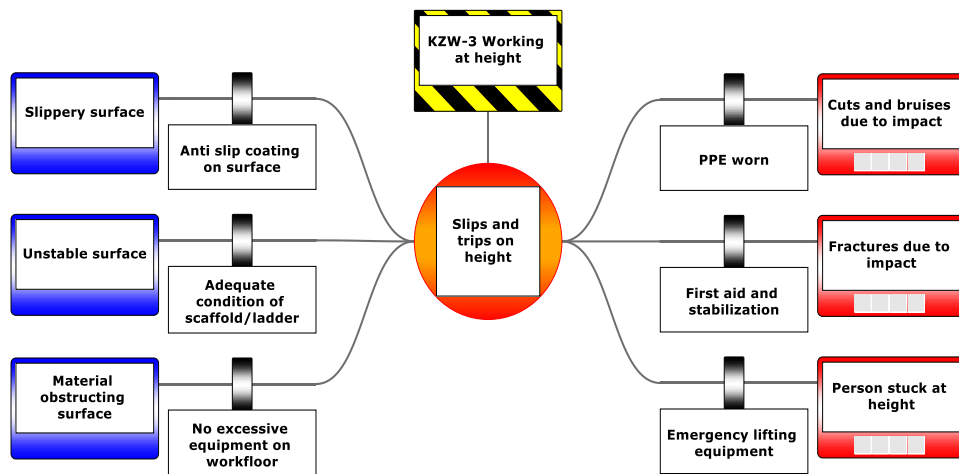


Figure 5: An illustrative BowTie risk model for working at height at Kaziwiziwi coal mine

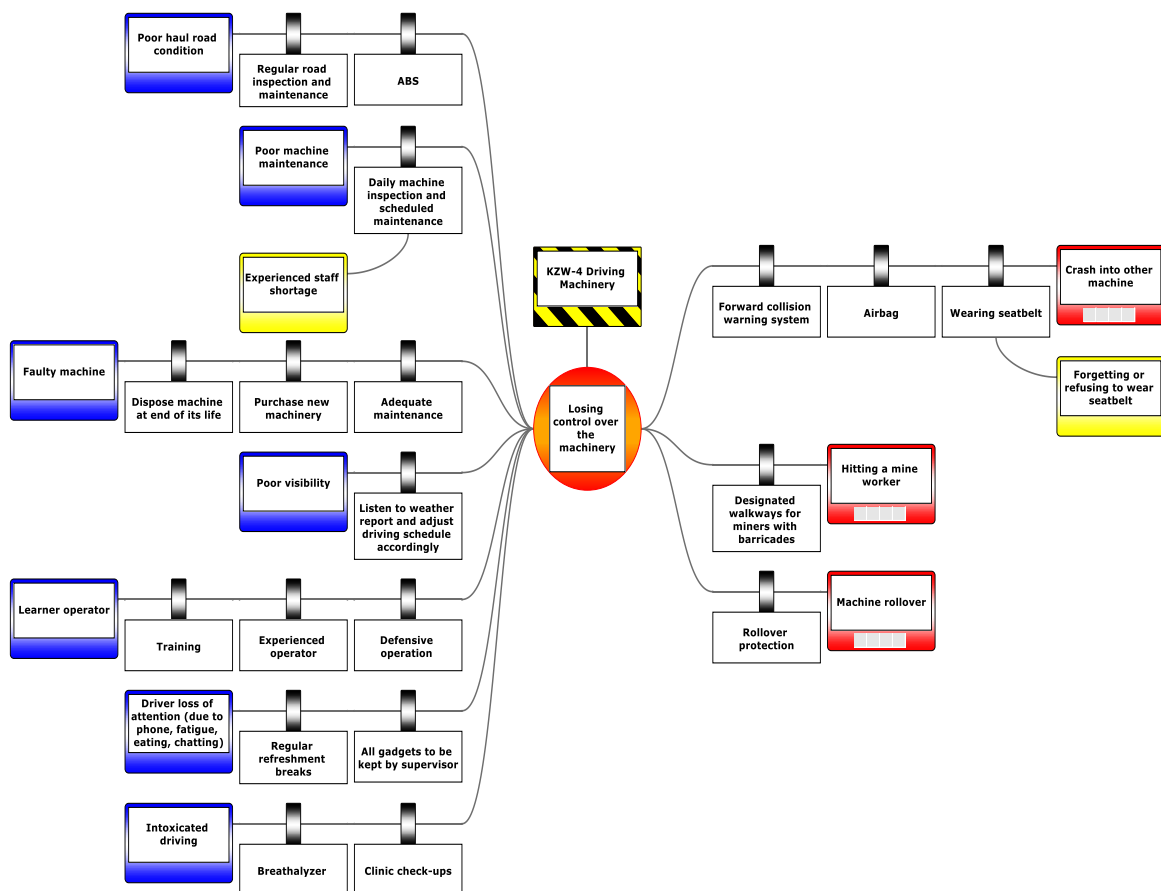


Figure 6: An illustrative BowTie risk model for driving machinery at Kaziwiziwi coal mine

4. Conclusion and Recommendation

Present study has applied the bowtie method to assess the most significant underground mining hazards being faced by mineworkers at Kaziwiziwi coal mine. The application of the bowtie method to identifying risk barriers from accident/incident reports in the mining industry uncovers a large number of different preventative and mitigation risk barriers. The authors demonstrated that the bowtie method is an effective visualization tool that can be used to analyze the hazard, top event, threats, consequences, barriers and escalation factors of mining accidents; and therefore give an overview of everything not wanted around a certain hazard. This new knowledge will help mining companies improve in their identification of risk controls during accident/incident investigation studies. Best practices comprising engineering design, mining methods, hoisting systems, ground/roof support, human factors and equipment choice will prevent mining risks from happening so far as is reasonably practicable, and create safer working environments at Kaziwiziwi coal mine.

In relation to the improvement of safety at the mining site which directly correlates with the welfare of mine workers, the labour statistics by the Annual Economic report 2012 indicates that a total of 21,022 workers were employed in the mining sector by 2011 representing an increase of 82 % from 11,565 in 2009. Of the total 2011 sector employees, 907 were in coal, 859 in uranium mining activities, 12,030 in the quarry aggregate production, 1,260 in gemstones minerals specimens, 195 in minerals exploration activities and the rest in other mineral production activities (Malema 2017). Therefore, to improve the safety and risk awareness culture, it is recommended to have a safety database of all possible accidents/incidents at mining sites in Malawi, and introduce safety training workshops in the mining industry. The bowtie risk analysis model is a reliable tool which will be used by the private and public sector to visualize their safety adherence. The Department of Mines will find this bowtie visualization tool useful when carrying out accident analyses in the future which in turn will promote safety awareness and policy development in the mining industry, and suggest ways on how to keep the normal but hazardous aspects from turning into something unwanted. In addition, mining companies will apply this new knowledge to proactively conduct situational audits of unwanted scenarios, and identify barriers to prevent accidents from happening so far as is reasonably practicable.

Future work can look into the impact of mental illness to mining related injuries and how mental awareness can be incorporated into safety management programmes at mining sites.

Conflict of Interest

The authors have not declared any conflict of interest.

Acknowledgements

The authors would like to thank University of Malawi, The Polytechnic for supporting the research.

References

- Annual Economic Report. (2012). Published report. Lilongwe: Malawi Government Publishing services.
- Acfield, A.P. and Weaver, R.A. (2012), "Integrating Safety Management through the Bowtie Concept. A move away from the Safety Case focus". Paper presented at the *Proceedings of the Australian System Safety Conference*-Volume 145.
- Burgess-Limerick, R., Horberry, T. and Steiner, L. (2014), "Bow-tie analysis of a fatal underground coal mine collision". *Ergonomics Australia*, 10(2), 1-5.
- CGE. (2020), "Risk Management Solutions: creating bowtie diagrams". Retrieved from <https://www.cgerisk.com/products/bowtiexp>
- Dodshon, P. and Limerick, R. (2015), "Using Bow-Tie analyses to enhance incident investigation activities". *Proceedings 19th Triennial Congress of the IEA*, Melbourne 9-14 August.
- Face of Malawi. (2012), "One killed, another injured in an accident at Kaziwiziwi coal mine in Rumphi". Retrieved from <https://www.faceofmalawi.com> on 6th June 2020.
- Maneya GJ. (2012). An Integrated Study of Coal Geology and Potential Environmental Impact Assessment at Mchenga Coal Mine in Livingstonia Coalfield in Malawi [unpublished Master of Science thesis on the Internet]. Pretoria: University of Fort Hare.

- Malema, K. (2017), "The working conditions in the mining sector: the case of Mchenga and Kaziwiziwi coal mines in Malawi". *Open Science Journal* 2(1).
- Mining Safety Regulations. (1982), "Laws of Malawi-Mines and Minerals Cap. 61:01". *Government of Malawi*.
- Pitblado, R. and Weijand, P. (2014). Barrier diagram (Bow Tie) quality issues for operating managers. *Process Safety Progress*, 33(4), 355-361.
- Safe Work Australia. (2012), "Guide for Major Hazard Facilities: Safety Case, Demonstrating the Adequacy of Safety Management and Control Measures".ed underground coal mines in Malawi". *Hindawi Advances in Civil Engineering Volume 2019*, Article ID 5350686.
- Saud, Y.E., Israni, K.C. and Goddard, J. (2014), "Bowtie diagrams in downstream hazard identification and risk assessment". *Process Safety Progress*, 33(1), 26-35.
- Yasidu, U. (2019), "Influences of water vapor on Roof Fall accidents in selected underground coal mines in Malawi". *Hindawi Advances in Civil Engineering Volume 2019*, Article ID 535

Assessment of Safety Culture and Maturity in Mining Environments: Case of Njuli Quarry

Jabulani Matsimbe¹, Steven Ghambi¹, Abdul Samson¹

¹ Department of Mining Engineering, Faculty of Engineering, The Polytechnic, University of Malawi, Blantyre, Malawi. Email: jmatsimbe@poly.ac.mw

Abstract

Due to an ever increasing concern for safety at most mines in Malawi, this paper aimed at assessing the safety culture and maturity in mining environments by applying the Safety Culture Maturity Model (SCMM). The SCMM is a practical and reliable diagnostic tool to use in the context of Malawian mining environments because it emphasizes the importance of employee involvement in assessing and improving safety culture. Njuli quarry is used as a case study due to its adoption of modern mining technologies and long existence in the mining industry. The methods used to assess the level of maturity of safety culture comprised questionnaires, interviews and behavioral observations. To test the reliability of the questionnaire, the respondents were interviewed using the same questions and comparing the results. There was good reliability of the measures used since the correlation coefficients between questionnaire and interview ranged from $r = 0.9$ to 1 . The results demonstrate that Njuli quarry has more characteristics of the Managing Level 2 or Developing Stage with percentages ranging 55% - 60% followed by the Emerging Level 1 ranging 33% - 36%. The Involving Level 3 ranged 4% - 10% showing improvement in some items of the dimensions of the safety framework. The company had the lowest percentages of 0% - 2% in Cooperating Level 4, and 0% - 1% in Continually Improving Level 5. This was expected because most mining companies in Malawi focus on maximizing production regardless of the safety implications, and also employees do not take safety issues seriously despite minor accidents and near misses. Therefore, the company should carry out safety trainings, set up a safety department, provide PPE to employees, and introduce rewards for best safety performance. Present study has added new knowledge on levels of maturity of safety culture in Malawi's mining environments which will influence the Department of Mines in policy development, site safety inspections and safety audits.

Keywords: Malawi, Maturity Model, Safety Management

1. Introduction

Despite Malawi experiencing an increase in the number of open pit quarries, there is a research gap on the state of safety culture maturity in mining environments. Therefore, the question that arises is how safe are these mining environments. Present study seeks to address the research question by assessing the level of safety

culture and maturity in Malawi's mining environments with Terrastone Njuli quarry used as a case study. The mining site is chosen due to its adoption of modern mining technologies and long existence in the mining industry. Research by Chiocha et al. (2011) found that optimum health and safety leadership, management commitment to and management involvement in health and safety, increasing awareness, and appropriate enforcement of legislation can lead to a decline in the number of construction-related fatalities and injuries in Malawi. In recent years, there has been an increasing recognition of the importance of organisational, cultural and behavioural aspects of safety management in high reliability industries (Lardner, 2002). Management has realized that the general likelihood of an accident occurring in their plant depends not only on the actions of individual employees, but also on the "safety culture" of their organisation, defined by the Confederation of British Industry as "the way we do things around here" (Lardner, 2002). Research by Lardner (2002) also suggests that the Safety Culture Maturity Model (see Figure 1) aims at assisting organizations in establishing their current level of safety culture maturity and identifying the actions required to improve their safety culture.

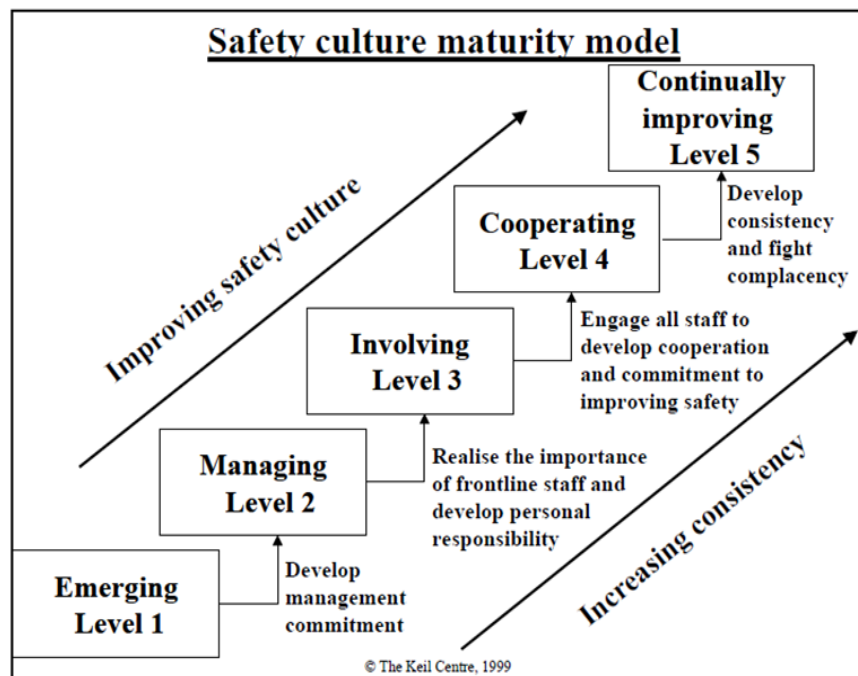


Figure 1: Safety culture maturity model (Fleming, 2001)

Figure 2 is based on Figure 1 and it shows how an improvement in safety culture lowers the rate of incidents occurring at a company. The key elements that constitute a good foundation for safety in an organization comprise strategic plans and action plans that integrate safety into all aspects of an organization's activities, presence and quality of the organization's risk control systems & safety management information system, the extent to which an organisation's safety management systems are reviewed and the extent to which every employee receives high quality integrated job and safety training (IAEA 2002a, Goncalves et al., 2010).

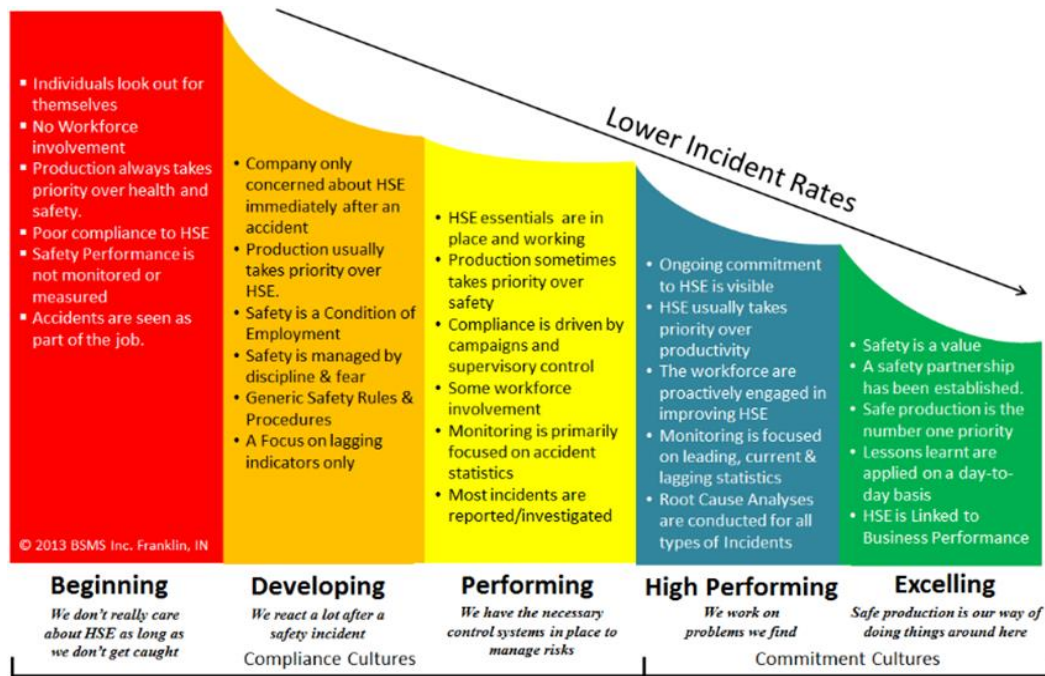


Figure 2. Maturity Model of Safety Culture (British HSE, 2007)

Njuli quarry is involved in high risk mining operations such as drilling, blasting, loading, hauling and processing of rock aggregates hence there is a need to assess the state of safety culture at the mining site. It is hoped that the output of this research will provide insights on how to assess and improve safety culture maturity in Malawi's mining environments.

2. Materials and Methodology

2.1. Study Area

Njuli Quarry is an aggregate mine located at Latitude -15.706495° and Longitude 35.118275° (see Figure 3). The quarry supplies construction materials to the surrounding areas. There are drilling, blasting, hauling and processing activities at the mine site which might affect mine workers as well as residents of Chakachaza, Chikuse, Luwanga and Namakhuwa villages.



Figure 3: Aerial view of Njuli quarry (Google Earth 2020)

2.2. Procedure

The Safety Culture Maturity Model (SCMM) used in this research is based on Fleming (2001) because the model emphasizes the importance of employee involvement in assessing and improving safety culture. In order to establish the level of maturity of Njuli quarry's safety culture, a framework of five dimensions (Fleming, 2001; IAEA 2002a; & Goncalves et al., 2010) was applied:

- i. Information: involves the way the organisation allows its employees to inform about any near misses and accidents as well as the confidence the employees have in the organisation.
- ii. Organisational Learning: describes how the organisation deals with the information, how the organisation analyses the accidents and near misses at the workplace, and if the organization keeps the employees informed about these events.
- iii. Involvement: explains the way the organisation leads the employees to a growing participation in safety issues, in accident analysis and in reviewing procedures and rules. It also includes if the employees participate in safety committees and safety meetings.
- iv. Communication: describes how, when and what to communicate regarding safety issues to employees. Also, if there is an open communication channel between employees and managers. It also describes if the communication reaches the employees and is understood by them.
- v. Commitment: describes the support given by the organisation as far as Health and Safety is concerned: planning, priorities, training, auditing, contractor, rewards, investment, procedures and teaming. It also describes there is a Health, Safety and Environment Management System. Truthful commitment means more than writing political statements to say that Health and Safety are important, it needs to have coherence between words and reality.

2.2.1. Questionnaire (Based on Fleming, 2001; & Goncalves, 2010)

The five dimensional frameworks had items which were used as statements to develop a safety maturity questionnaire for Njuli Quarry. Tables 1–5 show the framework and how each one of the five dimensions is treated in each one of the five stages of maturity of safety culture. Each item represented one level: 1 – Emerging, 2 – Managing, 3 – Involving, 4 – Cooperating and 5 – Continually Improving. The questionnaire had 22 questions: 14 questions with five items and 8 questions with four items, hence totalling 102 items. For each question, the respondents were required to select the item that best represented the position of the company.

Table 1: Framework to identify maturity of safety culture in information

I. Information				
Emerging Level 1	Managing Level 2	Involving Level 3	Cooperating Level 4	Continually Improving Level 5
1. The unusual events which occur in the organisation are not reported by the employees 2. There is not a formal system that allows the employees to inform any unusual events, including accidents and serious ones, occurred in the organisation 3. The employees do not inform any unusual	1. Only the serious accidents are reported by the employees 2. There is a formal system which allows the employees to inform only the serious accidents occurred in the organisation 3. The employees do not inform any unusual events occurred because they do not feel comfortable enough in relation to the organisation	1. Most of the unusual events which occur in the organisation are not reported by the employees 2. There is a formal system that allows the employees to inform only the accidents, including the serious ones, occurred in the organisation 3. The minority of the employees feel comfortable enough	1. Most of the unusual events which occur in the organisation are reported by the employees 2. There is a formal system that allows the employees to inform all the unusual events, including accidents and serious accidents, occurred in the organisation 3. The majority of the employees feel comfortable enough	1. All the unusual events which occur in the organisation are reported by the employees 2. There is a formal system that allows the employees to inform all the unusual events, including accidents and serious accidents, occurred in the organisation 3. All the employees feel comfortable enough to inform the unusual events occurred in the

events occurred because they do not feel comfortable enough in relation to the organisation 4. There are no performance indicators of safety at work	4. The only performance indicators of safety at work are the serious accidents occurred in the workplace	to inform the unusual events occurred in the organisation 4. The only performance indicators of safety at work are the accidents and work-related illnesses rates	to inform the unusual events occurred in the organisation 4. The organisation has other performance indicators of safety at work as well as the accidents and work-related illnesses rates	organisation 4. Besides having performance indicators of safety at work, the company has indicators of performance in the environmental area
---	--	--	---	---

Table 2: Framework to identify maturity of safety culture in organisational learning

I. Organisational Learning				
Emerging Level 1	Managing Level 2	Involving Level 3	Cooperating Level 4	Continually Improving Level 5
1. The organisation does not analyse any unusual events 2. The analysis of unusual events aims to identify the guilty ones only 3. The organisation does not propose any improving actions for safety at work 4. The organisation does not inform the analyses results of unusual events to its employees	1. Only the serious accidents are reported by the employees 2. There is a formal system which allows the employees to inform only the serious accidents occurred in the organisation 3. The employees do not inform any unusual events occurred because they do not feel comfortable enough in relation to the organisation 4. The only performance indicators of safety at work are the serious accidents occurred in the workplace	1. Most of the unusual events which occur in the organisation are not reported by the employees 2. There is a formal system that allows the employees to inform only the accidents, including the serious ones, occurred in the organisation 3. The minority of the employees feel comfortable enough to inform the unusual events occurred in the organisation 4. The only performance indicators of safety at work are the accidents and work-related illnesses rates	1. Most of the unusual events which occur in the organisation are reported by the employees 2. There is a formal system that allows the employees to inform all the unusual events, including accidents and serious accidents, occurred in the organisation 3. The majority of the employees feel comfortable enough to inform the unusual events occurred in the organisation 4. The organisation has other performance indicators of safety at work as well as the accidents and work-related illnesses rates	1. All the unusual events which occur in the organisation are reported by the employees 2. There is a formal system that allows the employees to inform all the unusual events, including accidents and serious accidents, occurred in the organisation 3. All the employees feel comfortable enough to inform the unusual events occurred in the organisation 4. Besides having performance indicators of safety at work, the company has indicators of performance in the environmental area

Table 3: Framework to identify maturity of safety culture in involvement

I. Involvement				
Emerging Level 1	Managing Level 2	Involving Level 3	Cooperating Level 4	Continually Improving Level 5
1. The employees do not engage in safety issues 2. The employees have no interest in participating in safety-related issues	1. The employees are invited to participate in safety-related issues only when serious accidents occur 2. The employees are interested in participating in safety-related issues only when serious accidents occur	1. The minority of the employees is engaged in safety-related issues 2. The minority of employees is interested in participating in safety related issues	1. The majority of the employees are engaged in safety-related issues 2. The majority of employees are interested in participating in safety related issues	1. All employees are engaged in both safety-related and environmental issues 2. All the employees are interested in participating in safety-related issues

Table 4: Framework to identify maturity of safety culture in communication

I. Communication				
Emerging Level 1	Managing Level 2	Involving Level 3	Cooperating Level 4	Continually Improving Level 5
1. The organisation does not communicate its employees any safety-related issues 2. There is not an open channel of communication between the organisation and its employees about safety-related issues 3. The organisation does not check if the communication about safety-related issues is effective	1. The organisation communicates its employees the safety-related issues only when serious accidents occur 2. There is an open channel of communication between the organisation and its employees only when serious accidents occur 3. The organisation checks if the communication about safety related issues is effective only when serious accidents occur	1. The organisation communicates its employees the least part of the safety-related issue 2. There is an open channel of communication between the organisation and its employees; however, it is still incipient and bureaucratic and it is based on norms and procedure 3. The organisation checks if the communication about safety-related issues is effective only in areas where there are risks of accident and work-related illnesses	1. The organisation communicates its employees the most part of the safety related issue 2. There is an open channel of communication between the organisation and its employees because the former considers safety-related issues relevant 3. The organisation checks if most part of the communication about safety related issues is effective	1. The organisation communicates its employees all the safety-related issues 2. There is an open channel of communication between the organisation and its employees because the former considers safety-related issues relevant 3. The organisation checks if all the communication about safety-related issues is effective

Table 5: Framework to identify maturity of safety culture in commitment

I. Commitment				
Emerging Level 1	Managing Level 2	Involving Level 3	Cooperating Level 4	Continually Improving Level 5
<p>1. Planning for safety at work is not done by the organisation</p> <p>2. The organisation does not audit in safety at work</p> <p>3. The organisation does not invest in safety at work</p> <p>4. The organisation does not provide any safety at work training</p> <p>5. The organisation does not have a team to give support in safety at work</p> <p>6. The organisation considers safety at work only an expense</p> <p>7. The procedures in safety at work are seen as limiting as far as activities are concerned</p> <p>8. The organisation does not adopt a rewarding system to stimulate safety at work</p> <p>9. The organisation hires outsourced companies for a lower price and shows no concern with safety</p>	<p>1. Planning for safety at work is focused only on what went wrong in the past</p> <p>2. The organisation audits in safety at work only after serious accidents and work-related illnesses occur</p> <p>3. The organisation invests in safety at work only after serious accidents and work-related illnesses occur</p> <p>4. The organisation provides resources so that specific training program in safety at work can take place only after serious accidents occur</p> <p>5. The organisation has a small team to give support in safety at work</p> <p>6. The organisation considers safety at work important only when serious accidents or work-related illnesses occur</p> <p>7. The procedures in safety at work are written only in face of serious accidents that occur</p> <p>8. The organisation adopts a rewarding system to stimulate safety at work only in specific situations, that is, after serious accidents and work-related illnesses occur</p> <p>9. The organisation worries about safety at work in relation to outsourced</p>	<p>1. Planning for safety at work is focused only on the identification and analysis of existing risks in the workplace</p> <p>2. The organisation has an auditing program in safety at work only in areas where risk of accident and work-related illness exist</p> <p>3. The organisation invests only to avoid risks of accident and work-related illnesses on the job</p> <p>4. The organisation has standard safety at work training only for the employees who work in places where risks of accident and work-related illnesses exist</p> <p>5. The organisation has a team that is big enough to give support in safety at work</p> <p>6. The organisation considers safety at work important, but it emphasises production</p> <p>7. The procedures in safety at work focus only the sectors where risks of accident and work-related illnesses exist</p> <p>8. The organisation adopts a rewarding system for good</p>	<p>1. Planning for safety at work is well structured with problem prevention and work procedures improvement, but It is not integrated with the other areas of the organisation</p> <p>2. The organisation has an auditing program in all its sectors for safety at work</p> <p>3. The organisation invests systematically in safety at work in all its sectors</p> <p>4. The organisation has a continuous training process in safety at work for all its employees</p> <p>5. The organisation has a team that is big enough to give support in safety at work</p> <p>6. The organisation seeks to prioritise safety at work, but it is not a reality yet</p> <p>7. The procedures in safety at work are done the best way possible, but they are not periodically reviewed</p> <p>8. The organisation adopts a rewarding system for all its sectors due to the employees' performance in safety at work</p> <p>9. The organisation</p>	<p>1. Planning for safety at work is well structured with problem prevention and work procedures improvement and It is integrated with the other areas of the organisation</p> <p>2. The organisation has an auditing program in all its sectors for both safety at work and environment</p> <p>3. The organisation continuously evaluates the need for new investment in both safety at work and the environment</p> <p>4. The organisation has a continuous training process in safety at work for all its employees</p> <p>5. The organisation does not have a team to give support in safety at work specifically because the responsibility for it is shared by all the organisation members</p> <p>6. The organisation, in fact, prioritises safety at work and production equally</p> <p>7. The procedures in safety at work are done the best way possible and are constantly reviewed for better effectiveness</p> <p>8. The organisation considers its</p>

	employees only when serious accidents or work-related illnesses occur	performance in safety at work only for those sectors where risks of accident and work-related illnesses exist 9. The organisation has a pre-qualification process in safety at work before contracting outsourced companies. Nevertheless, there is no follow-up afterwards	has a pre-qualification process in safety at work before contracting outsourced companies. Nevertheless, there is no follow-up afterwards	employees are highly motivated by both safety at work and the environment; therefore, it does not see the need for a rewarding system 9. The organisation considers the outsourced companies as part of its safety and environmental management system
--	---	--	---	---

2.2.2. Respondents

The sample of respondents was randomly selected from the production, maintenance and management teams. A total of 10, 10 and 4 respondents from the production, maintenance and management teams were selected respectively. Respondents from the management team comprised of the Managing Director, Quarry Manager, Safety Manager and Safety Officer. The respondents were advised to maintain anonymity when filling out the questionnaire.

2.2.3. Interviews

In order to correlate the respondents' answered questionnaires, all 24 respondents were interviewed by the researcher a week later after questionnaire submission and the interview lasted 30 minutes. Due to the non-parametric nature of the data, the verification of the questionnaire and interview scores were done by Kendall' tau, τ (Field 2005). During the time of this research, three students from The Polytechnic were on industrial attachment at the mining company thereby making it convenient for the researcher to observe the behaviour of management and employees towards safety. In addition, the researcher was given one month unlimited access to the site so as to observe employee' behavior, and carry out situational audits on safety culture. This on-site experience assisted in getting reliable responses from the interviewees.

3. Results and Discussion

All 24 respondents answered their questionnaire and returned it a week later. Interviews done on the respondents showed a correlation of between 0.9 and 1 indicating a good reliability of responses to questionnaire.

Table 6: Correlation between questionnaire and interview scores

Dimensions	Kendall' tau, τ
Information	0.915
Organizational Learning	1
Involvement	0.9
Communication	1
Commitment	0.908

Collected data was analyzed using Microsoft Excel statistical package. Table 7 shows the percentage of responses from 22 questions for each one of the five dimensions from all the 24 respondents. The use of the questionnaire, on-site behavioral observation, and interviews provided a satisfactory correlation on the maturity

of safety culture at Njuli Quarry. The researcher was taken through all sections at the quarry mine and this provided a better perspective on the company's adherence to the five dimensions and frameworks of safety.

Table 7: Maturity of safety culture scores for each one of the dimensions

Dimensions	Emerging (%)	Managing (%)	Involving (%)	Cooperating (%)	Continually Improving (%)
Information	36	60	4	0	0
Organizational Learning	34	56	7	2	1
Involvement	33	55	10	1	1
Communication	33	59	8	0	0
Commitment	34	58	8	0	0

Njuli quarry's maturity of safety culture varies across the five different maturity levels. The different levels of maturity found in this Njuli Quarry sample are consistent with the safety culture maturity concept in that safety culture does not develop at the same pace in all dimensions (IAEA, 2002a; Goncalves et al., 2010; Fleming, 2001). From the results, it is clear that Njuli quarry has more characteristics of the Managing Level 2 or Developing Stage with percentages ranging 55% - 60% followed by the Emerging Level 1 ranging 33% - 36%. The Involving Level 3 ranged 4% - 10% showing improvement in some items of the dimensions of the safety framework. The company had the lowest percentages of 0% - 2% in Cooperating Level 4, and 0% - 1% in Continually Improving Level 5. The results were anticipated by the researcher due to the fact that there is little to no literature available on safety culture in Malawi's mining environments, and through observation, most mining companies mainly focus on maximizing production regardless of the safety culture. Njuli quarry has no designated safety department thereby making it difficult for employees to report on near misses and non-compliance. The employees blame the company for not providing them with enough personal protective equipment and safety training thereby fostering complacency. However, the company indulges in safety talks and equipment inspection at 6:45am every morning before any work starts thereby showing the companies' commitment to improving safety culture. In addition, before blasting is carried out the company notifies the surrounding community of a date when blasting will be done. Blasting is normally carried out at 12pm noon and warning sirens are done 15 minutes prior to ignition of blast.

4. Conclusion and Recommendation

Fleming's (2001) safety culture maturity model was successfully applied to Njuli quarry mining environment and it has proven to be a reliable diagnostic tool for assessing safety culture maturity. The Emerging and Managing Levels of safety culture represent a true reflection of the maturity of safety culture in Malawi's mining environments because mining is still at the developing phase in Malawi and mining companies are mostly focused on maximizing production regardless of the safety culture. Present study findings will assist the Department of Mines when carrying out safety inspections in mining environments. In addition, mining companies will apply this new knowledge when carrying out safety audits on their operations thereby complying with the Malawi government's safety regulations. According to the Mining Safety Regulations (1982), all mining companies are encouraged to adhere to safety rules but most of these companies take shortcuts and reduce safety budgets so as to maximize production. Therefore, to continually improve safety culture in Malawi's mining environments, it is recommended to:

- Provide PPE to all employees at all working times
- Encourage housekeeping
- Carry out safety trainings, audits, and provide scenarios of near misses
- Set up an on-site safety department and develop a risk management system
- Introduce rewards for best safety performance to increase motivation amongst employees.

Future research work can look into the application of the safety culture maturity model to a heterogeneous environment like the construction sector so as to test its dimensional validity. In addition, a comparative analysis can be done on safety culture maturity between the construction and mining sectors in Malawi.

Conflict of Interest

The authors have not declared any conflict of interest.

Acknowledgements

The authors would like to thank University of Malawi, The Polytechnic for supporting the research.

References

- British HSE. (2007). Safety Culture Maturity Model. *Health and Safety Executive*.
- Chiocha, C., Smallwood, J., & Emuze F. (2011). Health and safety in the Malawian construction industry. *Acta Structilia* 18(1).
- European Union. (2011). Malawi National Occupational Safety and Health Programme-Moving towards zero accidents and diseases at work. *International Labour Organization*.
- Goncalves, A.P. F., Andrade, C.O., Marinho, M.M.O. (2010). A safety culture maturity model for petrochemical companies in Brazil. *Safety Science* 48, 615-624. <https://doi.org/10.1016/j.ssci.2010.01.012>
- Field, A. (2005). Statistics Using SPSS. *SAGE, London*.
- Fleming, M. (2001). Safety Culture Maturity Model. Report 2000/049. *Health and Safety Executive. Colegate, Norwich*.
- International Atomic Energy Agency, IAEA (2002a). Safety Culture in Nuclear Installations: Guidance for Use in the Enhancement of Safety Culture. *International Atomic Energy Agency, Vienna*.
- Lardner, R. (2002). Towards a mature safety culture. *The Keil Centre Ltd*.
- Mining Safety Regulations. (1982). Laws of Malawi-Mines and Minerals Cap. 61:01. *Government of Malawi*.